

O C T O B E R 1 9 9 9

SNCC

***Swiss Needle Cast
Cooperative***

A N N U A L R E P O R T

1 9 9 9



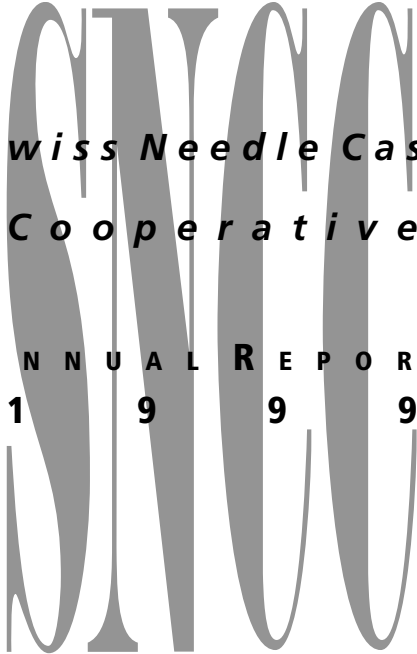
OREGON STATE
UNIVERSITY
COLLEGE OF
FORESTRY

Forest Research Laboratory



**MEMBERS OF THE SWISS NEEDLE CAST COOPERATIVE AND
THEIR 1999 CONTRIBUTIONS**

Boise Cascade Corporation	\$15,000
Champion International	\$5,000
Coos County Forestry Department	\$5,000
Confederated Tribes of the Grand Ronde	\$5,100
Confederated Tribes of the Siletz	\$700
Davidson Industries	\$5,000
Hampton Resources, Inc.	\$20,000
Longview Fibre Co.	\$45,000
Menasha Corporation	\$15,000
Miami Corporation	\$5,000
Oregon Department of Forestry	\$45,000
Port Blakely	\$15,000
Rayonier	\$3,000
Rosboro Lumber Co.	\$10,000
Simpson Timber Co.	\$45,000
Starker Forests	\$45,000
Swanson Superior Forest Products, Inc.	\$10,000
The Timber Company	\$45,000
Weyerhaeuser Corporation	\$5,000
Willamette Industries	\$45,000
USDA Forest Service	In kind
USDI Bureau of Land Management	\$45,000
OSU Forest Research Laboratory	\$30,000 (salary)



**Swiss Needle Cast
Cooperative**

A N N U A L R E P O R T
1 9 9 9

Edited by Greg Filip, SNCC Director
Layout by Gretchen Bracher, FRL Publications

SNCC INCOME SOURCES AND EXPENDITURES 1999

Income

Membership Dues	\$433,800
-----------------	-----------

Expenditures (as of 9/99)

Salaries and Wages	\$129,545
OPE	24,125
Supplies and Services	54,964
Travel	13,263
Indirect Costs	22,189
Total Expenditures	\$244,086

Balance	\$189,714
----------------	------------------

CONTENTS

HIGHLIGHTS OF 1999	5
PLANS FOR 2000	5
SWISS NEEDLE CAST AERIAL SURVEY, 1999	6
Survey procedures:	6
Results of the survey:	7
Acknowledgments:	9
GENETICS OF SWISS NEEDLE CAST TOLERANCE -EARLY SCREENING AND FIELD RESULTS	10
IMPACTS OF SWISS NEEDLE CAST ON THE PHYSIOLOGY OF DOUGLAS-FIR NEEDLES	12
Goal I.	12
Goal II.	13
Goal III.	24
References	27
Appendix I. A/Ci Curve Analysis and Calculations	29
Appendix II. Abbreviations and Gas Exchange Parameters.	30
Appendix III. Abbreviations and Spectrophotometric Rubisco Activity Parameters	31
Appendix IV. Abbreviations and Chlorophyll Fluorescence Parameters	31
IDENTIFICATION OF ALTERNATIVE FUNGICIDES AND APPLICATION TIMINGS TO REDUCE SWISS NEEDLE CAST DAMAGE IN STANDS OF DOUGLAS-FIR TIMBER	32
Assessment Methods and Scales	33
Protectant Studies	34
Inoculum Disruption Studies	35
Additional Studies and Observations	37
Acknowledgments	38
EFFECT OF FERTILIZATION AND VEGETATION CONTROL ON SWISS NEEDLE CAST	
INFECTION AND GROWTH OF COASTAL DOUGLAS-FIR SEEDLINGS	39
Study #1	39
Materials and Methods — Study #1	39
Study #2	42
Materials and Methods — Study #2	42
Expected Study Outcomes	43
GROWTH IMPACT STUDY	44
Tree size	44
Stand density	44
Swiss needle cast severity	49
SWISS NEEDLE CAST INFECTION STUDIES	50
Summary of Specific Studies in Progress	51
Preliminary Results	52
PART 2	58
Genetics of Phaeocryptopus	58
Molecular Systematics	61
SWISS NEEDLE CAST RISK ANALYSIS AND MODELING	69
Introduction	69
Methods	70
Results and Discussion	71
Conclusions	75
References	75
Objections and notes	76



To: SNCC Members
From: Greg Filip
Date: September 1999
Subject: 1999 Annual Report

This is the third year for SNCC, and I thank the members for all of the support that they have given SNCC this year. This has been another busy year for SNCC. We were fortunate to receive \$250,000 from the Oregon State Legislature to support projects in 2000 and 2001. I want to thank all of those involved in doing the work to help secure these funds, especially Alan Kanaskie, Mark Gourley, and John Washburn. This year's annual report contains summaries on the progress made on our eight projects. We had two aerial survey flights this year, one in Oregon and one in Washington, that show a continuing intensification of Swiss needle cast. Information continues to be collected on the permanent growth impact and precommercial thinning plots. Progress continues on the basic infection biology research that is summarized in this report. Projects are continuing in needle physiology and tree genetics, and progress reports are contained in this report. New projects were started in alternative fungicides and in fertilizer and vegetation control.

I would like to especially thank our 1999 investigators for their fine efforts in generating new information concerning Swiss needle cast: Alan Kanaskie, Doug Maguire, Katy Kavanagh, Jeff Stone, Randy Johnson, Robin Rose, Scott Ketchum, Diane Haase, and Gary Chastagner. Hats off to the many graduate students who do so much of the work. I would also like to thank the members of the SNCC executive committee whose enthusiasm and creativity keep this cooperative moving in the right direction: Mark Gourley, John Washburn, Greg Johnson, Dale Claussen, Jim Carr, and Alan Kanaskie. We have at least eight projects planned for 2000; it should be another exciting and productive year.

Department of Forest Science
Oregon State University
Corvallis, OR 97331-5752
PH 541-737-6567
FAX 541-737-1393
EMAIL Greg.Filip@orst.edu



HIGHLIGHTS OF 1999

This report presents the Swiss Needle Cast Cooperative activities in Swiss needle cast research. Highlights of 1999 include:

- We received \$250,000 (\$125,000 for two years) from the Oregon State Legislature for projects in 2000 and 2001.
- An aerial survey was conducted over 2.9 million acres in Oregon. A total of 295,000 acres of Douglas-fir had obvious symptoms on Swiss needle cast. Survey maps can be obtained from Alan Kanaskie, Oregon Department of Forestry in Salem.
- An aerial survey was conducted in southwest Washington. In general, symptoms of Swiss needle cast were more severe in 1999 than in 1998. Survey maps can be obtained from Dan Omdal, Washington Department of Natural Resources in Olympia.
- Research continues on eight different projects in 1999 including: aerial and ground surveys, growth impact studies, tree physiology, infection biology, tree genetics, alternative fungicides, precommercial thinning, and fertilizer and vegetation management.

PLANS FOR 2000

- Aerial survey to monitor SNC in Oregon and Washington
- Monitor permanent plots from the growth impact study Phase III
- Determine stomata response to SNC infection in Douglas-fir on different sites
- Conduct infection biology studies: Infection and biomass quantification; inoculum type, concentration, phenology, and nutrition on foliage colonization and disease severity; fungus physiology and host-fungus interactions; aerobiology and epidemiology; and digital microphotography and image analysis
- Develop early screening techniques for SNC resistance in Douglas-fir families
- Determine growth response to precommercial thinning in Douglas-fir stands with varying intensity of SNC in the Coast Range of Oregon
- Identify alternative fungicides and application timings to reduce SNC damage in stands of Douglas-fir
- Determine the effects of fertilization and vegetation control on SNC infection and growth of coastal Douglas-fir

SWISS NEEDLE CAST AERIAL SURVEY, 1999

Alan Kanaskie, Mike McWilliams, Keith Sprengel, Dave Overhulser

Survey procedures:

Flights were made at 1,500 to 2,000 feet above the terrain, follow-

ing north-south lines separated by 2 miles. Observers looked for areas of Douglas-fir forest with obvious yellow to yellow-brown foliage, a symptom

of Swiss needle cast. Patches of forest with these symptoms (the patches are referred to as polygons) were drawn onto 1:100,000 scale topographic

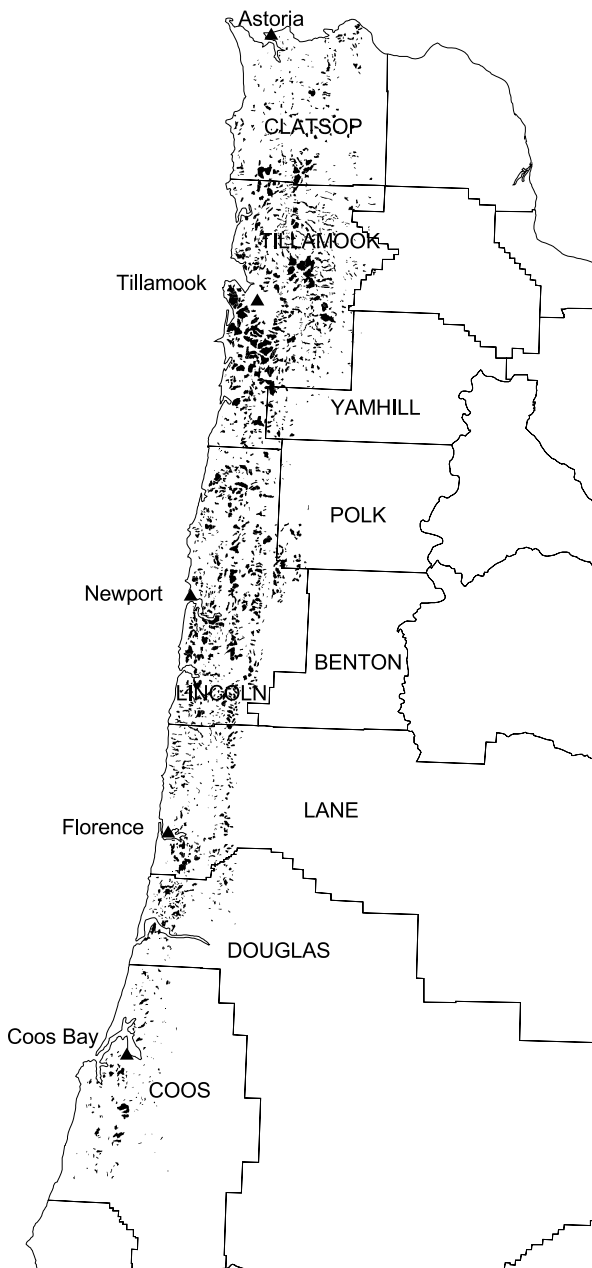


Figure 1. Areas of Douglas-fir forest in western Oregon with symptoms of Swiss needle cast detected during an aerial survey in April, 1999.

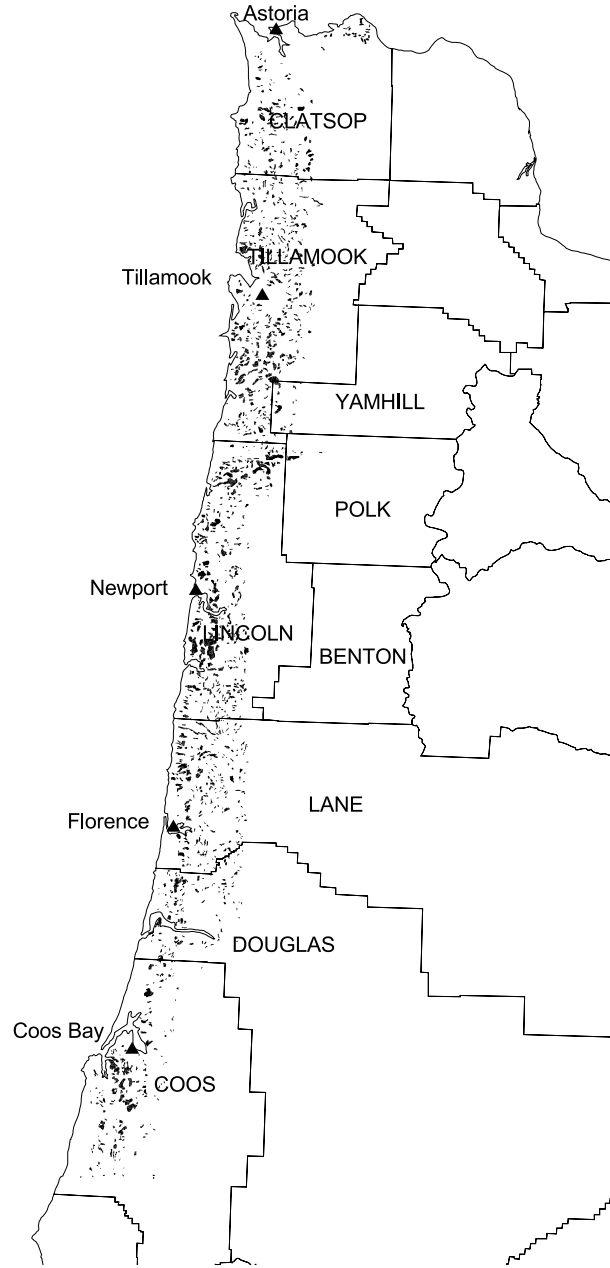


Figure 2. Areas of Douglas-fir forest in western Oregon with symptoms of Swiss needle cast detected during an aerial survey in April, 1996.

maps. Each polygon was classified for degree of discoloration as either “L” (light) or “H” (heavy). Polygons classified as “H” for discoloration had very sparse crowns and brownish foliage, while those classified as “L” were predominantly yellow to yellow-brown foliage and slightly more dense crowns than those classified as “heavy”.

The survey of the Coast range began on April 21 and ended on May 22, 1999. It extended from the coastline eastward until obvious symptoms were no longer visible, and from the Columbia river south to approximately the Coos/Curry county line.

Two flights were made over the west slopes of the Cascade Range;

one on May 6 and one on June 3, 1999. These flights extended from the Columbia river south to near Roseburg.

Results of the survey:

Figure 1 shows the approximate size and location of areas of Coast range Douglas-fir forest with symp-

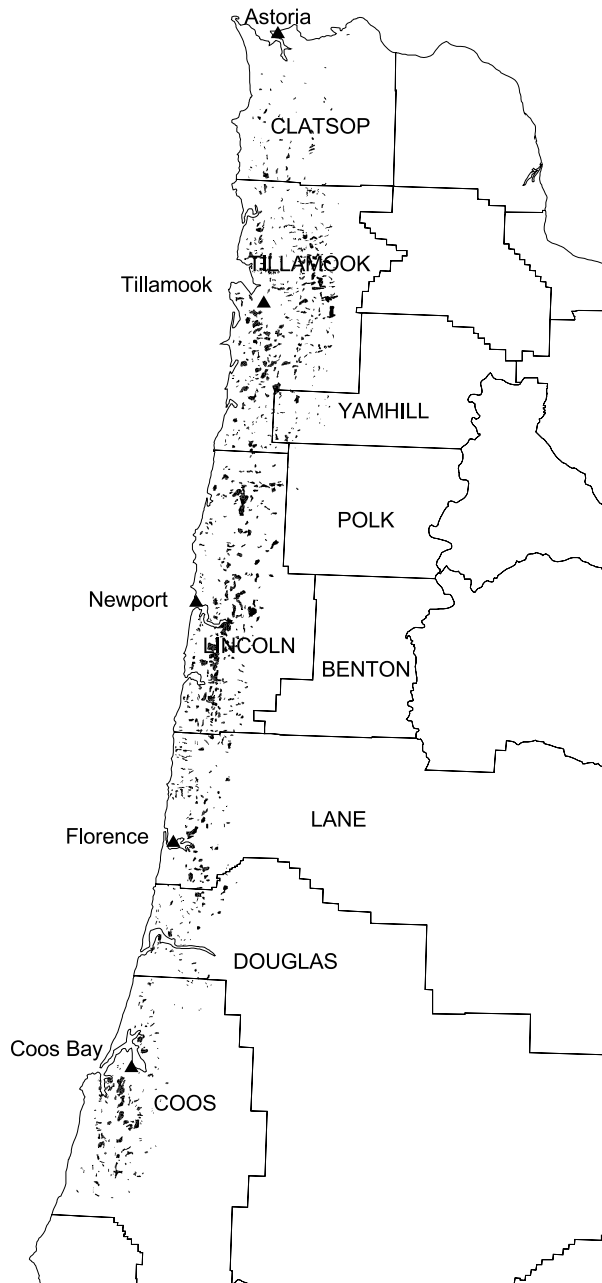


Figure 3. Areas of Douglas-fir forest in western Oregon with symptoms of Swiss needle cast detected during an aerial survey in April and May, 1997 (does **not** include re-fly of Nehalem and Yamhill quadrangles).

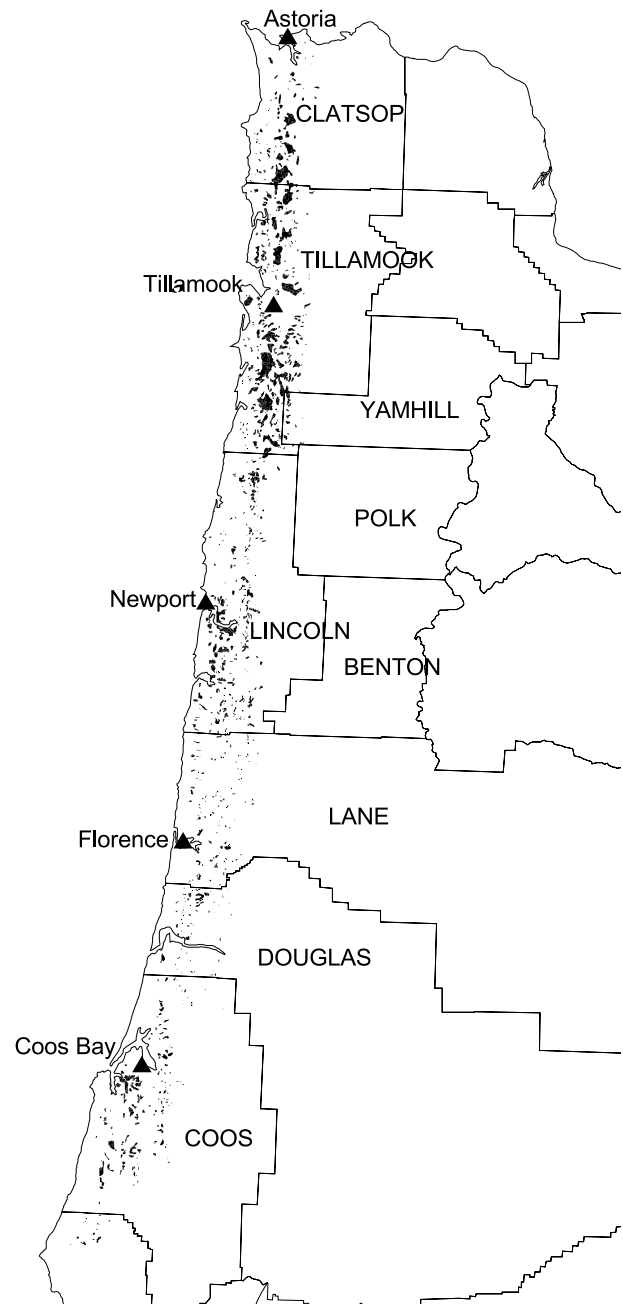


Figure 4. Areas of Douglas-fir forest in western Oregon with symptoms of Swiss needle cast detected during an aerial survey in April and May, 1998.

Table 1. Area of Douglas-fir forest in western Oregon with symptoms of Swiss needle cast detected during aerial surveys in 1996-1999.

Region	1996	1997	1998	1999
	acres			
North of Florence	106,000	130,000	135,000	260,000
South of Florence	24,000	30,000	38,000	35,000
TOTAL	130,000	160,000	173,000	295,000

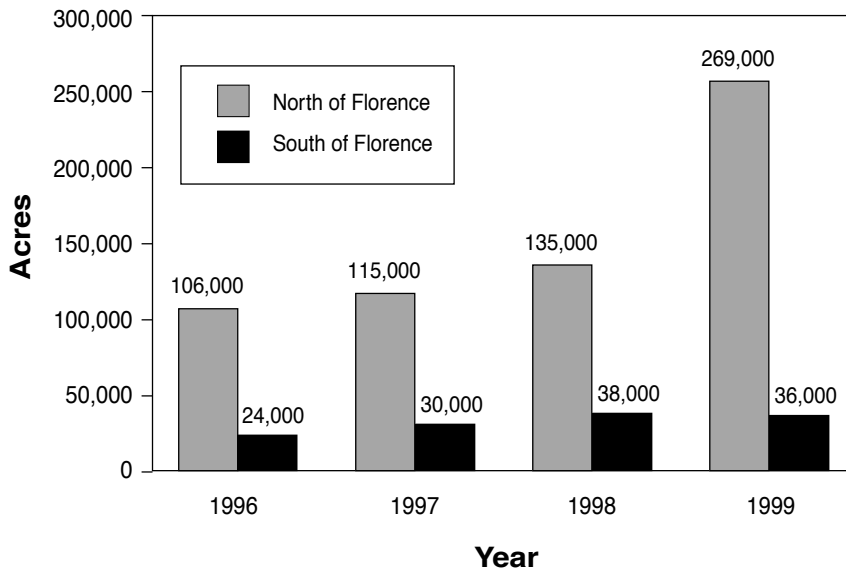


Figure 5. Trend in area of Douglas-fir forest in western Oregon with symptoms of Swiss needle cast detected during aerial surveys in April and May, 1996-1999.

toms of Swiss needle cast detected during an aerial survey in April and May, 1999. Figures 2,3, and 4 show survey results for 1996-1998. No obvious Swiss needle cast damage was mapped during the Cascade range survey. Although some areas of slightly yellow Douglas-fir were observed, none of the areas showed symptoms of severe Swiss needle cast damage.

The Coast Range survey covered about 2.9 million acres of forest. A total of 295,000 acres of Douglas-fir forest had obvious symptoms of

Swiss needle cast; 260,000 acres north of Florence, and 35,000 acres south of Florence. This is an increase of 122,000 acres over the 1998 survey (table 1, figure 5). Much of the increase in the number of acres with symptoms occurred in the eastern parts of Lincoln and Tillamook counties. The easternmost area with obvious SNC symptoms was almost 30 miles inland from the coast, which is an increase over previous surveys .

Some year-to-year variation in survey results is due to timing of the

flights. Because symptoms develop rapidly during April and May, later surveys detect more areas than those conducted earlier. This was very evident in 1997 when a few extra days of surveying at the time of bud break increased the estimate of acres with symptoms from 145,000 to 393,000. This happened to some degree in 1999, when about half of the survey was completed between April 21 and April 30, and the other half on May 21 and 22. However, the unseasonably cool spring temperatures in 1999 delayed bud-burst by about 2 to 3 weeks compared to previous years, so even though much of the survey was completed in late May, it was well within the target surveying window. Had the survey been flown later (in early June), we undoubtedly would have mapped even more acres of heavy discoloration.

After four years of surveys, we have little doubt that Swiss needle cast symptoms continue to intensify, especially in the northern half of the Coast range. We mapped it further inland, and the degree of discoloration has become more pronounced each year. It is also clear that even though the disease occurs throughout the Coast Range, most areas with symptoms that can be detected from the air are within about 18 miles of the coast.

These estimates still must be considered conservative because they represent only those areas where disease symptoms have developed enough to be visible from the air. Permanent monitoring plots and ground checks have shown that Swiss needle cast occurs throughout the survey area, but that symptoms

often were not developed enough to enable aerial detection. Factors other than the presence of the pathogen strongly affect disease development, and these factors remain poorly understood. The shape and distribution of survey polygons and the observer's comments suggest that symptoms are most obvious on southerly aspects and on exposed ridge tops, indicating a strong environmental interaction.

Brown needle tips were observed commonly during ground checks dur-

ing 1999. Cold temperatures during the week before Christmas in 1998 may have contributed to some of the discoloration observed during the aerial survey. The brownish discoloration was restricted to Douglas-fir, and even if it was partly due to low temperature injury, Swiss needle cast was an important factor as well. The upper crowns of many trees were barren of needles, apparently battered by the unusually frequent high-winds during the winter of 1998-1999.

Acknowledgments:

The survey was conducted by the Oregon Department of Forestry Insect & Disease and Air Operations sections, and was funded by the USDA Forest Service Forest Health Monitoring Program and the Oregon Department of Forestry. Jack Prukop (ODF) piloted the plane. Mike McWilliams (ODF), Keith Sprengel (US Forest Service), and Dave Overhulser (ODF) were the aerial observers.

GENETICS OF SWISS NEEDLE CAST TOLERANCE - EARLY SCREENING AND FIELD RESULTS

Randy Johnson and Fatih Temel

Four series of early screening trials were established this year. The plug seedlings used in the establishment were grown at the Dorena Tree Improvement Center and cold stored over the winter at The Timber Company's Cottage Grove facility. Two field trials were established on Simpson lands near Toledo and Pleasant Valley Oregon. Two artificial inoculation trials were conducted at the Dorena Tree Improvement Center near Cottage Grove using the mist chamber normally used for inoculating white pine with blister rust. Each trial contains 153 families collected from the Hebo, Alsea, and Waldport districts of the Siuslaw National Forest. Next spring/summer these trials will be assessed for foliage health and possibly other SNC traits. This data will be used to examine genetic variation and to see if early data are correlated with older field data from the same families.

The same 153 families are in raised beds at the Forest Science Lab in Corvallis where growth and bud burst data are being collected for a genecology study. Also at Corvallis is a smaller study examining the effect of defoliation on a subset of 20 families from the Hebo district. The same 20 families were established in a small plot on Juno Hill with Oregon Department of Forestry assistance.

Additional field data (DBH) were collected this year at six progeny test sites in the Hebo District and from three progeny test sites in the Nahalem breeding program of the Northwest Tree Improvement Cooperative. Data were used to examine the impact foliage scores on subsequent basal area growth. Foliage scores assessed in 1995/96 were: foliage color (1 = yellow, 2 = green, 3 = dark green), crown density (1 = sparse foliage to 6 = dense foliage), and needle retention (0 = < 10% to 9 = > 90% of second-year foliage). Basal area increment was calculated directly with the Nehalem data and but had to be estimated for the Hebo data because only height data were available from the 1995 assessment. DBH at age 10 for the Hebo trials was estimated with an equation developed from the age-11 Nehalem data. Both sets of data demonstrated that foliage scores

were highly correlated with subsequent basal area growth; families with good foliage scores had good basal area growth. Genetic correlations (Table 1) demonstrate that the genes controlling foliage health also impact basal area growth. The results were encouraging because previous analyses done on the age-10 Hebo data showed little correlation between height and foliage scores measured in the same year.

Foliage data from the 1996 and 1998 assessments of 55 families from the Hebo district were examined in relation to geographic and climatic conditions at the parent tree location. Distribution of parent trees ranged from 44E52'N to 45E18'N latitude and from 123E39'W to 123E57'W longitude, with 175 to 480m elevation range. Geographical data on parent tree locations (distance to the Pacific Ocean, latitude, longitude, elevation, aspect and slope) were obtained from

Table 1. Genetic correlation of age-10 or -11 growth and foliage variables at 5 sites with subsequent 3-year basal area growth.

	NWTIC-Nehalem			USFS-Hebo	
	Coal Creek	Acey Creek	Slick Rock	N. Gordy	Salal Dept.
DBH	0.93	0.93	0.95	n/a	n/a
Height	0.83	0.91	0.61	0.12	0.11
Crown Density	0.90	0.79	0.35	0.39	0.63
Color	0.53	0.0	0.70	0.48	0.68
Retention	0.49	-0.03	0.27	0.62	0.39

Geographic Information System. Climate data (mean monthly maximum and minimum temperatures, mean monthly precipitation and snowfall) were obtained using PRISM (Parameter-elevation Regressions on Independent Slopes Model). Regression was used to investigate the relationship between parent tree location and climate, and its resistance to

SNC. The only foliage variable showing a relationship with environment was crown density, which showed a pattern of better crown density as parent tree location got closer to the coast (figure 1).

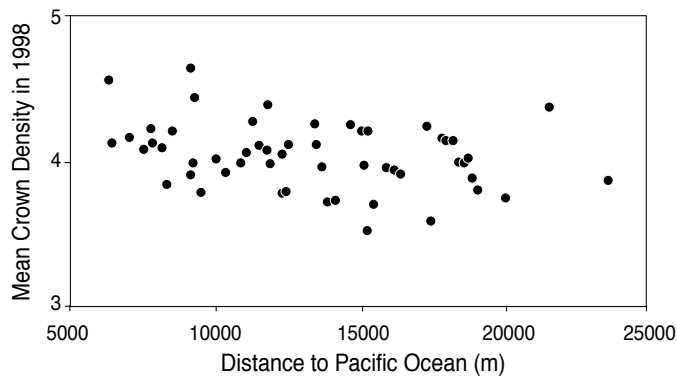


Figure 1. Relation between family crown density scores and distance to the ocean of the parent tree location.

IMPACTS OF SWISS NEEDLE CAST ON THE PHYSIOLOGY OF DOUGLAS-FIR NEEDLES

Daniel Manter and Kathleen Kavanagh

Cooperators: Barbara Bond, Greg Filip, Pablo Rosso, Jeffrey Stone, and Wendy Sutton

Our group is continuing its efforts to understand the physiological impacts of Swiss needle cast (SNC) on the physiology of Douglas-fir needles. Collaborative efforts between several OSU laboratories have been directed toward the following goals.

- I. Develop and compare methods for quantifying *Phaeocryptopus gaeumannii* infection, i.e., biomass index (ergosterol) and reproductive structures (pseudothecia counts).
- II. Determine the mechanism of SNC impact on Douglas-fir needle physiology (i.e., gas exchange).
- III. Determine potential interactions between SNC infected foliage and environment.

Goal I.

Introduction

Typically, SNC infection is measured by visible symptoms (needle retention and chlorosis) and/or pseudothecia production. How such measures correlate with one another, climatic factors, other aspects of fungal growth or their relation to host physiology is not known. Depending

on the mechanism by which SNC is influencing host physiology it may be preferable to quantify SNC by other methods. For example, a measure of fungal biomass may correlate better to fungal enzyme production and any fungal enzymatic control of host physiology, whereas pseudothecia production may best correlate with host function as determined by stomatal blocking and reduced CO₂ uptake.

Methods

Site selection - Three sites with varying levels of SNC infection were chosen for study. The most heavily infected site is located on the Siuslaw NF in Beaver, OR (i.e., Beaver), the medium infection site is located on the Siuslaw NF in Hebo, OR (i.e., Hebo), and the low infection site is located in the MacDonald Forest in Corvallis (i.e., Mac). At each site, 12 trees from a north and south-facing slope were selected, scored for visible symptoms of SNC infection and tagged for future analysis. Due to the uniform presence of *Phaeocryptopus gaeumannii* (PG) on these sites, six of the 12 trees were tagged as "controls" and sprayed with Bravo 720 (rate = 66 ml / gal., applied until run-off). Fungicide applications were conducted in 1998 and 1999 prior to

bud break, at bud break (90% trees had broken bud), and 1 month following bud break. All analyses from these trees (current section and Goal III) were limited to southern-aspect branches from the lower half of the tree canopy.

Pseudothecia Counts - the presence of *P. gaeumannii* was determined by visual estimates of fungal fruiting bodies or pseudothecia emerging from stomata on all needles used in gas exchange assessments. The average percent of needle stomata occluded with pseudothecia (i.e., "pseudothecia counts") was calculated from three sub-samples on each needle. Each sub-sample, one from each longitudinal third of the needle, was conducted by visually counting the number of pseudothecia emerging from 100 consecutive stomata from the first complete row closest to the needle mid-rib.

Ergosterol Content - ca. 25 needles from each age class were analyzed for the presence of ergosterol. Ergosterol is a cell membrane sterol found in most fungi, but not plant tissue, which may serve as an index of total fungal biomass present (e.g., Gessner et al. 1991). Analysis of ergosterol was estimated by HPLC (high performance liquid chromatography) with a LiChrosphere RP-18

column heated to 40°C and 100 % methanol as the solvent system. Elution of ergosterol occurred at 10.5-11.5 min and quantification of the eluent was assessed by comparison to known concentrations of pure ergosterol. Values reported are expressed as μg ergosterol g^{-1} dry weight of needles.

Results & Discussion

In general, ergosterol content showed a positive-linear relationship with pseudothecia counts ($R^2 = 0.539$, $p < 0.001$), and either measure may provide a useful estimate of infection at larger scales (i.e., for both ergosterol and pseudothecia counts Beaver > Hebo > Mac) (Figs. 1-3). However, within any given site the relationship between ergosterol content and pseudothecia counts may vary depending upon the sample date (Figs. 2-3). For example, during the winter survey, all southern slopes exhibited a higher pseudothecia count per unit ergosterol. We also observed, that the southern slopes tend to produce pseudothecia earlier in the season compared to their northern counterparts (Fig. 3). Similar results were observed in all needle age classes measured (data not shown).

Differences in the pseudothecia : ergosterol (biomass) ratios between slopes of the same site deserve further attention. In particular, climatic differences among sites and their impact on fungal growth should be investigated. We have been monitoring climatic data, at each site, and in general south slopes reach higher temperatures, lower humidities, and

higher light levels; any, or all of which, may induce earlier production of pseudothecia on the south slopes. Finally, the earlier development of pseudothecia on southern slopes, along with climatic differences (and its influence on needle physiology, see goal III) may explain the frequently observed pattern of higher symptom development on south slopes. As shown in goal II, pseudothecia development causes a decline in the ability of CO_2 to enter needles; and also a decline in the needles' ability to convert CO_2 to the carbon building blocks necessary for growth. As a result, the earlier development of pseudothecia on south slopes reduces the growth capacity by impacting these processes several months before that of their north slope counterparts.

Goal II.

Introduction

Approximately, 40 % of a plant's dry mass consists of carbon, fixed in photosynthesis (Lambers et al. 1998). Carbon is a vital component for growth and survival of all plants, and changes in its availability or rate of

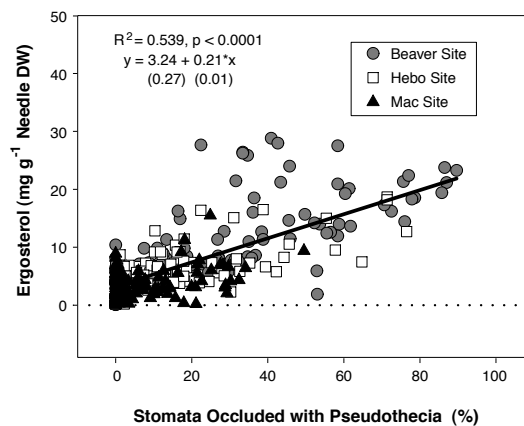


Figure 1. Ergosterol Content vs. Pseudothecia Counts, Sampled on 12/1998 & 5/1999.

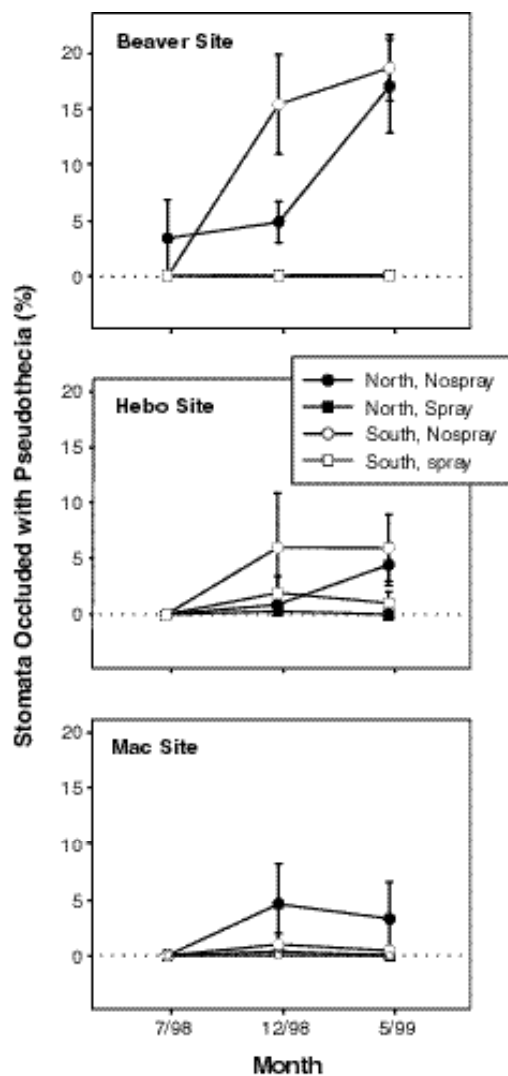


Figure 2. Development of Ergosterol Content, 1998 Needles. Each symbol represents the mean of six trees; error bars are the standard error of the mean.

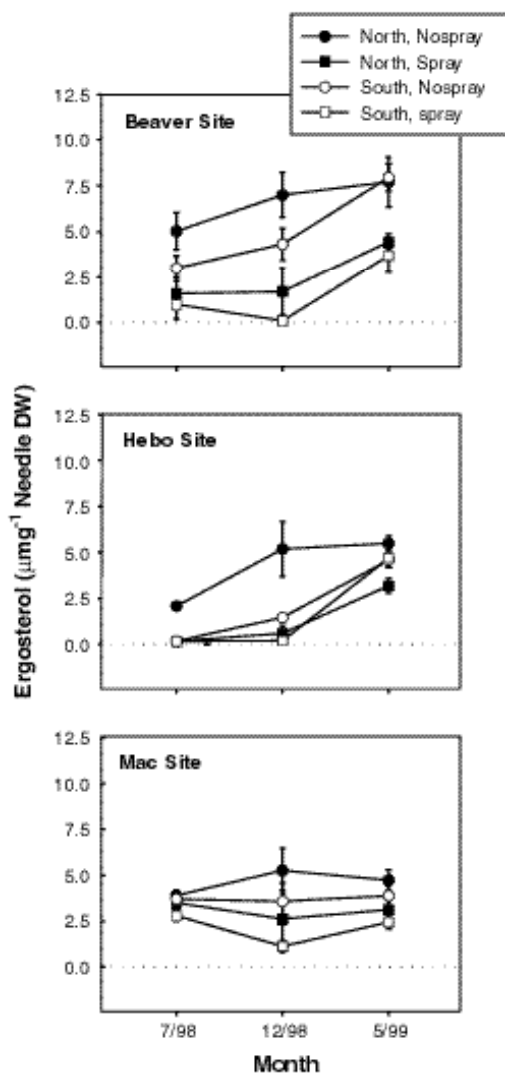


Figure 3. Development of *Pseudothecia*, 1998 Needles. Each symbol represents the mean of six trees; error bars are the standard error of the mean.

fixation will negatively affect both processes.

Parasitic fungi extract the nutrients necessary for their survival from the plant tissues that they invade; in some cases, reducing host growth and vigor. In addition to direct absorption of nutrients, fungi may also reduce host photosynthate production (e.g., Suti and Sinclair 1991, Scholes 1992) through a variety of biochemical and/or structural means. Biochemical processes include changes in host processes (e.g., electron transfer chain, Montalbini,

Buchanan and Hutcheson 1981) and enzymes (e.g., rubisco, Walters and Ayres 1984, Gordon and Duniway 1982) or the introduction of fungal enzymes, which regulate host physiology abnormally (e.g., invertase, Tang et al. 1996). Structural means include the loss of functional host tissue (e.g., necrosis) and physical blocking of intercellular spaces or stomata (Ayres 1976, 1981, Suti and Sinclair 1991). The latter has been suggested to be the major initial impact of *P. gaeumannii* due to the presence of fungal fruiting bodies (i.e., pseudothecia) that emerge from needle stomata.

The hypothesis that *P. gaeumannii* impacts Douglas fir needle gas exchange mainly through blockage of stomata is largely based on circumstantial evidence. For example, microscopic work has shown that internal colonization of *P. gaeumannii* is limited to intercellular spaces with no obvious development of haustoria, penetration or necrosis of needle tissue (Capitano 1999), and pseudothecia initials can be observed densely packed into needle stomata (Stone and Carroll 1986). Based on these observations and preliminary field data (Manter, unpubl.) showing reduced gas exchange in Douglas-fir stands infected with *P. gaeumannii*, we conducted the following studies in order to quantify the impacts of *P. gaeumannii* infection on Douglas-fir needle physiology, especially

on factors limiting the rate of CO₂ assimilation, and to determine the mechanism of impact.

Methods

Plant Material and Inoculations
 - All measurements were conducted on potted two-year old Douglas-fir seedlings (DL Phipps nursery, Elkton, OR). In May 1998, 50 seedlings were inoculated by placing seedlings in a chamber with an overhead misting system. Mist was applied for 15 sec every 60 min from 8 am to 8 pm, and 15 sec every 120 min from 8 pm to 8 am. An inoculum source was provided by branches infected with *P. gaeumannii*, collected from Sour Grass Summit, OR, suspended over the target seedlings. Inoculum levels were monitored by weekly spore counts, on glass slides suspended over the target seedlings, within the inoculation chamber (ca. 1 spore mm⁻²). After a two-week inoculation period, seedlings were incubated for two weeks in a greenhouse maintained at 70°F under ambient light and humidity conditions. Immediately following the incubation period, a second round of inoculation (using newly-collected inoculum-source branches) and incubation treatments were applied. Following treatments, seedlings were maintained in an outdoor cold frame at Oregon State University, Corvallis until future measurements. For each step of the inoculation procedure (i.e., inoculation, incubation and storage), seedling position was varied. To create uninfected control branches, two branches on each seedling were covered with bags ("D"-bag w/ polypropylene window,

Northwest Mycological Consultants, Corvallis, OR) during the inoculation and incubation periods. The bagging of branches was successful in reducing overall infection; however, some infection was eventually detected.

Gas Exchange Measurements - Using a LiCOR 6400 portable infrared gas exchange system (LiCor, Lincoln, NE) response curves of CO₂ assimilation (A/C_i curve, i.e., CO₂ assimilation rate versus calculated internal CO₂ concentration) were measured. CO₂ assimilation and its major biochemical limitations are described below. During measurements, cuvette conditions were maintained at or near optimum conditions: PAR 2000 mmol m⁻² s⁻¹, temperature 25 °C, [H₂O vapor] (18 mmol mol air⁻¹, [CO₂] 40 Pa, and flow rate 100 mmol m⁻² s⁻¹, unless otherwise noted. A/C_i curves were measured by varying the cuvette CO₂ concentration, allowing equilibration to a steady state (cuvette [CO₂] coefficient of variation < 2%), and logging measurements every 10 seconds for 1 minute. CO₂ was varied in the following order: 40, 30, 20, 60, 80, 100, 120, 160 and 200 Pa.

Gas exchange was measured each month from November 1998 to June 1999 using one bagged (i.e., control) and one unbagged (i.e., infected) branch from two-six randomly selected seedlings (i.e., 28 seedlings total). Within selected branches, samples of ca. 15 needles (1998 cohort of needles) were randomly selected for measurement (November-February). Beginning in March, low levels of infection were observed in most infected branches and some control branches. As

a result, control branch needles were preferentially selected based on the absence of pseudothecia, and infected branch needles were selected based on the presence of pseudothecia.

A/C_i curves were used to estimate some of the major limitations to net uptake of carbon into a plant following methods described by Farquhar et al. (1980), Sharkey (1985), Harley and Sharkey (1991) and Harley et al. (1992). All A/C_i curve calculations are in Appendix I, and a list of abbreviations and parameters can be found in Appendices II-IV.

A Brief Summary – Limitations to CO₂ Assimilation

The rate of CO₂ assimilation is the net uptake of CO₂ into plant tissues, which is ultimately used as the building blocks for tree growth and survival. Two types of processes determine the net rate of CO₂ assimilation or the amount of carbon available to the growing plant. They are CO₂ absorption (photosynthesis) and CO₂ evolution (photorespiration and respiration). The CO₂ evolution processes are necessary functions performed by a plant to provide energy and maintain proper physiological function; however, they do so at a cost of reducing the amount of carbon available to the plant for growth, etc. The CO₂ absorption process or photosynthesis is the process by which plants acquire carbon and capture energy from the sun to carry out cell metabolism. Photosynthesis is a cyclical process, which results

in the addition of atmospheric CO₂ to the 5-carbon-sugar ribulose 1,5-bisphosphate (RuBP), giving rise to the carbon building blocks necessary for plant survival. The rate of photosynthesis is determined by the concentrations within plant tissues of any of the following (also see Fig. A).

- (1) CO₂ – this is the source of all carbon to be used for plant growth.
- (2) Rubisco – the enzyme responsible for capturing CO₂ and combining it with its acceptor, RuBP, forming PGA. This is the first step in converting CO₂ into a usable form (i.e., the carbon building blocks). The rate of photosynthesis limited by rubisco is abbreviated as W_c.
- (3) Chemical Energy (ATP and NADH) –energy is required to convert PGA into the exported product, triose-P, some of which is exported and converted to sucrose. Sucrose is a mobile form of carbon that is transported to others plant tissues and used for growth and survival. The rate of photosynthesis limited by chemical energy is abbreviated as W_j.
- (4) Inorganic phosphate (P_i) – each exported triose-P molecule generated by photosynthesis temporarily removes phosphate which must be replenished. The rate of photosynthesis limited by inorganic phosphate is abbreviated as W_p.

Limitation 1 is commonly referred to as “stomatal or supply

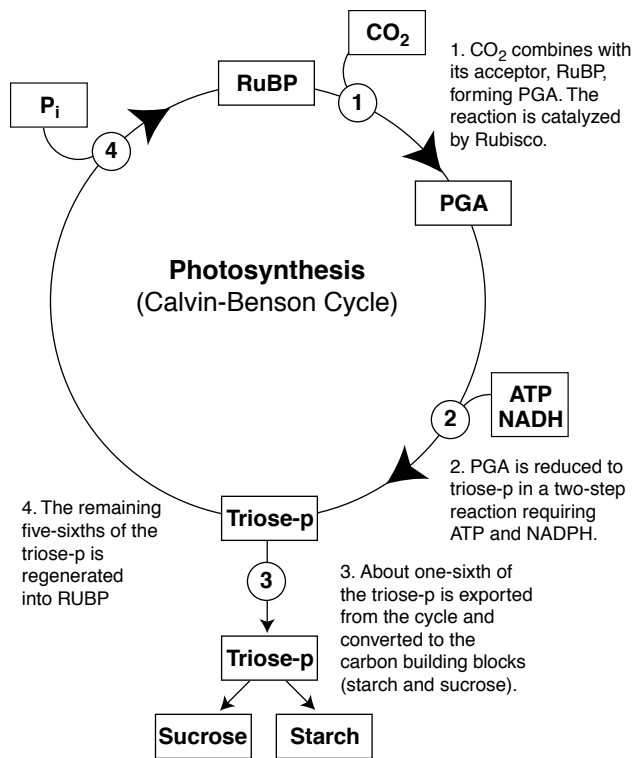


Figure A. Major Steps and Limitations of Photosynthesis.

limitations” to photosynthesis. This is because the amount of CO_2 available to the actively photosynthesizing leaf must diffuse through needle stomata (small openings on the needle surface). Limitations 2-4 are commonly referred to as “biochemical or demand limitations” to photosynthesis. And the response of photosynthetic rate to CO_2 concentration (A/C_i curve) is the principle tool to analyze the various demand components for CO_2 . Figure B shows the relationship between a typically observed A/C_i curve (solid line) and the rates of photosynthesis as determined by limitations 2-4 over a range of CO_2 concentrations (W_c ,

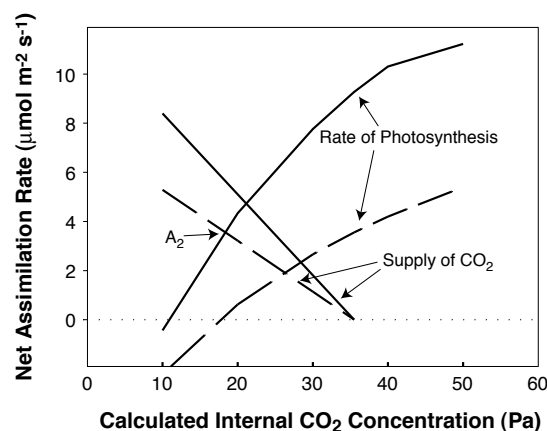


Figure B. Components of an A/C_i Curve.

W_j and W_p lines). By measuring an A/C_i curve we can estimate the relative contribution of each demand limitation on photosynthesis. This is achieved by employing regression techniques and previously defined mathematical equations relating each limitation to CO_2 concentration (see Appendix I).

Two important points regarding A/C_i curves. First, you will notice that as leaf CO_2 concentration increases, photosynthesis increases. Second, depending upon the CO_2 concentration within a leaf, the rate of photosynthesis will be determined by the factor that most limits photosynthesis. For example, at an internal CO_2 concentration of 30 Pa, the observed rate of photosynthesis will be most limited by rubisco (W_c)

or ca. $10 \text{ mmol m}^{-2} \text{ s}^{-1}$.

Finally, because the rate of photosynthesis as defined by any one of the three limitations above, (2-4) is dependent upon internal CO_2 concentration (which constantly changes); all comparisons between treatments are made at the maximum rate theoretically possible. Thus, for the rate of photosynthesis limited by rubisco (W_c), the maximum is $V_{c\text{max}}$; the rate of photosynthesis limited by chemical energy (W_j), the max is J_{max} ; and the rate of photosynthesis limited by inorganic phosphate concentration (W_p), the maximum is TPU.

Fungal Infection - See goal I.

Imaging Chlorophyll Fluorescence - In April 1999, a sub-sample of needles (1998 cohort) from the six seedlings selected for the April A/C_i curve analysis were also analyzed for chlorophyll fluorescence. Following gas exchange, sample branches (one infected and one control branch per seedling) were removed, re-cut under water, and then dark-adapted for 1 hr. After the dark treatment, 4-5 needles were removed from each branch, cut longitudinally in half, and placed side-by-side on index cards creating two samples per branch (i.e., one sample with 4-5 needle tip-halves, and one with 4-5 needle petiole-halves). For each sample, a 1 cm^2 region was measured for chlorophyll fluorescence. For each 1-cm^2 sample, a two-dimensional image of fluorescence was created using an imaging fluorometer that measures

time-dependent fluorescence from an array of 31,680 positions per sample. A description of the imaging fluorometer used can be found in Ning et al. (1995).

For each position, an estimate of quantum yield (Y') was calculated from measurements of F_m (the maximum fluorescence signal), F_s (the low, steady-state level of fluorescence 105 sec after illumination), and F_{dark} (the background level of fluorescence); where $Y' = (F_m - F_s) / (F_m - F_{\text{dark}})$. A more detailed explanation of the parameters and equations can be found in Ning et al. (1995) and Bowyer et al. (1998).

A Brief Summary - Chlorophyll Fluorescence

Light energy is absorbed by chlorophyll causing an electron to rise into a higher orbital. Up to 20 % of this energy may be transferred to the photosynthetic machinery in order to create the chemical energy needed to drive photosynthesis. The remainder, however, is given off as heat or fluorescence as the excited electron returns to its unexcited state. The downstream flow of energy (i.e., electrons) to the photosynthetic machinery is a function of both the chemical energy generating systems (ATP and NADPH production) and the Calvin-Benson cycles; and any perturbations in these systems may be observed by changes in the amount and timing of fluorescence.

The typical pattern of fluorescence of a dark-adapted leaf when illuminated with light can be defined by the following parameters.

F_m : The level of fluorescence as the electron acceptors of the photosystems become fully reduced (saturated with electrons). Downstream processes are slower to respond to the light stimulus; thus, fluorescence reaches a maximum at this point because the electrons essentially have nowhere to go but to decay back to the ground state.

F_s : The level of fluorescence after CO_2 assimilation (Calvin-Benson cycle) begins; increasing the demand for chemical energy production (ATP and NADPH).

F_{dark} : The background level of fluorescence detected by the fluorometer.

Rubisco Activity - In order to confirm A/C_i estimates of rubisco activity (i.e., V_{cmax} , see Appendix I), spectrophotometric assays of initial and total rubisco activity (R_i and R_T , respectively) were measured from a random sample of ten seedlings, as outlined in Cheng and Fuchigami (in preparation). From each seedling, two samples (one infected and one control branch) of six needles (1998 cohort) were analyzed and the percent of rubisco activated (i.e., rubisco activation, R_{ACT}) was calculated as $R_i / R_T * 100$.

In order to test the hypothesis that reduced stomatal conductance causes a decline in rubisco activity, we also measured rubisco activity on needles that were artificially induced to have lower stomatal conductance. To achieve this we covered the abaxial surface of selected needles (1999 needles with no visible pseudothe-

cia only) with one of three different amounts of petroleum jelly (0, 50 and 100 % of projected leaf area). Each treatment level was applied to one secondary lateral branch on each of six randomly selected seedlings. Pre (< 30 min) and post (one hour) treatment stomatal conductance was measured using a LiCor 6200 under natural conditions, and 1 day after treatment initial and total rubisco activity was measured on needles exposed to full sunlight.

Results

Seasonal Variation -The rate of net CO_2 assimilation differed seasonally in both infected and uninfected needles (Figure 4. A.) Net assimilation declined by ca. 40 % between December and January, associated with a reduction in stomatal conductance of ca. 60 % (Figure 4. B.). Assimilation rates remained constant at these reduced levels until March and the onset of bud-break. In March, assimilation declined another ca. 20 % for both infected and uninfected needles. At this time, respiration rates also increased ca. 50 % (e.g., $R_{\text{day}} \approx 4$ [March] and $R_{\text{day}} \approx 2 \mu\text{mol CO}_2 \text{ m}^{-2} \text{ s}^{-1}$ [October-February]) (Figure 4. C.). By June, assimilation rates of uninfected needles recovered to 87 % of pre-winter rates and conductance ca. 80 %. In infected needles, however, no recovery in assimilation rates and conductance were observed; in fact, assimilation and conductance were at their lowest observed values, i.e. 26 and 15 % of the pre-winter values, respectively.

Seasonal changes in rubisco activity mirrored changes in stomatal conductance (Figures 4.B. & 5.A.).

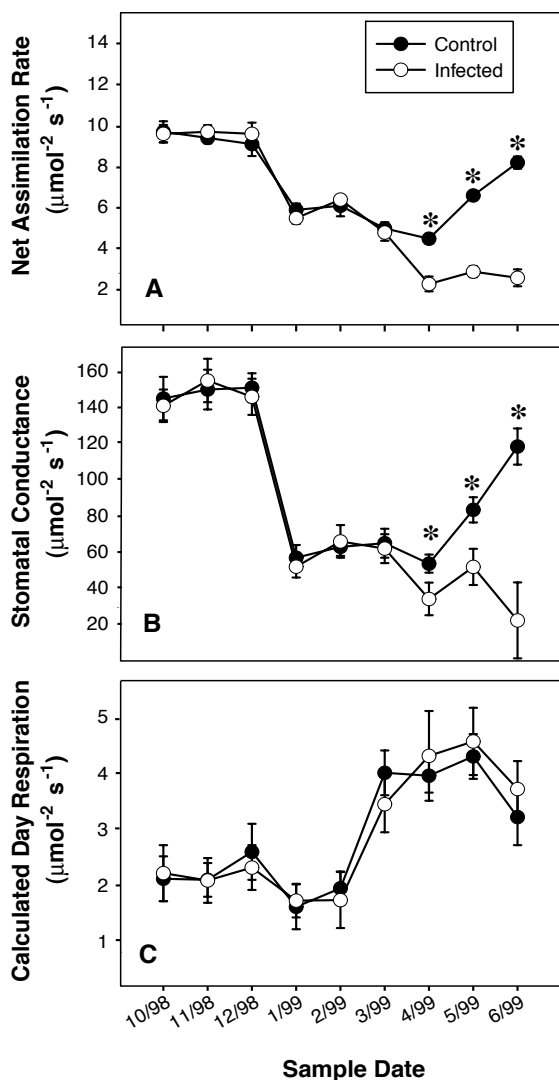


Figure 4. Seasonal Patterns of Needle Physiology (Gas Exchange) in Two-year-old Douglas-fir Seedlings Infected with *Phaeocryptopus gaeumannii*. For each sample date treatment differences were tested using a paired t-test, * denotes $p < 0.05$. Net assimilation rate was measured at PAR 2000 $\text{mmol m}^{-2} \text{s}^{-1}$, temperature 25 °C, $[\text{H}_2\text{O vapor}]$ (18 mmol mol air^{-1} , $[\text{CO}_2]$ 40 Pa, and flow rate 100 $\text{mmol m}^{-2} \text{s}^{-1}$. Stomatal conductance is the average rate of conductance measured during the entire A/C_i curve. Calculations of Day Respiration can be found in Appendix I.

V_{cmax} declined ca. 22 % between December and January (Figure 5.A) as compared to the 60 % decline in stomatal conductance (Figure 4.B). V_{cmax} remained depressed during the winter until recovery in the spring, which is also when stomatal conductance recovered. By May,

V_{cmax} recovered to pre-winter values (e.g., $V_{\text{cmax}} = 37.55$ [May] and $V_{\text{cmax}} = 37.53$ $\text{mmol CO}_2 \text{ m}^{-2} \text{ s}^{-1}$ [October-December]). Similar to rubisco activity, J_{max} showed some seasonal variation, declining in the winter and recovering during the spring months (Figure 5.B.). However, J_{max} proved to be quite variable, and especially during periods of low stomatal conductance (i.e., infected needles following pseudothecia development) not determinable at the CO_2 concentrations employed.

Fungal Impacts - In the spring reductions in net assimilation were associated with development of pseudothecia. For example, in April, when *P. gaeumannii* infection increased to 18.9 % of the stomata bearing pseudothecia, net assimilation rates in ambient conditions (i.e., PAR ca. 2000 $\text{mmol m}^{-2} \text{s}^{-1}$, $[\text{CO}_2]$ 35.5 Pa, $[\text{H}_2\text{O vapor}]$ ca. 18 mmol mol

air) declined by 50 %, compared to uninfected needles (Figures 4.A. & 6). *P. gaeumannii* internal and external hyphal colonization and biomass increases gradually following inoculation (Capitano 1999, Manter unpubl.); however, the first sign of physiological impact occurred

10 months after inoculation, or only after pseudothecia emerged from > 5 % of the needle stomata, i.e., March sample date (Figures 4-6).

At the onset of fungal impact, several changes in the physiology of infected needles were observed: stomatal conductance was reduced by 37 %, net assimilation was reduced by 50 %, and rubisco activity was reduced by 40 % compared with control branches (Table 1). Impacts on J_{max} due to fungal infection could not be determined in April and May; during these samples, A/C_i curves for the infected branches were entirely limited by rubisco activation or W_c .

The relationship between fungal infection and stomatal conductance was determined by a regression between the percent decline in stomatal conductance ($(g_{\text{sw,control}} - g_{\text{sw,infected}}) / g_{\text{sw,control}} * 100$) and pseudothecia presence (infected - control) using the observations from each seedling in April - June (Figure 7). A strong positive-linear relationship between pseudothecia presence and the percent decline in stomatal conductance was detected (Adj. $R^2 = 0.927$, $p < 0.0001$).

In addition to declines in stomatal conductance, some of the other measures of needle physiology were reduced following pseudothecia production, i.e., net assimilation and V_{max} . Analysis of the average A/C_i curve (calculated by inputting the mean values of V_{cmax} , J_{max} and R_{day} [from Table 1] in equation 2) from all six seedlings measured in April (Figure 8) suggests that the limitations to ambient net assimilation rates are caused by approximately equal amounts of biochemical and sto-

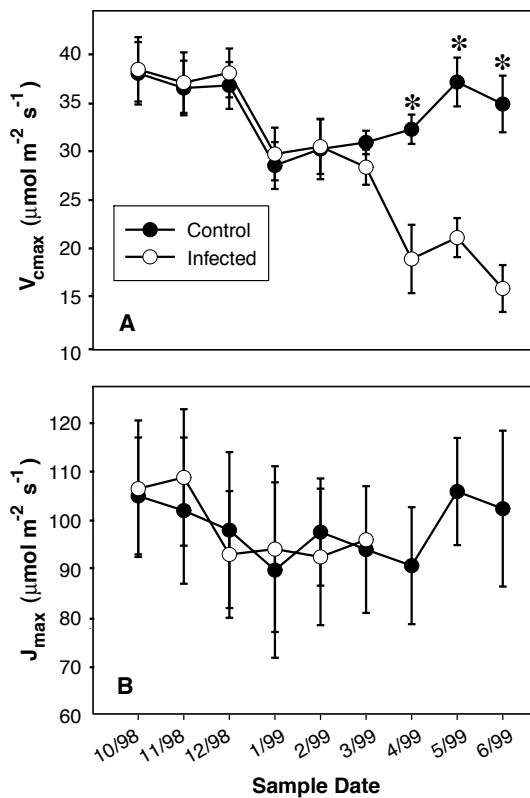


Figure 5. Seasonal Patterns of Biochemical Limitations to Gas Exchange in Two-year-old Douglas-fir Seedlings Infected with *Phaeocryptopus gaumannii*. For each sample date treatment differences were tested using a paired *t*-test, * denotes $p < 0.05$. Calculation of V_{cmax} and J_{max} can be found in Appendix 1.

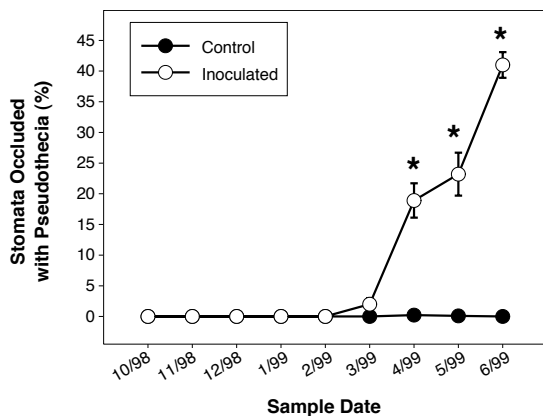


Figure 6. Seasonal Patterns of *Phaeocryptopus gaumannii* Infection in Inoculated Two-year-old Douglas-fir Seedlings. For each sample date treatment differences were tested using a paired *t*-test, * denotes $p < 0.05$.

Table 1. Infection Level And A/C_i Curve Parameters From Six Two-year-old Douglas-fir Seedlings Infected With *Phaeocryptopus gaumannii*, April 1999.

	Stomata Occluded with Pseudothecia (%) ¹	Stomatal Conductance ($\mu\text{mol H}_2\text{O m}^{-2} \text{s}^{-1}$)	Ambient Assimilation Rate ($\mu\text{mol CO}_2 \text{m}^{-2} \text{s}^{-1}$)	V_{cmax} ($\mu\text{mol CO}_2 \text{m}^{-2} \text{s}^{-1}$)	Day Respiration ($\text{mmol CO}_2 \text{m}^{-2} \text{s}^{-1}$)
Branch ²	Mean (SE)	Mean (SE)	Mean (SE)	Mean (SE)	Mean (SE)
Infected Branch	18.91 (2.83)	33.18 (5.02)	2.20 (0.24)	19.43 (1.52)	4.29 (0.30)
Control Branch	0.23 (0.14)	52.70 (9.32)	4.40 (0.36)	32.71 (3.55)	3.94 (0.76)
p-value ³	0.001	0.021	0.001	0.006	0.665

¹“Stomata Occluded with Pseudothecia” is the percent of all stomata occluded with pseudothecia (see “Methods” for further explanation). Stomatal conductance is the average value over the entire A/C_i curve measurement. Ambient assimilation rates are single point measurements of assimilation at $[\text{CO}_2]$ ca. 35.5 Pa, PAR ca. 2000 $\text{mmol m}^{-2} \text{s}^{-1}$, $[\text{H}_2\text{O vapor}] > 18 \text{ mmol mol}^{-1}$ air. V_{cmax} and respiration are derived from A/C_i curves as described in the text.

² One control and one infected branch from each of six two-year-old Douglas-fir seedlings were measured.

³p-value was calculated using a paired *t*-test between control and infected branches for the six seedlings sampled.

matal limitations. As suggested by Jones (1985) and based on the equations presented in Appendix 1, any observed assimilation rate, at equilibrium, will be determined by the intersection (“operating point”) of the demand for CO_2 (Appendix 1, equation 2) and the supply of CO_2 (Appendix I, equation 4). When this analysis is applied to our April measurements, predicted net assimilation rates at ambient CO_2 are ca. 4.7 and 1.9 $\text{mmol CO}_2 \text{m}^{-2} \text{s}^{-1}$ for control and infected needles, respectively. These rates

are similar to the measured rates of 4.4 and 2.2 $\text{mmol CO}_2 \text{m}^{-2} \text{s}^{-1}$, respectively (Table 1).

The assertion, that approximately equal biochemical and stomatal limitations to ambient net assimilation, is based on the following logic. If we assume stomatal conductance impacts infected needles first (see discussion below), then the path of assimilation reduction from uninfected to infected needles will proceed from $A_{control} \rightarrow A_2 \rightarrow A_{infected}$ (Figure 8). The first step represents a shift in the slope of the supply curve or a decline in stomatal conductance, resulting in ca. 26 % of the decline in our infected seedlings measured in April. The second step involves a shift in the demand curve, which is due to a decrease in V_{cmax}

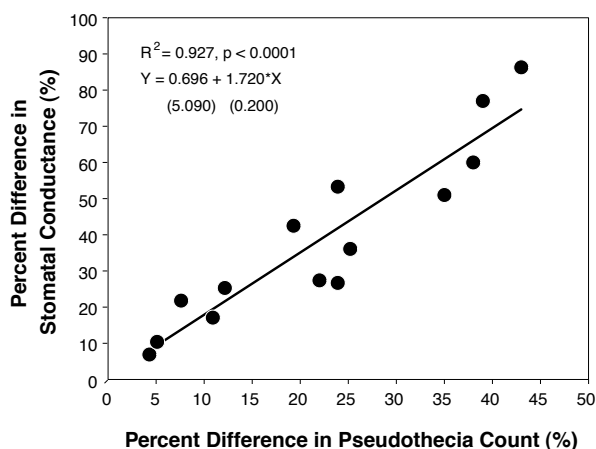


Figure 7. Relationship between Stomatal Conductance and *Phaeocryptopus gaeumannii* Pseudothecia in Two-year-old Douglas-fir Seedlings. Each observation represents differences between sample branches from each of the seedlings measured during the April–June sample dates. Percent Decline in Stomatal Conductance = $(g_{sw_control} - g_{sw_infected}) / g_{sw_control} * 100$. Percent Difference in Pseudothecia Count = infected - control.

rates in infected foliage. This change represents ca. 34 % or slightly more than half of the total decline in net ambient assimilation rate due to infection.

Rubisco Activity - Similar to the A/C_i curve analysis, spectrophotometric assays of rubisco activity also showed that needles infected with *P. gaeumannii* had a reduced amount of activated rubisco as compared to control needles. However, no difference in the total rubisco activity was detected (Table 2).

Spectrophotometric assays of rubisco activity using needles treated with petroleum jelly showed that rubisco activity is lower in treated needles (i.e., lower stomatal conductance). In these seedlings, pre-treatment stomatal conductance did not significantly differ between needle samples (stomatal conductance was 142.7 ± 9.07 , 143.7 ± 12.7 , and 139.5 ± 7.2 $\text{mmol m}^{-2} \text{s}^{-1}$ for 0, 50

and 100 % treatments, respectively); however, stomatal conductance was significantly reduced following treatment with petroleum jelly (stomatal conductance was 69.8 ± 8.67 , 48.86 ± 7.4 and 27.92 ± 4.5 for 0, 50 and 100 % treatments, respectively). A strong linear relationship (Adj. $R^2 = 0.736$, $p < 0.0001$) exists between the percent decline in stomatal conductance following treatment ($(g_{sw_treatment_0} - g_{sw_treatment_i}) / g_{sw_treatment_0} * 100$, where i is either the 50 or 100 % treatment level) versus the percent decline in rubisco activation ($(R_{ACT_treatment_0} - R_{ACT_treatment_i}) / R_{ACT_treatment_0}$, where i is either the 50 or 100 % treatment level) (Fig. 9.A.). A similar relationship between the percent decline in stomatal conductance due to *P. gaeumannii* infection ($(g_{sw_control} - g_{sw_infected}) / g_{sw_control} * 100$) versus the percent decline in rubisco activity ($(V_{cmax_control} - V_{cmax_infected}) / V_{cmax_control} * 100$) was obtained

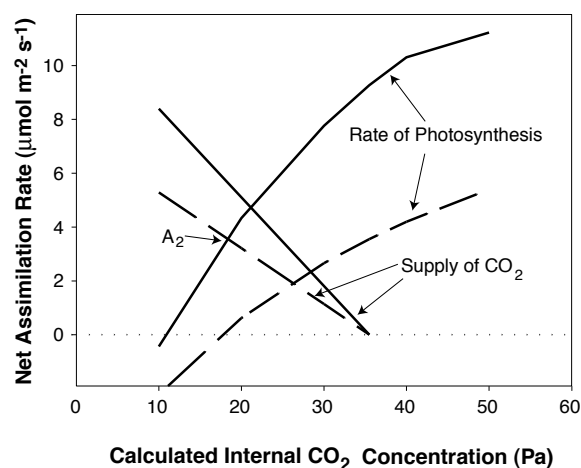


Figure 8. Average A/C_i Curves for Control and *Phaeocryptopus gaeumannii* Infected Branches in Two-year-old Douglas-fir Seedlings Sampled in April 1999. Supply and demand curves were determined from the average values of V_{cmax} , J_{max} , R_{day} and conductance (Table 1) for each treatment (control and infected) using the equations found in Appendix I.

using the A/C_i curve analysis of diseased seedlings ($R^2 = 0.777$, $p < 0.0001$) (Fig. 9.B.). Relationships only differed in their y intercept, which may be due to the varying conditions under which stomatal conductance was measured. For the petroleum jelly treated seedlings, stomatal conductance was measured under ambient conditions; and as a result, the reference value ($g_{sw_treatment_0}$) did not represent the maximum rate (see above). Whereas, for the *P. gaeumannii* infected seedlings stomatal conductance was measured under optimal conditions, and in this case, the reference value ($g_{sw_control}$) was at or near the maximum rate.

Chlorophyll Fluorescence - Images of quantum efficiency, from control and infected samples of needles from the same seedling, show no spatial variation in quantum efficiency. In other words, each set of needles measured had a quantum

Table 2. Spectrophotometric Assay Of Rubisco Activity In Ten Two-year-old Douglas-fir Seedlings Infected With *Phaeocryptopus gaeumannii*, July 1999.

Branch ²	Rubisco Activation (R_{ACT}) (%) ¹	Total Rubisco Activity (R_T) ($\mu\text{mol m}^{-2} \text{s}^{-1}$)
	Mean (SE)	Mean (SE)
Infected Needles	48.0 (2.7)	10.5 (0.9)
Control Needles	78.7 (3.2)	10.1 (1.0)
p-value ³	0.000	0.539

¹Rubisco activation is the percent of initial rubisco activity compared to the total rubisco activity from sun-adapted needles.

²One control and one infected branch from each of ten two-year-old Douglas-fir seedlings were measured.

³p-value was calculated using a paired t-test between control and infected branches for the six seedlings sampled.

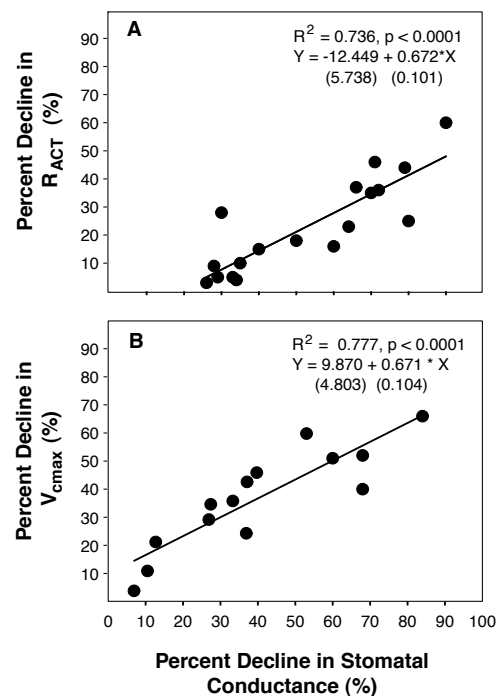


Figure 9. Relationship between changes in Stomatal Conductance and Rubisco Activity. Panel A was determined from spectrophotometric analysis of rubisco activation from petroleum jelly treated needles. Each observation represents differences between treated needles from each of six seedlings measured in July 1999. Percent decline in rubisco activation = $R_{ACT_treatment_0} - R_{ACT_treatment_i}$, where i is either the 50 or 100 % treatment level. Percent decline in stomatal conductance = $g_{sw_treatment_0} - g_{sw_treatment_i} / g_{sw_treatment_0} * 100$, where i is either the 50 or 100 % treatment level. Stomatal conductance was measured 1 hr after treatment under ambient conditions. Panel B was determined from A/C_i curve analysis of *P. gaeumannii* infected seedlings. Each observation represents differences between control and infected branches. Percent decline in rubisco activity = $V_{cmax_control} - V_{cmax_infected} / V_{cmax_control} * 100$. Percent decline in stomatal conductance = $g_{sw_control} - g_{sw_infected} / g_{sw_control} * 100$. Stomatal conductance is the average stomatal conductance measured during A/C_i curve analysis at optimal conditions.

same seedling (Table 3). In addition, no differences were detected in F_m , F_s or F_{dark} (data not shown).

Table 3. Quantum Efficiency, Y' , Calculated From Imaging Chlorophyll Fluorescence In Six Two-year-old *Phaeocryptopus gaeumannii* Infected Douglas-fir Seedlings.

Branch ²	Quantum Efficiency ¹ (Y')
	Mean (SE)
Infected Needles	0.686 (0.014)
Control Needles	0.693 (0.014)
p-value ³	0.326

¹Quantum efficiency was calculated from $(F_m - F_s) / (F_m - F_{dark})$.

²One control and one infected branch from each of 6 two-year-old Douglas-fir seedlings were measured.

³p-value was calculated using a paired t-test between control and infected branches for the six seedlings sampled.

Discussion

Seasonal Variation - Seasonal changes in needle physiology (i.e., gas exchange) were observed for both infected and non-infected needles of two-year-old Douglas-fir seedlings. However, no difference between infected and non-infected needles was noted until there were obvious pseudothecia present in infected needles. Depressions of needle physiology during the winter are a typical phenomenon in conifers, particularly at higher elevations (e.g., Havranek and Tranquillini 1995). In our work, winter depressions of Douglas-fir needle physiology have been detected in seedlings (present study) and saplings, ca. 15 years-old

(Kavanagh, unpubl.). Although the cause(s) of these depressions were not directly investigated, it is possible that increased levels of abscisic acid (Qamaruddin et al. 1993), and/or low water potentials created by xylem freezing (Havranek and Tranquillini 1995), are responsible for increased stomatal closure and a reduction in conductance. And similar to the disease mechanism presented below, the reduced supply of CO₂ from the low stomatal conductance causes a down-regulation in the activation of rubisco.

Fungal Impacts and Mechanism
 - Following pseudothecia emergence both stomatal conductance and carbon assimilation are reduced. Based on our studies here we propose the following mechanism through which *P. gaumannii* impacts Douglas-fir needle physiology.

In this mechanism, fungal impacts begin with the formation of

pseudothecia and a decline stomatal conductance (steps 1-3). Then, net CO₂ assimilation is reduced by both stomatal and biochemical means (steps 4a & 4b). These two processes together limit the amount of net CO₂ assimilation possible in an infected needle (step 5). Finally, once assimilation rates have been reduced, needles will be less productive and over time give rise to the common Swiss needle cast disease symptoms of chlorosis, needle abscission and growth loss (Step 6).

In our model, the first major impact of disease occurs with the emergence of fungal pseudothecia, despite the presence of internal and external hyphae, which develop many months prior to pseudothecia emergence. The lack of fungal impacts prior to pseudothecia formation is not surprising, however, considering that fungal penetration and necrosis of host cells is rarely if

ever observed (Capitano 1999). Furthermore, *P. gaumannii* is not known to produce any toxins; however this is currently under investigation. The strong relationship between pseudothecia presence and declines in stomatal conductance also suggests that pseudothecia presence is the causal factor reducing stomatal conductance in SNC infected Douglas-fir foliage. If the relationship presented in figure 4 is extrapolated to zero stomatal

conductance (i.e., 100% decline in stomatal conductance) then only ca. 58 % of the stomata need be occupied by pseudothecia. This may be due to the presence of other fungal structures, which also block gas exchange through needle stomata. One structure, pseudothecia initials (i.e., generative hyphae), may prove to be the best indicator of fungal impact on stomatal conductance, because these structures can be found densely packed into needle stomata with or without attached mature pseudothecia (Stone and Carroll 1986). Secondly, surface hyphae in SNC infected foliage can at times form relatively dense mats of hyphae on the needle surface (Capitano 1999), and these structures may also physically block needle gas exchange, as previously shown with powdery mildew (Ayres 1976, 1981).

Following the decline in stomatal conductance, net CO₂ assimilation is reduced through both stomatal and biochemical means. The former reduces net assimilation directly by reducing the amount of substrate, CO₂, available to the photosynthetically active needle. This relationship is expressed mathematically by equation 2 (Appendix I), and the impact of stomatal limitations to CO₂ assimilation can be seen graphically in figure 8.

Two possible mechanisms are likely to explain the relationship between stomatal conductance and V_{cmax} (i.e., biochemical limitation to net assimilation). The first potential mechanism involves what is commonly referred to as “patchy” stomatal closure (e.g., Terashima et al. 1988, Terashima 1992, Mott 1995).

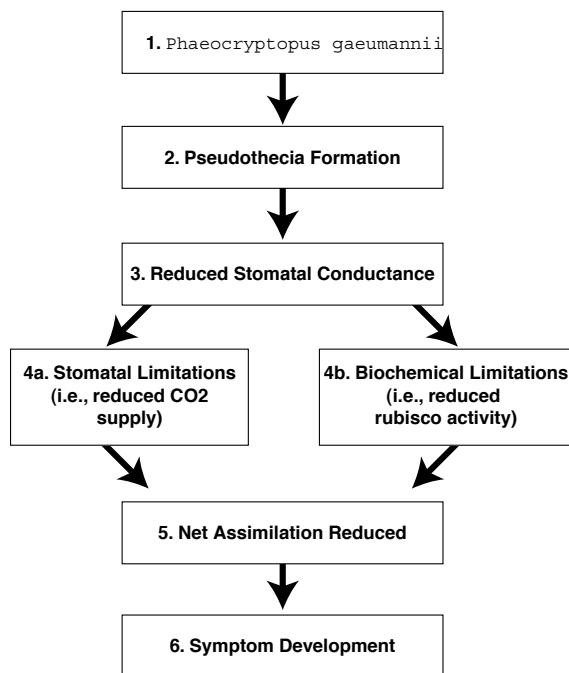


Figure 10. Mechanism of *Phaeocryptopus gaumannii* Impact on Douglas-fir Needle Physiology (Gas Exchange).

In this scenario, stomata are closed in groups, resulting in a needle-wide conductance distribution that has distinct modes; typically, it is bimodal with one region possessing a normal conductance and the other little to no conductance (e.g., Buckley et al. 1997). If such a distribution is present, and the internal conductance of CO_2 to the region of closed stomata is low, than this area effectively becomes non-functional. However, because typical A/C_i curves are reported on a total leaf area basis not a “functional” leaf area basis, these stomatal limitations that shift the A/C_i curve (the demand curve) may erroneously be considered biochemical limitations.

In the case of *P. gaumannii*-infected foliage, however, patchy stomatal closure does not appear to be responsible for our observed biochemical limitations to assimilation. First, spectrophotometric assays of rubisco activity confirmed that rubisco activity is reduced in infected needles. Second, chlorophyll fluorescence images show that quantum efficiency, in both infected and control needles, conforms to a uni-modal distribution.

The second possible mechanism is that the reduced CO_2 supply results in a reduction in the amount of activated rubisco. In order for rubisco to act as a carboxylase and fix carbon it must first be activated. One of the steps in activation involves carbamylation of the active site with a CO_2 molecule (Lorimer 1981). Therefore, following the decline in stomatal conductance and a reduced supply in internal CO_2 it is possible that the amount of activated rubisco

declines resulting in our observed reductions in V_{cmax} . In order to test this hypothesis, we measured rubisco activity from healthy needles that had an artificially reduced stomatal conductance. Based on these studies, rubisco activity in Douglas-fir is quite sensitive to stomatal conductance and the resulting decline in internal CO_2 concentration. In fact, rubisco activity showed a linear relationship with stomatal conductance, decreasing as stomatal conductance decreased. To the authors’ knowledge, a direct relationship between stomatal conductance and rubisco activity has not previously been shown. However, rubisco activity has been shown to decline below some threshold level of internal CO_2 , which varies between species (e.g., Sage et al. 1990, von Caemmerer and Edmondson 1986). Interestingly, under some conditions rubisco activation is unaffected by stomatal conductance. In measurements of rubisco activation in field trees (Manter unpubl.), diurnal changes in stomatal conductance (e.g., humidity response) did not lower rubisco activation. This suggests that early morning stomatal conductance (typically, maximum conductance) and internal $[\text{CO}_2]$ may be the major limitation of rubisco carbamylation and activation following nighttime inactivation. The exact relationship and mechanism still needs to be determined.

We also believe that the biochemical limitations observed arise directly from the decline in stomatal conductance for the following reasons. First, biochemical limitations to net assimilation were only observable once changes in stomatal conductance

were observed. Second, no changes in any of the chlorophyll fluorescence parameters were detectable following fungal infection. From this data we can infer that *P. gaumannii* infection appears to have no direct impact on the level and function of energy capture and electron transfer, or any of the other physiological processes typically associated with changes in chlorophyll fluorescence (e.g., Kraus and Weis 1991). Third, physical reductions in stomatal conductance (i.e., petroleum jelly treated needles) of healthy needles resulted in reduced rubisco activation.

Finally, only after the decline in net assimilation occurs do we reach the final stage of disease development or symptoms expression. During this stage, the commonly observed patterns of chlorosis, needle abscission and growth loss develop in *P. gaumannii*-infected foliage.

Goal III.

Introduction

In the above section, we discussed the impact of pseudothecia presence on the maximum rates of stomatal conductance and carbon assimilation. In this section, we are concerned with the ability of diseased trees to regulate stomatal function. Stomata open and close in response to environmental conditions such as light, temperature, humidity and soil and plant water content, in such a manner as to maximize CO₂ uptake and minimize water loss. For example, under conditions when water loss may be high (e.g., low humidity) or supply is low (e.g., low soil water content, reduced xylem function) plants respond by closing stomata and limiting the amount of water lost to the environment. This ability to close stomata reduces a plants risk to excess water loss and several forms of injury. One type of injury is cavitation, which may occur when water is lost from xylem tissues faster than it is replenished. The excess water loss creates tension in the xylem cells that can cause air bubbles to form that physically rupture xylem cells.

A second interest in understanding stomatal regulation in SNC infected trees is its potential influence on symptom development. For example, under favorable environmental conditions, infected foliage may be able to compensate for SNC infection by leaving its functioning stomata open longer during the day, thereby allowing transpiration and photosynthesis to continue. Even though there is less water movement per hour, the stomata remain open for more hours

during the day. However, once stomata become limited by environmental conditions, this compensation can no longer occur and symptom progression is accelerated. Preliminary reports of greater SNC symptom development on south slopes, which tend to have higher temperatures and less soil water than north slopes suggest that such an interaction may occur. We hypothesize that such an interaction between SNC infection and environmental conditions exists and may help to explain differences in symptom development.

Methods

Site Selection - See goal I.

Gas Exchange - Starting in June 1999 diurnal analysis of gas exchange (H₂O) and water potential were measured. Diurnal measurements included pre-dawn water potentials, bi-hourly gas exchange (Li-1600) and leaf water potential (Y_{leaf}, a measure of water content) measurements commencing at dawn or immediately after foliage dried-off. At the end of the day, all measured foliage was removed and measured for leaf

area, dry weight (used to express gas exchange on a unit basis) and fungal presence (pseudothecia counts and ergosterol content).

Results and Discussion

Figures 11 and 12 show typical patterns of diurnal stomatal conductance from the Beaver and Mac sites, respectively. At Beaver, non-sprayed trees (i.e., pseudothecia present, see Fig. 3) had lower rates of stomatal conductance as compared to their sprayed counterparts. The reduction in early morning stomatal conductance (ca. maximum) is consistent with the observations in inoculated seedlings. Also similar to the inoculated seedling study, diseased trees show a reduction in CO₂ assimilation through both stomatal (supply) and biochemical (demand) limitations (data not shown).

Several important changes in stomatal regulation for SNC trees are emerging that may be responsible for our observation of increased symptom development on southern slopes (more chlorosis and less needle retention). First, at any given time of the

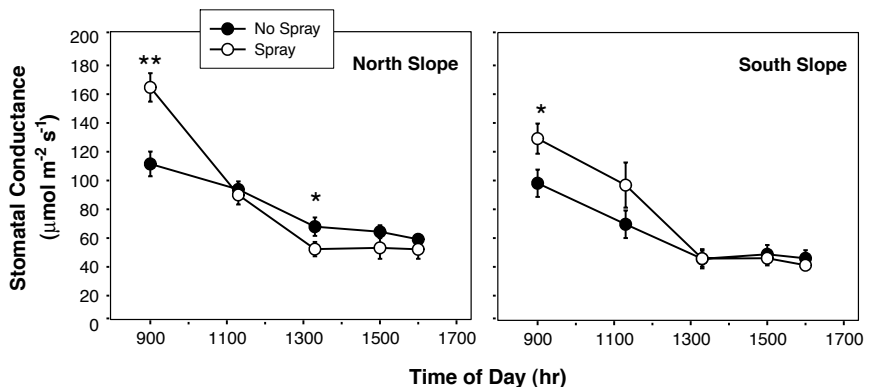


Figure 11. Diurnal Pattern of Stomatal Conductance, Beaver Site, 1998 Needles, Sampled on July 8, 1999. Each symbol represents the mean of six trees; error bars are the standard error of the mean. Treatment differences were tested using a grouped t-test. * denotes $p < 0.10$, ** denotes $p < 0.05$.

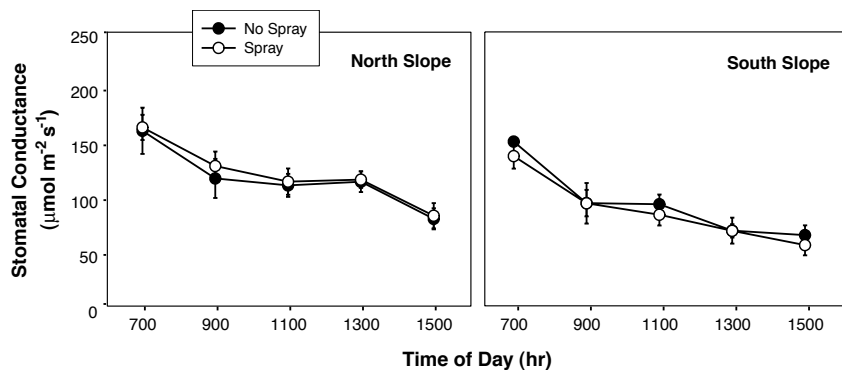


Figure 12. Diurnal Pattern of Stomatal Conductance, Mac Site, 1998 Needles, Sampled on July 6, 1999. Each symbol represents the mean of six trees; error bars are the standard error of the mean. Treatment differences were tested using a grouped t-test. * denotes $p < 0.10$, ** denotes $p < 0.05$.

day, north slope trees exhibit higher rates of stomatal conductance (and CO_2 assimilation) compared to south slope trees. This pattern is consistent for both healthy and diseased trees, and may be linked to environmental and/or host differences between north and south slopes. We have observed that on the north slopes the supply of water (soil content) is typically higher; and the demand for water loss (e.g., humidity) is lower (data not shown). And even when environmental conditions are similar (e.g., see VPD response curve, Fig. 14) stomatal conductance on the south slopes is lower. The mechanism is currently under investigation but may be related to a reduced ability to supply needles with water in the south slope trees, through either root damage or diminished xylem conductance (less sapwood and/or increased cavitation). Figure 13 shows a typical diurnal pattern of leaf water content from trees at the Beaver site. It should be noted that south slope trees have lower water content than north trees, and also that diseased trees have lower water contents than healthy (sprayed) trees. This pattern of water content was

similar throughout the entire summer (Table 4).

Second, during late afternoon, at the Beaver north site, diseased trees exhibit higher levels of stomatal conductance compared to sprayed trees; thus, compensating for the reduced early morning conductance. On the south slope, however, diseased trees do not show this late afternoon compensation effect. The result is that diseased trees on the north slopes can have a total daily rate of stomatal conductance that is similar to healthy trees. And as we discussed above,

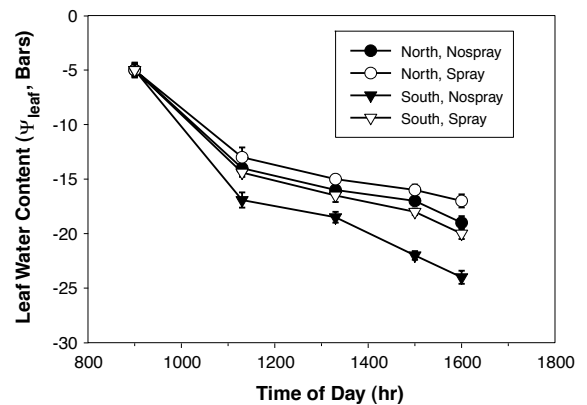


Figure 13. Diurnal Pattern of Leaf Water Content (Ψ_{leaf}), Beaver Site, 1998 Needles, Sampled on July 8, 1999. Each symbol represents the mean of six trees; error bars are the standard error of the mean.

Table 4. Average Leaf Water Content (Ψ_{leaf}) for Trees at the Beaver Site, Summer 1999.

Slope	South		North	
	Nospray	Spray	Nospray	Spray
Mean(SE) ¹	-14.8(1.2) ^a	-12.6(1.0) ^b	-12.2(1.1) ^b	-10.8(1.0) ^c

¹Means were determined by averaging bihourly measurements from six trees on four days during the summer of 1999. Means with different letters are significantly different ($p < 0.05$) as determined by paired t-tests.

this will increase the amount of carbon assimilated into the plant. The mechanism responsible is currently under investigation. However, as shown in figure 14, diseased trees respond differently to vapor pressure deficit (VPD is a measure of the dryness of the air) compared to sprayed trees (i.e., lower conductance at $\text{VPD} < 700 \text{ Pa}$ and higher conductance at $\text{VPD} > \text{ca. } 700 \text{ Pa}$ as compared to sprayed trees). We believe that the difference between diseased and healthy trees in response to VPD is due to pseudothecia development. Pseudothecia development results in stomata being both artificially “closed” and “open”. The first effect, artificially “closed”, reduces maximum conductance by their presence in fully open stomata. The second

effect, artificially “open”, results from pseudothecia interfering with the stomata’s ability to fully close. Even though pseudothecia reduce the maximum ability of water (and CO₂) to diffuse through stomata they are still “leakier” than fully closed stomata.

In figure 14, the south slope does not show the “blocked open” effect. Again, we contribute this to the impact of reduced water content levels in the south trees. In other words, at the high VPD levels on the south slope stomatal conductance is limited by water content not VPD. Furthermore, if we plot stomatal conductance against leaf water content (Ψ_{leaf}) then both sites show the “blocked open” and “blocked closed” effects (Fig. 15). However, in practice, this compensation is rarely if ever reached in the south slope diseased trees because they typically have lower water contents (see Table 4).

In summary, the following factors allow for the greater development of SNC symptoms on southern slopes (or dry sites).

Environmental Differences

Higher humidities, temperatures and light levels cause a greater demand for water loss on southern slopes.

Reduced soil water content limits water supply.

Host Differences

Water supply in southern slope trees may be further reduced by diminished root systems and/or stemflow (decreased sapwood area and/or cavitation).

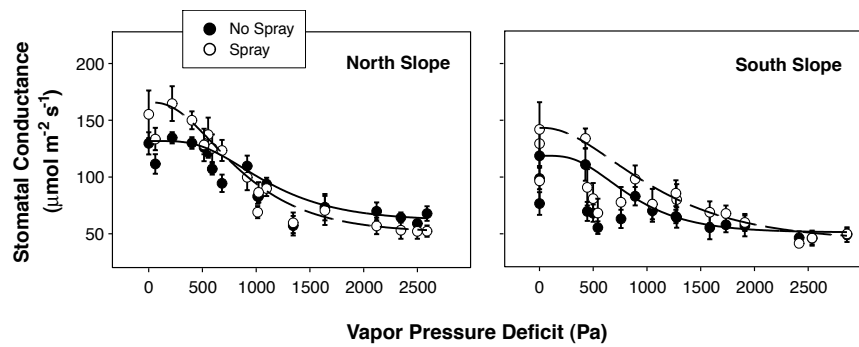


Figure 14. Response to Vapor Pressure Deficit (VPD), Beaver Site, 1998 Needles, Summer 1999. Model lines (Chapman 4-parameter sigmoid curve) were created using the upper boundary of stomatal conductance at a particular level of vapor pressure deficit. In theory, any observation below this line is limited by some other variable (light, water content, etc.).

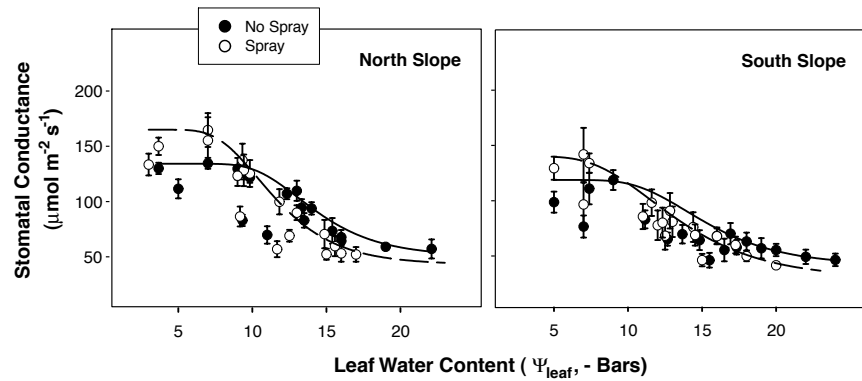


Figure 15. Response to Leaf Water Content (Ψ_{leaf}), Beaver Site, 1998 Needles, Summer 1999. Model lines (Chapman 4-parameter sigmoid curve) were created using the upper boundary of stomatal conductance at a particular level of vapor pressure deficit. In theory, any observation below this line is limited by some other variable (light, water content, etc.).

Pseudothecia Impacts on stomatal regulation

Stomata artificially “closed” – reduces maximum stomatal conductance (and carbon assimilation). Similar effect on both sites.

Stomata artificially “open” – despite the high demand for water loss or low leaf water content stomata remain open. This allows for a greater com-

ensation in the north slopes. However, on the southern slopes this effect is removed due to harsher environmental conditions and/or reduced host vigor.

Pseudothecia Development

Pseudothecia emerge earlier in the season on southern slopes decreasing the seasonal assimilation of CO₂.

References

- Ayres, P.G. 1976. Patterns of stomatal behavior, transpiration and CO₂ exchange in pea following infection by powdery mildew (*Erysiphe pisi*). *J. Exp. Bot.* 27:1196-1205.
- Ayres, P.G. 1981. Effects of disease on plant water relations. In: (P.G. Ayres, ed.). *Effects of Disease on the Physiology of the Growing Plant*. Cambridge University Press. p. 131-148.
- Bowyer, W.J., L. Ning, L.S. Daley, G.A. Strobel, G.E. Edwards and J.B. Callis. 1998. In vivo fluorescence imaging for detection of damage to leaves by fungal phytotoxins. *Spectroscopy*. 13:36-44.
- Buckley, T.N., G.D. Farquhar and K.A. Mott. 1997. Qualitative effects of patchy stomatal conductance distribution features on gas-exchange calculations. *Plant, Cell and Env.* 20:867-880.
- Capitano, B. The infection and colonization of Douglas-fir by *P. gaeumannii*. 1999. MS Thesis, Oregon State University, Corvallis.
- Cheng, L. and L. Fuchigami. (in preparation). Department of Horticulture, Oregon State University, Corvallis, OR.
- Ehrlinger, J. and R.W. Pearcy. 1983. Variation in quantum yield for CO₂ uptake among C₃ and C₄ plants. *Plant Physiol.* 73:555-559.
- Farquhar, G.D., S. von Caemmerer and J.A. Berry. 1980. A biochemical model of photosynthetic CO₂ assimilation in leaves of C₃ species. *Planta*. 149:78-90.
- Gessner, M.O., M.A. Bauchrowitz and M. Escautier. 1991. Extraction and quantification of ergosterol as a measure of fungal biomass in leaf litter. *Microb. Ecol.* 22: 285-291.
- Gordon, T.R. and J.M. Duniway. 1982. Effects of powdery mildew infection on the efficiency of CO₂ function and light utilization by sugar beet leaves. *Plant Physiol.* 69:139-142.
- Hansen, E.M. 1996. Swiss needle cast, why here, why now? A problem analysis. Oregon Dept. of Forestry. 22p.
- Harley, P.C. and T.D. Sharkey. 1991. An improved model of C₃ photosynthesis at high CO₂: Reversed O₂ sensitivity explained by lack of glycerate re-entry into the chloroplast. *Photosyn. Res.* 27:169-78.
- Harley, P.C., R.B. Thomas, J.F. Reynolds and B.R. Strain. 1992. Modelling photosynthesis of cotton grown in elevated CO₂. *Plant, Cell and Env.* 15:271-282.
- Havranek, W.A. and W. Tranquillini. 1995. Physiological processes during winter dormancy and their ecological significance. In: (W.K. Smith and T.M. Hinckley, eds.). *Ecophysiology of Coniferous Forests*. Academic Press, New York. p. 95-124.
- Jones, H.G. 1985. Partitioning stomatal and non-stomatal limitations to photosynthesis. *Plant, Cell and Env.* 6:671-674.
- Kraus, G.H. and E. Weis. 1991. Chlorophyll fluorescence and photosynthesis: The basics. *Annu. Rev. Plant Physiol. Molec. Biol.* 42:313-349.
- Lorimer, G.H. 1981. The carboxylation and oxygenation of ribulose 1,5-bisphosphate: The primary events in photosynthesis and photorespiration. *Annu. Rev. Plant Physiol.* 32:349-383.
- Montalbini, P., B.B. Buchanan and S.W. Hutcheson. 1981. Effect of rust infection on rates of photochemical polyphenol oxidase activity of *Vicia faba* chloroplast membranes. *Physiol. Plant Path.* 18:51-57.
- Mott, K.A. 1995. Effects of patchy stomatal closure on gas exchange measurements following abscisic acid treatment. *Plant, Cell and Env.* 18:1291-1300.
- Ning, L. G.E. Edwards, G.A. Strobel, L.S. Daley and J.B. Callis. 1995. Imaging fluorometer to detect pathological and physiological change in plants. *App. Spectroscopy*. 49:1381-1389.
- Qamaruddin, M., I. Dormling, I. Ekberg, G. Eriksson and E. Tillberg. 1993. Abscisic acid content at defined levels of bud dormancy and frost tolerance in two contrasting populations of *Picea abies* grown in a phytotron. *Physiol. Plant.* 87:203-210.
- Sage, R.G., T.D. Sharkey and J.R. Seemann. 1990. Regulation of rubulose-1,5-bisphosphate carboxylase activity in response to light intensity and CO₂ in the C₃ annuals *Chenopodium album* L. and *Phaseolus vulgaris* L. *Plant Physiol.* 94:1735-1742.
- Scholes, J.D. 1992. Photosynthesis: cellular and tissue aspects in diseased leaves. In: (P.G. Ayres, ed.). *Pests and Pathogens*. Bios Scientific Publ., Oxford. p. 85-106.

- Sharkey, T.D. 1985. Photosynthesis in intact leaves of C_3 plants: Physics, physiology and rate limitations. *The Bot. Rev.* 51:53-105.
- Stone, J.K. and G.C. Carroll. 1986. Observations on the development of ascocarps of *Phaeocryptopus gaeumannii* and on the possible existence of an anamorphic state. *Sydowia.* 38:317-323.
- Suti, D.D. and J.B. Sinclair. 1991. *Anatomy and Physiology of Diseased Plants.* CRC Press, FL. 232 Pp.
- Tang, X., S.A. Rolfe and J.D. Scholles. 1992. The effect of *Albugo candida* (white blister rust) on the photosynthetic and carbohydrate metabolism of leaves of *Arabidopsis thaliana*. *Plant, Cell and Env.* 19:967-975.
- Terashima, I. 1992. Anatomy of non-uniform leaf photosynthesis. *Photo Res.* 31:195-212.
- Terashima, I., S.-C. Wong, C.B. Osmond and G.D. Farquhar. 1988. Characterization of non-uniform photosynthesis induced by abscisic acid in leaves having different mesophyll anatomies. *Plant Cell. Physiol.* 29:385-394.
- von Caemmerer, S. and D.L. Edmondson. 1986. Relationship between steady-state gas exchange, in vivo ribulose biphosphate carboxylase activity and some carbon reduction cycle intermediates in *Raphanus sativus*. *Aust. J. Plant Physiol.* 13:669-88.
- Walters, D. and P.G. Ayres 1984. Ribulose biphosphate carboxylase protein and enzymes of CO_2 assimilation in barley infected by powdery mildew (*Erysiphe graminis hordei*). *Phytopathologie Zeitschrift Bd.* 109:208-218.
- Woodrow, I.E. and J.A. Berry. 1988. Enzymatic regulation of photosynthetic CO_2 fixation. *Annu. Rev. Plant Physiol. Mol. Biol.* 39:533-594.
- Wullschlegel, S.D. 1993. Biochemical limitations to carbon assimilation in C_3 plants - A retrospective analysis of the A/C_i curves from 109 species. *J. Exp. Bot.* 44(262):907-920.

Appendix I. A/C_i Curve Analysis and Calculations

A/C_i curves can be used to estimate some of the major underlying biochemical processes influencing gas exchange and the net uptake of carbon into a plant (assimilation) (Farquhar et al. 1980, Sharkey 1985, Harley and Sharkey 1991, and Harley et al. 1992). According to their models, CO₂ assimilation (mmol m⁻² s⁻¹) can be modeled by equations 1 and 2. See Appendix II for variable definitions.

$$A = V_o - 0.5V_o - R_{day} \quad (1)$$

$$A = \left(1 - 0.5 \frac{O}{\tau \cdot C_i}\right) \cdot \min\{W_o, W_j, W_p\} - R_{day} \quad (2)$$

$$\tau = \exp(-3.9489 + 28.9/0.00831 \cdot T_k) \quad (3)$$

Implicit in equation 1 is that for each carboxylation event one molecule of CO₂ is assimilated, and for every two oxygenations one CO₂ molecule is released. C_i is the calculated internal CO₂ concentration (Pa) based on equations 4-6.

$$A = g_{sc}(C_a - C_i) \quad (4)$$

$$E = g_{sw}(W_a - W_i) \quad (5)$$

$$g_{sc} = \frac{g_{sw}}{160} \quad (6)$$

Furthermore, according to Farquhar et al. (1980) if rubisco assumes Michaelis-Menton enzyme kinetics based on a competitive two-substrate (O₂ and CO₂) system, then

$$W_o = \frac{V_{o,max} \cdot C_i}{C_i + K_c \left(1 + \frac{O}{K_o}\right)} \quad (7)$$

$$K_c = \exp(35.79 - 80.47/0.00831 \cdot T_k) \quad (8)$$

$$K_o = \exp(9.59 - 14.51/0.00831 \cdot T_k) \quad (9)$$

$$W_j = \frac{J \cdot C_i}{4 \left(C_i + \frac{O}{\tau}\right)} \quad (10)$$

assuming that for every four electrons produced enough ATP and NADPH are generated for completion of the Calvin cycle and regeneration of RuBP. And the potential rate of electron transport is dependent upon the follow-

$$J = \frac{\alpha \cdot I}{\left(1 + \frac{\alpha^2 I^2}{J_{max}^2}\right)^{0.5}} \quad (11)$$

ing.

Quantum-use efficiency, was assumed to be 0.18 (mol e⁻ mol⁻¹ absorbed photons) for both control and inoculated branches, based on the work of Ehrlinger and Pearcy (1983) that showed that quantum-use efficiency and light-absorption is relatively constant among several C₃ plants.

And,

$$W_p = 3 \cdot TPU + \frac{V_o}{2} = 3 \cdot TPU + \frac{V_o \cdot 0.5 \cdot O}{C_i \cdot \tau} \quad (12)$$

Finally, equation (2) was solved iteratively for V_{\max} and R_{day} by assuming that W_c occurs at low C_i values. Wulscleger (1993) suggests using the portion of the curve where $C_i < 30$ Pa, however when V_{cmax} values are low, the best fit may be obtained using larger portions of the curve (e.g., $C_i < 50$ Pa). Therefore, for each curve the largest range of C_i values that produced the best fit to the W_c form of equation 2 was used to determine V_{cmax} and R_{day} . After determining V_{\max} and R_{day} , J_{\max} and TPU were determined by solving the entire A/C_i response curve for the full-version of equation two.

Appendix II. Abbreviations and Gas Exchange Parameters.

Abbreviation	Parameter	Units
A	Assimilation rate	$\text{mmol m}^{-2} \text{s}^{-1}$
C_a	Atmospheric CO_2 concentration	35.5 Pa
C_i	Internal CO_2 Concentration	Pa
E	Transpiration rate	$\text{mmol m}^{-2} \text{s}^{-1}$
g_{sc}	Stomatal conductance to CO_2	$\text{mmol m}^{-2} \text{s}^{-1}$
g_{sw}	Stomatal conductance to H_2O	$\text{mmol m}^{-2} \text{s}^{-1}$
I	Incident light	$\mu\text{mol m}^{-2} \text{s}^{-1}$
J	Potential rate of electron transport	$\mu\text{mol m}^{-2} \text{s}^{-1}$
J_{\max}	Light saturated rate of electron transport	$\mu\text{mol m}^{-2} \text{s}^{-1}$
K_c	Michaelis-Menton constants for CO_2	Pa
K_o	Michaelis-Menton constants for O_2	kPa
O	Internal oxygen concentration	21 kPa
R_{day}	Evolution of non-photorespiratory CO_2 in light	$\mu\text{mol m}^{-2} \text{s}^{-1}$
(Specificity of rubisco for O_2/CO_2	$\mu\text{mol m}^{-2} \text{s}^{-1}$
TPU	Rate of phosphate release in triose phosphate utilization	$\mu\text{mol m}^{-2} \text{s}^{-1}$
V_c	Rubisco carboxylation	$\mu\text{mol m}^{-2} \text{s}^{-1}$
V_o	Rubisco oxygenation	$\mu\text{mol m}^{-2} \text{s}^{-1}$
V_{cmax}	Rubisco activity	$\mu\text{mol m}^{-2} \text{s}^{-1}$
W_a	Vapor pressure of the air	$\mu\text{mol H}_2\text{O mol air}^{-1}$
W_c	Rate of carboxylation limited by rubisco activation	$\mu\text{mol m}^{-2} \text{s}^{-1}$
W_i	Internal leaf vapor pressure	$\text{mmol H}_2\text{O mol air}^{-1}$
W_j	Rate of carboxylation limited by RuBP regeneration	$\mu\text{mol m}^{-2} \text{s}^{-1}$
W_p	Rate of carboxylation limited by inorganic phosphate	$\mu\text{mol m}^{-2} \text{s}^{-1}$

Appendix III. Abbreviations and Spectrophotometric Rubisco Activity Parameters

Abbreviation	Parameter	Units
R_{ACT}	Rubisco Activation, $R_I / R_T * 100$	$\text{mmol m}^{-2} \text{s}^{-1}$
R_I	Initial rubisco activity	$\text{mmol m}^{-2} \text{s}^{-1}$
R_T	Total rubisco activity	$\text{mmol m}^{-2} \text{s}^{-1}$

Appendix IV. Abbreviations and Chlorophyll Fluorescence Parameters

Abbreviation	Parameter	Units
F_m	Maximal fluorescence	NA
F_s	Steady state fluorescence at 150 sec	NA
F_{dark}	Machine background fluorescence	NA
Y'	Quantum efficiency, $(F_m - F_s) / (F_m - F_{dark})$	NA

IDENTIFICATION OF ALTERNATIVE FUNGICIDES AND APPLICATION TIMINGS TO REDUCE SWISS NEEDLE CAST DAMAGE IN STANDS OF DOUGLAS-FIR TIMBER

Progress Report 1999

Gary Chastagner, Washington State University, Research and Extension Center, Puyallup, WA

Although this project was initially supported by the SNCC in 1998, portions of this research were initiated in 1997 with support from the Pacific Northwest Christmas Tree Association and the Washington State Commission on Pesticide Registration. This project has two objectives: 1) to identify fungicides that are effective in controlling Swiss needle cast (SNC) when applied as protectants in the spring and 2) determine the effectiveness of fall applications of selected fungicides in disrupting inoculum production and reducing subsequent disease development.

Fungicides have played an important role in the management of SNC in Christmas tree plantations and there is increasing interest in using them as a short-term approach to mitigate damage to trees in selected stands of timber. Chlorothalonil (various formulations of Bravo or Daconil) is the most common fungicide used to control SNC. Application timing is critical in that this protectant fungicide must be applied shortly after new growth has emerged from the buds to be effective. This presents a number of problems because of tree to tree variability in bud break

and poor weather conditions which often prevent applications from being made during this critical period of time. In addition, there are increasing environmental concerns about the use of chlorothalonil.

During the past two years a number of replicated field trials have been established to identify alternative types of fungicides that are effective in protecting newly developing Douglas-fir needles from infection by *P. gaeumannii*. A summary of these fungicide protection trials is provided below.

Another approach to controlling SNC with fungicides is to use fungicides to disrupt inoculum production. SNC is a single-cycle disease. This means that there is only one infection cycle per year. Pseudothecia initially appear in the stomates on the underside of the current season needles during fall to winter. As they mature, they increase in size and can easily be seen with a hand lens during March or April when they begin producing spores. Spores are released upon wetting of mature pseudothecia from April through September, but the peak release period coincides with bud break and shoot elongation in the spring. Newly emerging needles are very susceptible to infection, which

is favored by cool moist conditions and occurs through the stomates. Growth of the fungus inside the needle and the subsequent production of pseudothecia in the stomates completes the disease cycle.

Disrupting the development of fruiting bodies and subsequent production of inoculum is a form of sanitation, and sanitation is a very effective way of reducing the development of single-cycle diseases such as SNC. Taxonomically, *P. gaeumannii* is in the same family as *Venturia inaequalis*, which causes apple scab. Several systemic fungicides have been shown to be effective in disrupting the development of pseudothecia of *V. inaequalis* when they are applied to foliage in the fall. Studies were initiated in 1997 and expanded in 1998 to examine the effectiveness of some of these fungicides in disrupting SNC inoculum production.

Assessment Methods and Scales

We use a number of different assessment methods to evaluate the effects various treatments have on disease development and develop-

ment of pseudothecia. Pseudothecia assessments are typically done by examining the lower surfaces of needles with a dissecting microscope. The following is a description of the assessment methods and scales we commonly use.

Disease Incidence - This is the number of needles out of ten that have one or more SNC pseudothecia on them.

Disease Severity - Initially we rated disease severity on a 0 to 5 scale where 0 = none, 1 = < 1%, 2 = 1 - 10%, 3 = 11-25%, 4 = 26-50%, and 5 = > 50% of stomates on the needles are plugged with pseudothecia. During 1999, we have changed the 5 to 50-75% and added a 6th category for > 75% of the stomates plugged with pseudothecia. These ratings are made with the aid of a card that illustrates sections of needles with 180 stomates that have 1, 10, 25, 50, and 75% of the stomates plugged with pseudothecia.

We have compared our severity ratings with one based on counting the number of pseudothecia to determine the proportion of stomates with pseudothecia. One counting method used at Oregon State University involves counting the number of pseudothecia per 80 stomates on one side of the midrib. These counts are made at two locations on each needle. By counting a total of 160 stomates on each of ten needles per sample and dividing the total number of pseudothecia by 160, one obtains a rating that ranges for 0 to 10. To compare our rating method with this counting method, we examined sets of 10 needles from 20 different samples that had a wide range in the

number of stomates plugged with pseudothecia. There was a very high correlation between these two rating methods (Figure 1).

Disease Index - A disease index is calculated by multiplying the disease incidence times disease severity. Thus our disease index ranges from 0 to 50 or 0 to 60 depending on the severity scale used.

Pseudothecia Maturity - The development or maturity of pseudothecia are rated on a 0 to 4 scale where 0 = none, 1 = < 10%, 2 = 10-25%, 3 = 25-50%, and 4 = > 50% of the pseudothecia are fully erupted out of the stomates.

Inoculum production - We determine the ability of pseudothecia on needles to release ascospores by mounting ten needles across a 1 cm wide window in a piece of filter paper that is mounted in the top of a petri plate lid. The exposed lower surfaces of the needles are then sprayed with water and the lid is positioned above a plate of water agar. Plates are sealed and incubated at 20°C. After 24 hours, the surface of the agar is then sprayed

with rose bengal to stop the germination of spores and the number of spores released are counted using a compound microscope. This provides us with the number of spores released from ten 1-cm-long sections of needle.

Needle Loss - Needle loss is rated on a scale of 0 to 10, where 0 = none, 1 = 1-10%, 2 = 11-20%, 3 = 21-30%, ..., and 10 = 91-100% loss.

Needle Color - We rate needle color on a 1 to 5 scale, where 1 = healthy appearing dark green needles, 2 = healthy appearing green needles, 3 = needles with a slight yellow mottling on a green background that may also have brown spots or tips on the needles, 4 = dull green needles with moderate chlorosis that may also have brown spots or tips on the needles, and 5 = uniformly yellow needles that may have some brown spots or tips.

Protectant Studies

1997 Trials - Applications of eight fungicides were applied to newly developing needles on branches on ten trees at Weyerhaeuser's McDonald Tree Farm and eight trees at a site near Kapowsin, WA.

A single application of each material was applied to a branch on each tree when the new growth was 1 to 3.25 inches long at the McDonald site and 0.75 to 5.25 inches long at the Kapowsin site. The following spring the effect of these treatments on disease incidence, severity and disease index was assessed as described above. Ad-

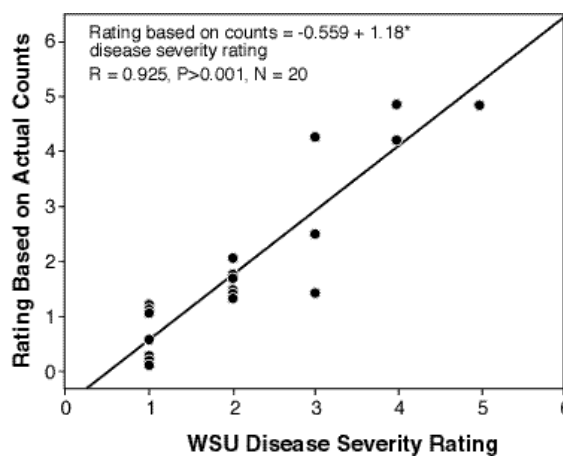


Figure 1. Correlation between WSU's disease severity rating and ratings based on actual counts of pseudothecia in stomates.

ditional data on the effect of treatments on needle loss and color were also obtained from the trees at the Kapowsin site during June 1999.

At the McDonald site, there was only moderate disease pressure and applications of Banner, Benlate, Fore, and Bravo significantly reduced disease severity and the disease index (Table 1). Bravo was the most effective material tested.

Disease pressure was much higher at the Kapowsin site and the only fungicide that controlled SNC was Bravo (Table 2). Applications of Bravo 720 at 5.5 pts/100 gallons provide significantly better control than applications at 2.75 pts/100 gallons. The effects of applying Bravo during spring 1997 were still evident during June 1999. Branches sprayed with Bravo had lost significantly fewer needles and the needle color was much greener compared to the other treatments (Table 2).

1998 Trial - During 1998, a protectant test was established on trees at a Manke Timber site near Cinnebar, WA. Newly developing needles on individual branches on seven trees were sprayed with each treatment on May 21, 1998 using a handheld sprayer. The new growth at the time of application was 1 to 3.5 inches long. The following spring samples were collected from each shoot on March 26, 1999 and rated for SNC.

Although disease incidence was high at this site, disease severity and index ratings were fairly low. Applications of Rally plus Fore, Bravo, Benlate, and Benlate plus Fore were the only materials that resulted in significantly lower disease index ratings than the checks (Table 3).

Table 1. Effect of protectant applications of fungicides on Swiss needle cast at the McDonald Tree Farm.

Treatment	Product/ 100 gallons	Disease evaluations on March 30, 1998		
		Incidence ¹	Severity ²	Index ³
Check	-	9.4 a ⁴	3.6 a	34.4 a
Cleary's 3336 50W	1 lb	8.9 ab	2.9 ab	26.1 ab
Heritage 40W	2 oz	8.3 a	2.9 ab	26.1 ab
Eagle 40W	4 oz	8.7 a	2.9 ab	25.9 ab
Syllit 65W	2 lb	7.8 abc	3.0 ab	25.5 ab
Banner 1.1EC	2 fl oz	6.9 bc	2.2 b	19.9 b
Benlate 50W	1 lb	7.8 abc	2.1 b	17.0 b
Fore 80W	1.5 lb	5.9 c	2.1 b	15.7 b
Bravo 720	2.75 pt	2.1 d	0.9 c	3.4c

¹ Incidence = Number out of ten 1997 needles with SNC pseudothecia.

² Severity rated on a 0 to 5 scale where 0 = no disease, 1 = < 1%, 2 = 1-10%, 3 = 11-25%, 4 = 26-50%, and 5 = > 50% of the stomates on 1997 needles plugged with SNC pseudothecia.

³ Disease index is a 0 to 50 scale where 0 = no disease to 50 = > 50% of the stomates plugged with SNC pseudothecia on all of the 1997 needles.

⁴ Numbers followed by the same letter are not significantly different, P = 0.05, DMRT.

Table 2. Effect of protectant applications of fungicides on Swiss needle cast, needle loss and needle color at Kapowsin test site.

Treatment	Product/ 100 gallons	Disease evaluations on March 20, 1998			June 6, 1999	
		Incidence ¹	Severity ²	Index ³	N. loss ⁴	Color ⁵
Check	-	10 a ⁶	4.8 a	47.5 a	7.5 ab	4.7 a
Cleary's 3336 50WP	1 lb	10 a	4.9 a	48.9 a	6.6 ab	4.6 a
Heritage 40W	2 oz	10 a	4.8 a	47.8 a	6.3 ab	4.4 a
Eagle 40W	2.5 oz	10 a	4.8 a	47.8 a	7.8 a	4.3 a
Eagle 40W	10 oz	10 a	4.7 a	46.7 a	7.0 ab	3.9 a
Syllit 65W	1 lb	10 a	5.0 a	50.0 a	6.3 ab	4.2 a
Syllit 65W	3 lb	10 a	4.8 a	47.8 a	8.4 a	4.7 a
Banner 1.1 EC	2 fl oz	10 a	4.8 a	47.8 a	6.1 ab	4.1 a
Benlate 50W	1 lb	9.9 a	4.9 a	48.4 a	4.8 b	3.8 a
Fore 80W	1.5 lb	10 a	5.0 a	50.0 a	5.6 ab	3.9 a
Bravo 720	2.75 pt	5.1 b	3.6 b	19.4 b	1.0 c	2.3 b
Bravo 720	5.5 pt	3.0 c	1.8 c	11.1 c	1.4 c	1.4 b

¹ Incidence = Number out of ten 1997 needles with SNC pseudothecia.

² Severity rated on a 0 to 5 scale where 0 = no disease, 1 = < 1%, 2 = 1-10%, 3 = 11-25%, 4 = 26-50%, and 5 = > 50% of the stomates on 1997 needles plugged with SNC pseudothecia.

³ Disease index is a 0 to 50 scale where 0 = no disease to 50 = > 50% of the stomates plugged with SNC pseudothecia on all of the 1997 needles.

⁴ Loss of 1997 needles was rated on a scale of 0 to 10 where 0 = no loss, 1 = 1-10%, 2 = 11-20%, 3 = 21-30%, ..., 10 = 91-100% loss.

⁵ 1997 needle color rated on a scale of 1 to 5 where 1 = dark green, 2 = green, 3 = slightly yellow, 4 = dull green with portions being yellow or brown, and 5 = uniformly yellow.

⁶ Numbers followed by the same letter are not significantly different, P = 0.05, DMRT.

A combination treatment of low rates of Benlate and Fore was much more effective than either material alone. Bravo 720 at 5.5 pts/100 gallons of water was the most effective material tested. The effects of these treatments on needle retention and color will be assessed during spring 2000.

1999 Trials - A series of three tests were established during this past spring. Two sites, Yankee/Beaver and Starker are located in Oregon, while the third site is located in a Grays Harbor County timber stand in Washington. A total of 19 or 20 treatments were applied to whole

trees or branches on trees between June 2nd and 10th at these sites. Materials in these tests include, Heritage 50W, Daconil Weather Stik 720, Daconil Ultrex 82.5WDG, Benlate, Dithane 80 DF, UltraFine oil, Golden Dew Sulfur, Compass 50W and two melanin inhibitors. These materials are being tested alone as well as in various combinations. The UltraFine oil is being used to determine if it is possible to increase the activity of Benlate by increasing the movement of this fungicide into the needles. Applications were applied by hand held sprayers and each test was set up as a randomized complete block design with five blocks. The effectiveness

of these treatments in protecting needles from SNC will be assessed during spring 2000.

Inoculum Disruption Studies

1997/98 Trial - During 1997/98 a trial was established to determine the effectiveness of single applications of several different systemic fungicides in disrupting the development of SNC pseudothecia and subsequent production of inoculum. Individual branches on eight Douglas-fir trees were sprayed to run off with one of five fungicides on November 10, 1997. During the following spring and summer, ten randomly selected needles were periodically harvest from the treated and untreated branches on each tree to determine the effects of these fall treatments on pseudothecia development and release of ascospores.

The disease index for the trees in this test was very high and the fall treatments had no effect on the index (Table 4). Applications of Syllit 50W (3 lbs/100 gallons), Cleary's 3336 50W (2 lbs/100 gallons), and especially Benlate 50W (2 lbs/100 gallons) significantly delayed the development of pseudothecia during early spring (Table 5). Heritage 40W (4 oz/100 gallons) partially delayed development in March while applications of Eagle 40W (8 oz/100 gallons) had no effect on pseudothecia development (Table 5). Fungicide treatments also had a significant effect on the release of ascospores. By mid May, pseudothecia on Benlate treated needles had produced only about 10% as many spores as those on the nontreated

Table 3. Effect of protectant applications of fungicides on Swiss needle cast at the Manke test site.

Treatment	Product/ 100 gallons	Disease evaluations on March 26, 1998		
		Incidence ¹	Severity ²	Index ³
Check	-	10.0 a ⁴	2.0 a	20.0 a
Banner 1.1 EC	2 fl oz	10.0 a	2.0 a	20.0 a
Banner 1.1 EC	4 fl oz	10.0 a	2.0 a	20.0 a
DPX-MU 752 30F	6.4 fl oz	10.0 a	1.8 ab	18.6 a
Rally 40W	5 oz	8.8 abc	1.7 abc	15.9 ab
Fore 80W	2 lb	9.0 ab	1.6 abcd	14.7 ab
Benlate 50W	1 lb	7.7 abcd	1.6 abcd	13.3 abc
RH-7592 75W	2 oz	10.0 a	1.3 bcde	12.9 abc
Syllit 65W	3 lb	9.9 a	1.3 bcde	12.7 abc
Rally 40W plus Fore 80W	5 oz 4 lb	6.7 bcde	1.1 cde	8.1 bcd
Fore 80W	4 lb	4.4 ef	1.1 cde	5.8 cd
Bravo 720	2.75 pt	5.9 cdef	1.0 def	5.9 cd
Benlate 50W	2 lb	5.5 def	0.8 ef	5.5 cd
Benlate 50W plus Fore 80W	1 lb 2 lb	3.3 fg	1.0 def	3.3 d
Bravo 720	5.5 pt	1.0 g	0.4 f	0.4 d

¹ Incidence = Number out of ten 1998 needles with SNC pseudothecia.

² Severity rated on a 0 to 5 scale where 0 = no disease, 1 = < 1%, 2 = 1-10%, 3 = 11-25%, 4 = 26-50%, and 5 = > 50% of the stomates on 1998 needles plugged with SNC pseudothecia.

³ Disease index is a 0 to 50 scale where 0 = no disease to 50 = > 50% of the stomates plugged with SNC pseudothecia on all of the 1998 needles.

⁴ Numbers followed by the same letter are not significantly different, P = 0.05, DMRT.

branches (Figure 2).

1998/98 Trials – During fall 1998, inoculum disruption trials were established at three sites to verify the 1997/98 results and determine the optimal timing to apply fungicides to disrupt pseudothecia development and the production of inoculum. Applications of Cleary's 3336 50W (2 lbs/100 gallons), Syllit 65W (3 lbs/100 gallons), and Benlate 50W (2 lbs/100 gallons) were applied to whole trees or branches on trees at two sites along the Oregon coast (Starker and Yankee/Beaver) and the Manke Timber site near Cinnebar, WA. Unsprayed trees and branches served as checks. Plots were designed as a randomized split block design with 10 blocks. Fungicides were applied at the Yankee/Beaver site on Sept. 30, Oct. 20, Nov. 12 and 30, at the Starker site on Sept. 29, Oct. 21, Nov. 11 and 29, and at the Manke site on Oct. 7 and 28, Nov. 18 and Dec. 3, 1999.

Samples of 1998 growth were harvested during the third week of April, the last week of May, and the last week of June and the numbers of fruiting bodies and fruiting body size were assessed as described above. The effects of treatments on inoculum production was also determined by exposing needles over media and counting the number of spores released by fruiting bodies on the needles as described above.

There have been a number of difficulties encountered in trying to process all of the samples collected from these plots. Data from the check trees and branches indicate that there are significant differences in disease severity and production of spores among the sites (Table 6). The disease index for the check trees at the

Table 4. Effect of fungicide applications on November 10, 1997 on Swiss needle cast development the following spring.

Treatment	Product/ 100 gallons	Disease Index (0-50) ¹				
		March 20	April 15	April 27	May 19	June 23
Check	-	47.5	47.8	46.9	48.8	48.8
Heritage 50W	4 oz	48.8	50.0	48.8	46.3	46.3
Eagle 40WP	8 oz	45.6	45.6	43.0	45.0	43.9
Cleary's 3336 50W	2 lb	50.0	46.7	47.5	46.3	46.9
Syllit 65W	3 lb	45.6	47.3	43.0	45.0	45.0
Benlate 50W	2 lb	50.0	48.3	46.3	46.3	45.0
		NSD ²	NSD	NSD	NSD	NSD

¹ Rated 0 to 50 where 0 = no disease and 50 = > 50% of the stomates plugged with pseudothecia on all the needles.

² NSD = no significant difference, P = 0.05.

Table 5. Effect of fungicide applications on November 10, 1997 on the development of Swiss needle cast pseudothecia the following spring.

Treatment	Product/ 100 gallons	Development rate (0-4) ¹				
		March 20	April 15	April 27	May 19	June 23
Check	-	3.4 a ²	3.7 a	3.8 a	3.8 a	3.5 a
Heritage 50W	4 oz	2.4 bc	3.0 ab	3.3 a	3.1 a	3.4 a
Eagle 40WP	8 oz	2.8 ab	2.9 ab	3.1 a	3.4 a	3.3 a
Cleary's 3336 50W	2 lb	1.9 cd	2.4 b	3.0 a	3.1 a	2.9 a
Syllit 65W	3 lb	1.4 de	2.1 bc	1.8 b	3.1 a	3.4 a
Benlate 50W	2 lb	0.8 e	1.3 c	1.8 b	2.6 b	2.6 a

¹ Rated 0 to 4 where 0 = none and 4 = 75% of the pseudothecia were fully erupted out of the stomates.

² Numbers followed by the same letter are not significantly different, P = 0.05, DMRT.

Yankee/Beaver site is significantly higher than the index for the trees at Starker, which is higher than the index for the trees at the Manke site. Needles from only four of the 480 samples processed in April produced spores. In May, needles from the check treatments at the Yankee/Beaver site

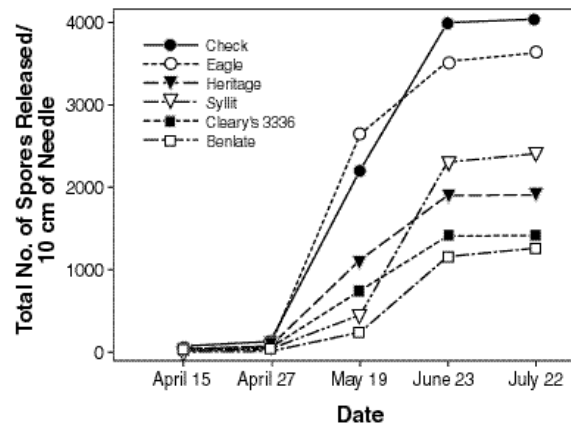


Figure 2. Effect of a single fall fungicide treatment on November 10, 1997 on the number of ascospores released by Swiss needle cast pseudothecia the following spring.

produced more spores than needles from the Starker and Manke sites. In June, the number of spores increased dramatically and the needles from the Starker site produced the highest number of spores.

The large number of spores produced by the needles in June has made it very difficult to complete the spore counts from all of the samples. In addition, on some plates there are large numbers of other fungal spores that slow the counting process. As of the first week in September, about 15 percent of the June samples have yet to be processed. A preliminary examination of the data that has been collected indicates that there is considerable variability between replications within treatments. Treatments appear to have had very little effect on pseudothecia maturation. There appear to be some trends of reduced inoculum associated with some of the fungicide treatments, but these differences may not be significant because of the variability in the data. Data for the third application date at the Manke site has been completed and indicates that Syllit was the only material that reduced spore production (Figure 3). Upon completion of the June sample counts, all of the data from these plots will be analyzed to determine if there are significant differences among any of the treatments.

Additional Studies and Observations

This past spring, some stands of Douglas-fir timber along the central Washington coast exhibited extensive discoloration and

Table 6. Comparison of SNC disease evaluations and numbers of spores released from check trees at three inoculum disruption test sites.

Site	1999 Sample date					
	April 20-22		May 25-26		June 29-30	
	D.I. ¹	No. of spores	D.I.	No. of spores ¹	D.I.	No. of spores
Starker	34.0 b ²	0 a	33.3 b	60.0 b	35.0 b	3,895.0 a
Yankee/Beaver	51.5 a	0 a	49.5 a	826.5 a	48.0 a	1,535.2 b
Manke	26.4 b	0 a	26.3 c	158.5 b	19.9 c	1,229.2 b

¹ D.I. = Disease index on a 0 to 60 scale.

² Numbers followed by the same letter are not significantly different, P = 0.05, DMRT.

trees had very sparse crowns because of the premature loss of needles. Trees that were examined in these stands had high levels of SNC sporulation on their needles. Samples of 1998 spring growth and lammas growth were collected from several trees and rated for disease incidence and severity, needle color, and needle loss. No SNC was found on the lammas growth, which had dark green needles with minimal needle loss. There was extensive loss of the discolored needles on the spring growth, which had fairly high levels of SNC on the remaining needles (Table 7).

In an effort to obtain some information on the impact of SNC in these stands, two plots were established. A series of paired plots were installed at two sites. Applications of Daconil Weather Stik 720 (5.5

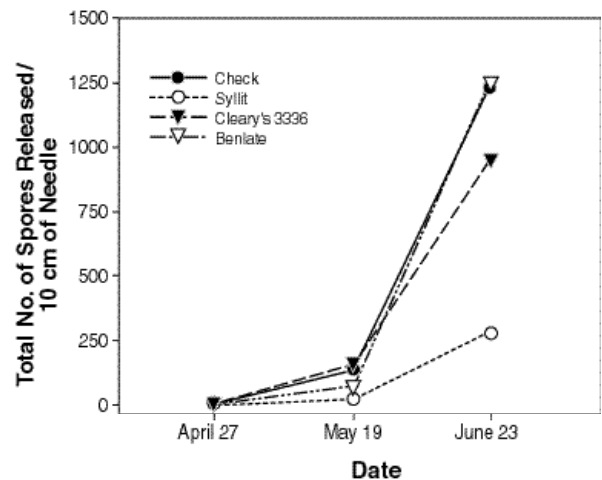


Figure 3. Effect of a single fall fungicide treatment on November 18, 1998 at the Manke timber site on the number of ascospores released by Swiss needle cast pseudothecia the following spring.

pts/100 gallons) were applied to half of the trees at each site using a high pressure sprayer. At a Grays Harbor County timber site, there are three replications of ten treated and check trees. At a Rayonier timber site, all of the trees within 60' X 100' plots that have a minimum 20' wide buffer between plots were sprayed. Data were collected on shoot development on all of the trees in the sprayed and paired check plots and the effects of the Daconil spray on SNC will be evaluated during spring 2000.

Table 7. Swiss needle cast levels and the color and loss of needles on the 1998 spring and lammas growth on Douglas-fir trees growing north of Hoquiam, WA.

Growth	Swiss needle cast		Needle	
	Incidence	Severity	Color	Loss
Spring	10 a ¹	3.2 a	Yellow w/ brown spots	8.3 a
Lammas	0 b	0 b	Dark green	0.6 b

¹ Average of six samples collected on June 8, 1999, P = 0.05.

Acknowledgments

In addition to the SNCC, during 1998/99 portions of this work were supported by the Northwest Christmas Tree Association and the Washington State Commission on Pesticide Registration. The assistance of Starker Forest, Rayonier, and Grays Harbor County Forestry Department is greatly appreciated.

EFFECT OF FERTILIZATION AND VEGETATION CONTROL ON SWISS NEEDLE CAST INFECTION AND GROWTH OF COASTAL DOUGLAS-FIR SEEDLINGS

Progress Report September 1999

Robin Rose, Scott Ketchum, and Diane Haase

(Associate Professor and Senior Faculty Research Assistants, OSU Department of Forest Science)

Study #1

Rationale

Rapid successful establishment of forest tree seedlings has been a major goal for decades on private, state, and federal lands in the Pacific Northwest. Improvements in seedling quality through better nursery practices and early herbaceous and woody control after outplanting have led to improved reforestation in the region. However, the increasing incidence of Swiss needle cast (SNC) infestation, caused by the fungus *Phaeocryptopus gaeumannii*, in coastal Douglas-fir (*Pseudotsuga menziesii* Mirb. Franco) threatens reforestation success.

In 1994, a problem analysis workshop was held regarding coastal Douglas-fir foliage disease (Filip et al. 1994). An important research gap identified was to determine the effects of competing vegetation and fertilizer on disease severity. Vegetation control and fertilizer treatments have resulted in significantly greater seedling growth and vigor in previous research (Vegetation Management Research Cooperative). However, the relationship with Swiss needle cast

has yet to be examined. This study would meet that research gap.

One problem with SNC research is the lack of a consistent, objective, quantification of infection. Chlorophyll fluorescence may be an ideal test for this purpose. Fluorescence technology has ranked highest among seedling physiological tests now available. Under optimum conditions of photosynthesis, the dissipation of absorbed light energy via chlorophyll fluorescence is minimal. However, when plant conditions change, chlorophyll fluorescence emissions can also change. The ratio F_{var}/F_{max} has been shown to be linearly correlated with the quantum yield of net photosynthesis. Hence, any factor that affects the photosynthetic rate (as would be expected from SNC infection) will produce corresponding changes in fluorescence emission. Thus, fluorescence can provide information about the overall photosynthetic activity of the plant and its responses to disturbances.

Objective

The objective of this project is to determine how fertilization and veg-

etation control influence Swiss needle cast infection and subsequent growth of coastal Douglas-fir seedlings. The hypothesis is that increased seedling vigor resulting from weed control and fertilization will lower the infection rate or reduce the impact of infection on seedling growth. An additional objective is to evaluate the usefulness of chlorophyll fluorescence as a tool to detect SNC infection.

Materials and Methods — Study #1

Sites

The study was installed at three different sites across an east/west transect of the Oregon coast range. This gradient for installation of the study replicates was chosen because the greatest level of growth losses associated with SNC have been observed in the coastal regions and tend to decrease eastward toward the drier environments nearer the Willamette Valley. Thus, we expect to find decreased SNC infection and growth reduction along the west-east gradient.

The first site is near Toledo (South Drake). The second is mid-

way between the coast and the Willamette Valley near Eddyville (Bushy Peterson). The third is near the western valley fringe close to Summit (Charlie Olson). Each site has existing 7-9-year-old plantations of Douglas-fir saplings. All three sites were installed during the last two weeks of May 1999.

Study Design

On each site, the study is a randomized complete block design with 5 replications (blocks) of each treatment plot. The six treatments consist of a 2x3 factorial with two levels of weed control and three levels of fertilization. Each treatment plot is 70 ft. x 70 ft. and encompasses 25-35 operationally-planted trees of which the center-most 15 trees were identified for evaluation in the study. An effort was made to select trees well inside the perimeter of each plot. Trees with forked stems or which originated from natural regeneration were not used for measurement trees.

Each tree is clearly identified with an aluminum tag, marking paint, and flagging.

Treatments

There are two vegetation control treatments:

1. no control
2. control of all competition for three consecutive years

During September 7-9, 1999, woody vegetation on the South Drake and Bushy Peterson sites was manually cut to ground level. The Charlie Olson site does not have a significant amount of woody competition and

therefore did not necessitate manual crews. In addition, vegetation control will be accomplished by herbicides broadcast over each treatment plot designated for vegetation control. A fall herbicide treatment (late September 1999) followed by spring and fall herbicide applications as needed will be applied to eliminate all woody and herbaceous competitors thereby maintaining weed-free conditions for three years. The herbicides used will vary by site and target weed species (most likely Oust and Accord in the fall and Atrazine and Transline in the spring).

The three fertilizer treatments are:

1. unfertilized control
2. 200 grams of 17-17-17
3. 200 grams of 9-17-17

The controlled-release fertilizer formulations with minor elements included are from Simplot Company and are identical with the exception of the nitrogen content. Applications were made September 8-10, 1999 to each of the 15 trees in the plots designated for fertilization. The fertilizer blends were surface-applied around the tree base. Applications will be made again in mid-to late-September each year of the study.

Measurements

Morphology. Initial DBH and height were measured on the 15 study trees in each plot at all sites in late May 1999 (Table 1). In mid-October 1999 and at the end of each growing season (after budset) trees will be measured for total height and DBH. In addition, any other details about each tree's condition will be recorded

(i.e. chlorosis, etc.). Seasonal growth will be calculated by subtracting height values and DBH values. Stem volume will also be calculated using the formula for a cone: $1/3(1/4 \pi d^2) h$, where d is the DBH and h is the height. Basal area will be calculated as the area of a circle with diameter equivalent to DBH.

SNC Infection. An initial SNC assessment was made in mid-July 1999 on a branch at approximately DBH (Table 1). This same branch will be used for all further assessments of SNC infection. The assessment consisted of estimating the percentage of needle retention for each year of needles on the main stem of the branch and also on a lateral marked for future assessments.

SNC severity will be evaluated each spring.

Chlorophyll fluorescence. Photosynthetic yield and electron transport rate (calculated via fluorescence measurements) will be assessed on needles from each age class from selected trees in each treatment plot using the the Nursery Technology Cooperative's portable instrument (OptiSciences OS5-FL). The same needles that are measured will then be frozen and later examined under a microscope for number of stomates with pseudothecia.

Nutrient Analyses. Initial foliar and soil nutrient analyses were done on samples from each site in late October 1998 (Tables 2-4). One and two-year-old foliage was collected from mid-canopy on 10 trees at each site and a composite sample from each site was sent for analyses.

Periodically, a sample of current year's foliage will be collected from

Table 1. Average morphology and SNC infection (needle retention by age class) at each site prior to treatment applications. Standard deviation is in parentheses.

Morphology		% needle retention on age classes of a branch				
Height (cm)	DBH (mm)	1 yr - main	2 yr - main	3 yr - main	1 yr - side	2 yr - side
Charlie Olson site						
392.4 (66.8)	49.9 (12.6)	84.3 (17.9)	53.9 (29.7)	19.6 (24.8)	93.0 (14.5)	74.2 (29.5)
Bushy Peterson site						
460.0 (66.1)	60.5 (11.7)	61.5 (24.2)	47.3 (23.4)	10.1 (15.7)	82.6 (29.4)	71.8 (24.9)
South Drake site						
411.9 (69.5)	57.0 (13.6)	27.8 (20.4)	21.6 (16.9)	5.0 (10.2)	64.6 (26.9)	45.2 (28.9)
Sulfur study (South Drake site)						
431.2 (44.8)	59.2 (8.1)	24.8 (17.8)	17.2 (15.8)	1.5 (2.9)	57.6 (26.7)	42.2 (29.4)

Table 2. Initial soil exchangeable nutrient levels.

	pH	P ppm	K ppm	Ca meq/ 100g	Mg meq/ 100g	Na meq/ 100g	N %	NH ₄ -N ppm	NO ₃ -N ppm	
Light Infection—Charlie Olson										
A-Horizon	4.80	28.48	448.5	5.0	2.30	0.08	0.38	8.10	1.24	
B-Horizon	5.40	2.81	390.0	3.2	2.10	0.06	0.09	5.59	0.89	
Moderate Infection—Bushy Peterson										
A-Horizon	5.00	4.73	241.8	2.2	1.40	0.10	0.19	4.96	0.98	
B-Horizon	5.10	2.59	265.2	1.2	0.91	0.08	0.12	3.95	0.67	
Heavy Infection—South Drake										
A-Horizon	4.80	1.65	429.0	0.8	1.20	0.20	0.401	0.00	3.31	
B-Horizon	4.60	1.46	237.9	0.8	1.20	0.19	0.35	7.51	2.87	
	Fe ppm	Mn ppm	Cu ppm	Zn ppm	SO ₄ -S ppm	CEC meq/100g	Incub. N ppm	C %	S %	B ppm
Light Infection—Charlie Olson										
A-Horizon	58.0	32.80	0.18	0.70	9.00	48.04	59.58	10.69	<0.01	0.51
B-Horizon	1.4	3.88	0.02	0.02	51.50	25.20	5.96	1.25	<0.01	0.17
Moderate Infection—Bushy Peterson										
A-Horizon	12.4	10.66	0.10	0.16	9.60	26.07	20.85	2.96	<0.01	0.26
B-Horizon	2.0	4.28	0.06	0.06	43.40	25.40	5.35	1.60	<0.01	0.20
Heavy Infection—South Drake										
A-Horizon	5.8	10.28	0.04	0.24	15.50	53.32	32.16	6.55	<0.01	0.47
B-Horizon	7.4	9.62	0.04	0.34	18.10	52.82	16.37	5.97	<0.01	0.39

3-5 trees from the top 1/3 of the crown from each treatment replication for foliar nutrient analyses. Foliar samples will be dried for 48 h at 68 °C. Needles will be removed from the stems and the weight of 100 needles will be determined. Samples then will be pooled by block and treatment and assessed for nutrient concentration using standard laboratory procedures. Nutrient content will be calculated by taking the product of nutrient concentration and average dry weight of 100 needles. Relative nutrient concentration, content, and dry weight will be calculated (relative to the control treatments) and vector diagrams will be constructed (Haase and Rose 1995) to facilitate a thorough examination of nutrient responses to the fertilizer treatments.

Statistical analyses

Using a factorial model, data will be analyzed independently by site using analysis of variance to determine if there are differences in SNC infection, growth, and other measurements which can be attributed to fertilization and/or vegetation control. Regression analyses will be performed to determine if there is a relationship between SNC infection and F_{var}/F_{max} . All data will be analyzed using SAS software (SAS Institute Inc. 1994).

Study #2

Rationale

In 1997, a few individual members of the Swiss Needle Cast Cooperative ran an unreplicated study to examine if elemental sulfur would

Table 3. Initial soil total nutrient levels.

	P ppm	K ppm	Ca ppm	Mg ppm	Mn ppm	Fe ppm	Cu ppm	Zn ppm	Na ppm
Light Infection—Charlie Olson									
A-Horizon	1477.4	1754.5	2032.1	3311.8	1569.4	35754	23.8	87.0	89.6
B-Horizon	851.4	1906.2	1035.6	4054.4	1168.2	41285	27.8	97.1	87.2
Moderate Infection—Bushy Peterson									
A-Horizon	542.6	1410.6	739.1	4609.4	667.9	31305	19.2	84.5	99.0
B-Horizon	485.7	1245.3	475.6	4371.6	553.0	37954	23.1	85.9	88.2
Heavy Infection—South Drake									
A-Horizon	729.1	1468.6	452.9	2736.4	463.8	42345	26.3	85.3	109.6
B-Horizon	757.0	1262.1	415.5	2759.2	506.1	48199	26.5	79.1	102.3

Table 4. Initial foliar nutrient levels.

Site	Needle Wt/200	N %	P %	K %	Ca %	Mg %	B ppm	Fe ppm	Mn ppm	Cu ppm	Zn ppm	S %
Charlie Olson	1.40	1.85	0.21	0.92	0.32	0.09	18	94	518	4	20	0.12
Bushy Peterson	1.25	1.82	0.20	1.02	0.33	0.08	19	61	371	4	18	0.13
South Drake	1.22	1.81	0.16	0.79	0.21	0.10	20	50	25	3	15	0.16

have an impact on SNC infection as well as improve tree growth. The observational study indicated that Douglas-fir saplings had an 18% increase in growth when treated with an unknown amount of sulfur suspended in water and sprayed onto the trees. This study is an experimental follow-up to that study.

Objective

The objective of this project is to determine how applications of sulfur influence Swiss needle cast infection and subsequent growth of coastal

Douglas-fir seedlings. The hypotheses are that SNC infection is not reduced as a result of sulfur treatments and Douglas-fir growth and nutrition are not significantly affected by sulfur application.

Materials and Methods — Study #2

Site

This study was installed adjacent to the Study #1 installation at the South Drake site near Toledo.

Study Design

The study is a completely randomized design with 10 replications (trees) for each of the five treatments. Selected trees were at least 6 m apart to avoid treatment drift from nearby applications. Trees with forked stems or which originated from natural regeneration were not used for measurement trees. Each tree is clearly identified with an aluminum tag, marking paint, and flagging.

Treatments

There are five sulfur treatments in the study:

1. untreated control
2. Bravo fungicide @ 3.75 pts /100 gallons sprayed on the foliage
3. Sulfur (Thiolux) diluted with water (25 lb per 100 gallons) sprayed on the foliage
4. Sulfur (Thiolux) diluted with water (25 lb per 100 gallons) with TacTic sticker (8 oz per 100 gallons) sprayed on the foliage
5. Sulfur (Thiolux) diluted with water (25 lb per 100 gallons) sprayed on the ground under each tree within the drip line

Treatments were applied on June 8, June 25, and July 10 using a truck tank sprayer at 38psi. Each tree was sprayed for 14 seconds resulting in an application rate of 2 oz Thiolux per tree.

Measurements

The same measurements are being done on this study as described for Study #1. See Table 1 for sum-

mary of initial morphology and SNC infection.

Statistical analyses

Data will be analyzed using analysis of variance to determine if there are differences in SNC infection, growth, and other measurements which can be attributed to sulfur application. All data will be analyzed using SAS software (SAS Institute Inc. 1994).

Expected Study Outcomes

This research will result in a better understanding of the relationship between SNC infection and seedling response to fertilization and vegetation control. The data will give a statistical evaluation of this relationship necessary for the scientific and operational understanding of these treatments.

Studies of this type tend to become more valuable with time. If the three-year report suggests that additional useful information may be generated by further monitoring of the study, we may propose additional funding.

It is anticipated that a research publication as well as articles in regional publications for forestland owners will be produced.

GROWTH IMPACT STUDY

Phase III Progress Report

Doug Maguire, Alan Kanaskie, Bill Voelker, Randy Johnson, and Greg Johnson

Growth Impact activities over the past year were limited to final entry and editing of the Phase III permanent plot data. A total of 76 one-fifth-ac plots was established in the spring of 1998, with measurement planned after two years of growth. Swiss needle cast severity has been assessed by ODF crews on an annual basis (spring of 1998 and 1999), and will be re-assessed next spring (year 2000). This fall a contract for the first re-measurement will be initiated through the SNCC at OSU, with data entry following contract completion in January or February. Data analysis will begin in April and will extend through August, incorporating the new SNC severity ratings recorded in April and/or May.

A brief description of the range in initial plot and tree conditions, prior to the 1998 growing season, follows.

Tree size

The database consists of 7,978 trees distributed across 76 plots (Table 1). The most common species after Douglas-fir is western hemlock, although it occurs on only 48 plots (Table 1).

Douglas-fir mean tree diameter ranged from 1.4 to 13.1 inches and

Table 1. Number of trees and plots by species that comprise the growth impact study in northwest Oregon.

Species	Number of sample trees	Number of plots
Douglas-fir	4052	76
western hemlock	1401	48
cascara	840	31
red alder	549	43
elderberry	490	33
sitka spruce	331	40
bitter cherry	172	19
grand fir	54	1
western redcedar	34	6
bigleaf maple	28	6
other hardwoods	26	6
noble fir	1	1
Total	7978	76

maximum height from 10.1 to 88.2 ft, with an overall average crown ratio of 79 % (Table 2).

Stand density

Because the plots are located in young (10-30 year-old), intensively managed plantations, few relative densities exceeded 60% for Douglas-fir only (Table 3; relative density is regarded as the plot SDI, or stand density index, as a percentage of the maximum SDI for coastal Douglas-fir, assumed here to be 600). The bulk of

the plots fell between relative density bounds of 30% and 60% (Fig. 1). When other species were included in the Stand Density Index computations, the number of trees per acre increased while the quadratic mean diameter declined, but the net result was an increase in the SDI (Fig. 2).

Swiss needle cast severity

The distribution of plots by SNC severity class was described previously in this volume (see Kanaskie

Table 2. Mean diameter (in), height (ft), height to lowest live branch (ft), crown ratio and height:diameter ratio (ft:ft) by plot.

Plot	Douglas-fir						Western hemlock					
	Ave. dbh	Ave. ht	Max ht	Ave. hllb	Ave. cr	Ave. ht/dbh	Ave. dbh	Ave. ht	Max ht	Ave. hllb	Ave. cr	Ave. ht/dbh
1	5.4	36.0	46.8	11.5	0.66	86	1.9	24.1	24.1	4.0	0.84	150
3	6.0	35.7	47.1	3.5	0.90	72	2.4	35.6	43.4	3.9	0.89	114
4	5.6	36.8	47.6	6.5	0.81	79	3.0					
5	9.9	54.1	64.8	5.7	0.90	66						
6	11.3	65.9	74.6	17.8	0.72	71						
7	6.9	48.2	64.6	9.8	0.80	87						
8	8.9	46.4	59.1	7.4	0.84	62						
9	7.6	42.8	53.9	6.0	0.85	70	4.3	36.9	49.2	5.5	0.85	85
11	7.8	37.9	46.7	5.6	0.84	59	1.5	30.1	35.0	4.8	0.83	103
13	3.3	18.1	30.9	0.4	0.98	66	1.5	20.9	26.6	1.4	0.98	84
14	5.1	32.4	41.4	3.9	0.88	72	0.9					
15	2.8	18.8	27.5	3.4	0.81	67						
16	5.7	35.5	47.4	5.4	0.83	75	1.1	26.9	26.9	1.8	0.93	126
17	4.3	23.7	39.9	2.4	0.86	97						
18	6.5	42.7	56.7	7.0	0.82	85	7.1	41.9	60.6	3.6	0.86	78
19	6.6	34.9	45.4	7.8	0.78	70						
20	10.7	62.2	75.8	22.6	0.63	70	3.2	38.1	65.9	6.4	0.83	88
22	10.0	54.7	63.1	10.7	0.80	67						
23	9.3	45.3	55.8	12.3	0.73	60	3.0	36.4	47.7	6.8	0.79	86
27	6.5	33.9	45.6	6.7	0.79	69	2.9	30.5	48.0	4.2	0.86	91
28	7.0	41.6	52.5	7.1	0.83	71	1.0	28.4	28.7	4.1	0.86	104
30	8.4	46.0	57.9	13.9	0.69	72	3.5	41.4	49.7	9.6	0.77	104
31	10.2	42.0	54.3	3.3	0.92	52	2.2	37.6	49.0	2.4	0.93	74
32	5.0	30.8	61.7	4.2	0.86	80						
33	10.4	59.9	76.1	17.9	0.71	71	5.4	48.3	62.5	7.5	0.84	74
34	3.7	22.7	28.1	2.5	0.89	76	4.1	32.4	49.2	3.0	0.92	66
35	5.9	35.3	48.1	2.6	0.93	70	2.9	22.4	22.4	0.4	0.98	92
36	10.1	58.9	65.9	17.5	0.70	71	14.9	64.2	64.2	5.9	0.91	52
38	3.5	20.9	25.1	1.1	0.94	68	3.0	22.6	25.7	1.5	0.93	80
39	9.0	44.9	55.8	6.4	0.85	62	3.7	40.8	56.9	3.0	0.93	63
40	9.0	48.0	68.7	10.1	0.77	66	3.1	39.2	51.7	5.1	0.87	89
41	7.9	58.5	64.4	14.7	0.70	91	4.0	41.5	58.8	10.0	0.73	107
42	3.5	22.3	35.3	1.7	0.91	97	1.3	18.9	18.9	0.6	0.97	80
43	7.8	45.9	61.7	7.6	0.82	68						
47	3.5	23.7	30.8	0.9	0.96	67	1.5	23.2	26.7	0.7	0.97	84
48	7.7	48.6	60.8	13.5	0.72	76	5.8	46.8	56.6	8.4	0.82	78
49	3.4	19.8	30.6	0.6	0.96	76						
51	4.0	24.5	30.1	3.2	0.87	75	2.6	25.7	33.3	3.7	0.86	99
53	3.2	19.0	33.2	1.0	0.95	75	2.6	27.2	36.3	0.5	0.98	67
54	5.0	26.5	40.6	1.1	0.95	70						
55	9.0	61.5	71.1	22.1	0.63	85						
56	7.4	49.8	61.5	13.4	0.73	85	1.5					
57	8.2	53.8	65.9	17.3	0.67	81						
58	4.5	30.6	41.9	4.0	0.87	74						
59	7.4	50.0	60.4	14.7	0.71	80						
60	8.7	43.8	57.4	2.6	0.94	61	2.0	16.8	43.9	2.8	0.78	131
61	6.2	43.2	76.0	17.9	0.66	83	2.2					
62	8.0	39.7	53.0	8.5	0.77	61	3.8	25.8	37.7	2.5	0.90	73

Table 2. continued

Plot	Douglas-fir						Western hemlock					
	Ave. dbh	Ave. ht	Max ht	Ave. hllb	Ave. cr	Ave. ht/dbh	Ave. dbh	Ave. ht	Max ht	Ave. hllb	Ave. cr	Ave. ht/dbh
63	9.9	57.6	77.9	16.4	0.69	82	8.5	52.0	70.9	13.5	0.68	77
68	8.9	50.3	67.4	13.6	0.71	74	5.9	43.0	49.2	11.4	0.74	87
70	6.2	29.7	40.0	2.1	0.93	62	0.8	10.6	20.2	0.9	0.88	466
72	6.0	36.1	43.9	8.1	0.77	73	3.9	35.9	43.3	6.3	0.82	90
76	8.4	52.0	66.4	6.4	0.88	71	0.0					
77	10.2	50.3	62.6	7.4	0.85	74	0.0					
81	11.7	57.3	71.9	19.3	0.66	61	0.0					
83	9.6	61.8	97.1	18.7	0.69	80	1.6	31.2	31.7	9.8	0.69	147
85	12.8	67.3	79.5	14.6	0.78	68	0.4					
94	13.1	88.2	102.6	41.0	0.53	84						
101	4.8	31.6	43.4	11.3	0.63	83	4.0	28.5	36.3	4.9	0.80	87
105	9.0	63.1	79.8	24.4	0.61	86	7.0	58.9	77.4	12.1	0.72	79
108	4.6	34.7	41.5	2.6	0.92	76	0.6					
119	12.8	10.1	17.8	1.0	0.89	100	0.5					
121	13.1	31.5	38.3	2.3	0.93	64	1.6	21.9	26.8	1.7	0.93	80
122	4.8	39.3	56.8	8.4	0.77	80						
124	9.0	56.8	70.4	16.7	0.71	75						
126	4.6	47.3	58.0	9.9	0.79	64						
127	1.4	68.1	81.8	17.3	0.74	69	5.8	54.7	92.5	6.8	0.87	75
128	6.1	21.3	30.4	1.3	0.94	76						
132	5.8	65.5	88.6	31.4	0.50	115	4.6	57.3	80.6	19.3	0.64	100
133	9.4	42.7	56.7	7.7	0.80	68	0.9					
138	9.1	19.9	49.6	0.7	0.96	106						
139	10.9	59.1	86.1	29.1	0.46	112	15.1	48.3	99.5	2.8	0.93	47
140	3.5	48.2	61.9	15.0	0.69	73	0.2					
141	6.8	54.0	64.5	18.1	0.67	65						
142	7.9	40.6	48.5	5.2	0.87	56						
143	3.5	36.9	44.9	5.8	0.83	73						
Mean	7.3	42.6	59.8	9.8	0.79	75	3.2	35.1	46.9	5.2	0.85	99

Table 3. Trees per acre, quadratic mean diameter, and stand density index by plot and species group.

Plot	Douglas-fir			Western hemlock			Other conifer			Hardwoods			All species		
	Tpa	Dq (in)	SDI	Tpa	Dq (in)	SDI	Tpa	Dq (in)	SDI	Tpa	Dq (in)	SDI	Tpa	Dq (in)	SDI
1	625	5.67	251	5	1.93	0	50	3.09	8	50	3.47	9	730	5.38	270
3	285	6.20	132	230	2.88	31	.	.	.	30	5.36	11	545	5.02	180
4	270	5.63	107	20	3.03	3	440	3.35	76	160	3.80	34	890	4.24	224
5	155	9.96	154	10	4.54	3	165	9.71	158
6	155	11.42	192	65	0.61	1	220	9.59	206
7	250	7.24	149	60	3.18	10	310	6.65	161
8	295	9.07	252	.	.	.	10	5.28	4	605	1.54	30	910	5.34	333
9	180	7.84	122	125	5.47	47	10	1.10	0	90	2.89	12	405	6.20	188
11	295	7.99	206	80	2.25	7	90	1.26	3	5	4.49	1	470	6.44	232

Table 3. Continued.

Plot	Douglas-fir			Western hemlock			Other conifer			Hardwoods			All species		
	Tpa	Dq (in)	SDI	Tpa	Dq (in)	SDI	Tpa	Dq (in)	SDI	Tpa	Dq (in)	SDI	Tpa	Dq (in)	SDI
13	315	3.03	46	990	1.41	43	1305	1.93	93
14	350	5.44	132	5	0.94	0	.	.	.	140	3.24	23	495	4.89	157
15	335	2.98	48	70	1.45	3	405	2.78	52
16	350	5.94	152	40	1.42	2	330	1.90	23	135	2.90	19	855	4.16	209
17	460	4.81	142	180	3.67	36	640	4.52	179
18	165	6.82	89	190	7.70	125	355	7.30	214
19	265	6.79	142	.	.	.	5	1.77	0	55	2.94	8	325	6.25	153
20	195	11.14	232	120	4.55	34	45	3.93	10	250	4.27	64	610	7.24	363
22	175	10.13	179	215	1.63	12	390	6.89	215
23	230	9.58	215	115	4.40	31	75	3.39	13	45	3.43	8	465	7.29	280
27	210	6.73	111	445	3.55	85	15	2.49	2	115	3.26	19	785	4.58	224
28	315	7.20	186	70	1.47	3	.	.	.	50	1.44	2	435	6.18	201
30	300	8.69	240	145	4.19	36	215	2.78	27	.	.	.	660	6.38	321
31	130	10.54	141	230	3.97	52	10	0.24	0	20	2.84	3	390	6.83	212
32	380	5.17	132	195	0.71	3	575	4.22	144
33	170	10.71	190	70	6.93	39	.	.	.	5	2.24	0	245	9.67	232
34	115	3.47	21	525	3.78	110	5	2.48	1	910	0.96	21	1555	2.51	169
35	390	6.20	181	5	2.91	1	10	1.19	0	180	1.47	8	585	5.14	201
36	160	10.22	166	5	14.92	10	5	0.51	0	200	3.26	33	370	7.34	225
38	305	3.61	59	95	3.28	16	35	3.03	5	40	0.55	0	475	3.35	82
39	170	9.16	148	95	5.73	39	25	1.36	1	485	1.43	21	775	4.88	245
40	165	10.50	179	710	3.67	142	40	1.70	2	.	.	.	915	5.52	353
41	185	8.32	138	435	6.03	193	25	9.72	24	.	.	.	645	6.93	358
42	655	3.80	139	20	1.61	1	55	0.97	1	65	3.00	9	795	3.58	153
43	220	8.67	175	65	2.31	6	285	7.70	187
47	315	3.91	70	155	2.11	13	.	.	.	30	3.59	6	500	3.44	90
48	260	7.87	177	85	6.57	43	10	0.88	0	10	3.00	1	365	7.38	224
49	290	3.50	54	290	3.50	54
51	85	4.13	21	190	2.83	25	5	0.94	0	.	.	.	280	3.26	46
53	220	3.38	39	995	2.93	139	5	0.59	0	25	2.97	4	1245	3.01	181
54	230	5.31	83	20	1.31	1	250	5.11	85
55	245	9.22	215	.	.	.	5	2.09	0	35	1.53	2	285	8.57	222
56	390	7.65	254	85	1.58	4	.	.	.	550	3.15	86	1025	5.27	367
57	210	8.34	157	260	0.97	6	470	5.62	187
58	515	4.83	160	.	.	.	25	1.01	1	80	2.38	8	620	4.49	171
59	245	7.56	156	25	6.01	11	270	7.43	168
60	170	8.86	140	55	2.82	7	10	0.48	0	5	3.11	1	240	7.59	154
61	390	6.86	213	20	3.31	3	10	5.60	4	60	6.37	29	480	6.66	250
62	150	8.60	118	105	4.75	32	270	7.91	185	.	.	.	525	7.60	338
63	275	13.74	458	50	9.17	44	50	4.80	15	265	2.35	26	640	9.58	597
68	245	9.39	221	15	6.07	7	40	4.80	12	25	4.61	7	325	8.52	251
70	295	6.43	145	30	1.09	1	75	1.14	2	30	0.84	1	430	5.36	158
72	325	6.12	148	135	4.47	37	5	1.42	0	85	1.18	3	550	5.22	194
76	220	8.82	180	170	1.15	5	390	6.67	204
77	200	10.44	214	90	3.29	15	290	8.86	239
81	215	11.99	288	.	.	.	5	1.73	0	10	3.16	2	230	11.62	293
83	285	9.95	283	20	1.89	1	55	4.13	13	210	2.27	19	570	7.29	343
85	105	13.34	167	15	0.66	0	.	.	.	360	0.30	1	480	6.25	226
94	110	13.65	181	40	10.68	44	150	12.92	226

Table 3. Continued.

Plot	Douglas-fir			Western hemlock			Other conifer			Hardwoods			All species		
	Tpa	Dq (in)	SDI	Tpa	Dq (in)	SDI	Tpa	Dq (in)	SDI	Tpa	Dq (in)	SDI	Tpa	Dq (in)	SDI
101	155	5.19	54	10	4.21	2	85	2.92	12	600	4.27	153	850	4.34	223
105	175	9.22	154	215	8.53	167	5	0.75	0	5	10.04	5	400	8.81	326
108	485	4.92	155	15	0.85	0	.	.	.	325	2.80	42	825	4.16	202
119	225	1.48	10	150	0.60	2	115	1.11	3	30	1.26	1	520	1.19	17
121	340	6.24	159	260	1.94	19	10	2.15	1	45	1.79	3	655	4.69	194
122	385	6.14	176	205	3.64	40	590	5.40	220
124	170	9.57	158	415	0.72	6	585	5.19	204
126	225	9.17	196	80	0.17	0	305	7.88	208
127	40	11.71	52	250	8.30	185	85	2.71	10	20	2.27	2	395	7.71	260
128	355	3.53	67	210	1.79	13	565	3.01	82
132	465	7.16	272	410	5.48	156	50	3.82	11	15	11.54	19	940	6.43	463
133	470	8.22	343	5	0.94	0	10	7.24	6	575	3.92	128	1060	6.23	496
138	165	4.91	53	165	4.91	53
139	730	7.75	485	50	19.86	150	.	.	.	1730	2.42	177	2510	5.42	939
140	265	8.24	194	10	0.20	0	5	0.59	0	.	.	.	280	8.02	196
141	210	10.59	230	.	.	.	15	2.58	2	15	1.42	1	240	9.93	237
142	135	8.90	112	140	1.29	5	275	6.31	131
143	175	6.66	91	15	1.55	1	190	6.41	93

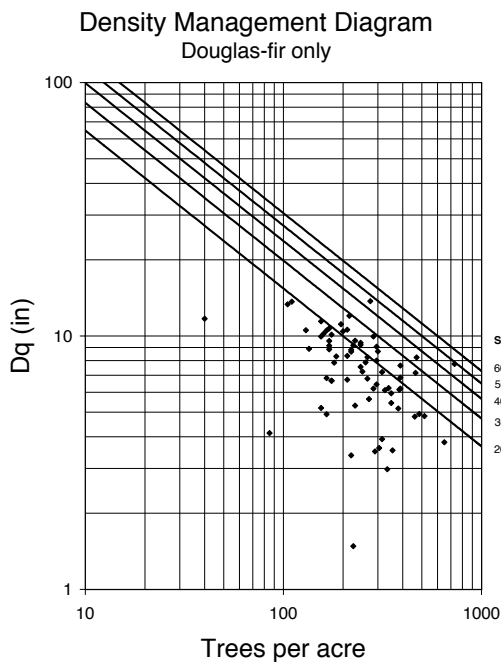


Figure1. Locatin of the 76 permanent plots regarding their stand density index (SDI) for Douglas-fir only.

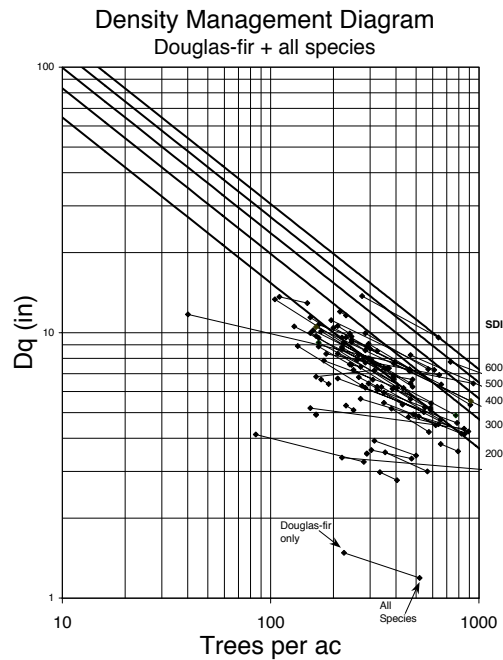


Figure2. Locatin of the 76 permanent plots regarding their stand density index (SDI) for all tree species.

report on ODF Plantation Survey). The bivariate distribution between 1998 SNC severity and three other variables - Douglas-fir stand density, Douglas-fir quadratic mean diameter, and percentage of Douglas-fir by basal area - yielded another view of plot distribution by initial SNC severity and initial levels of several important plot covariates (Figs. 3-5).

Figure 3. Plot distribution by mean needle retention and Douglas-fir SDI.

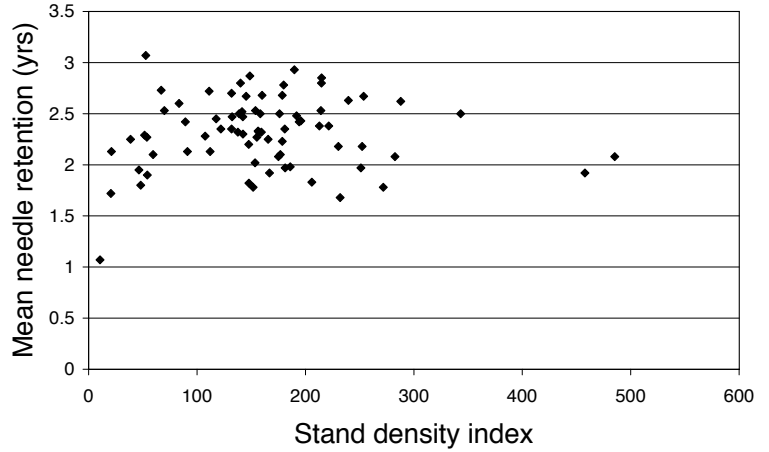


Figure 4. Plot distribution by mean needle retention and Douglas-fir quadratic mean dbh.

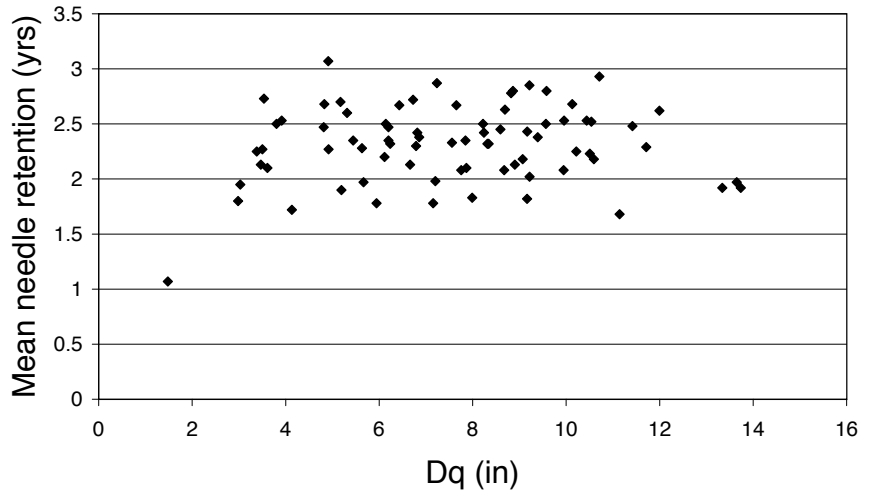
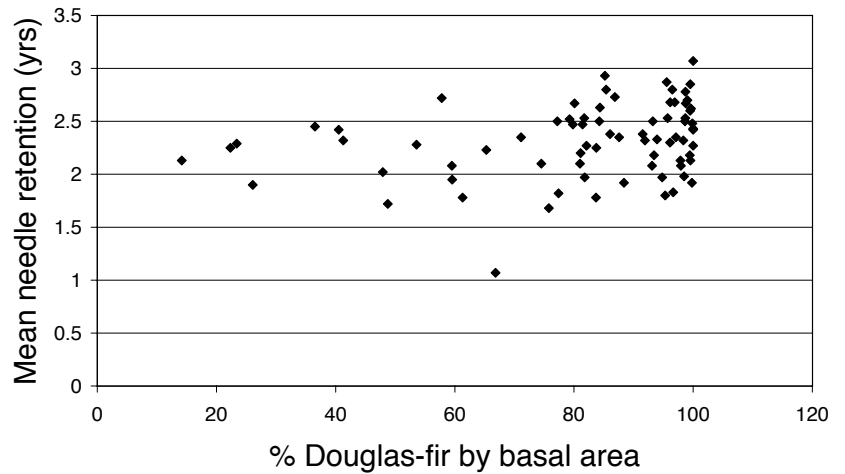


Figure 5. Plot distribution by mean needle retention and % Douglas-fir by basal area.



SWISS NEEDLE CAST INFECTION STUDIES

Progress Report 1999

Jeffrey Stone, Loretta Winton, Bryan Capitano, Dan Manter, Pablo Rosso, Paul Reeser, Wendy Sutton, Everett Hansen

Cooperators: Alan Kanaskie, Katy Kavanagh, Randy Johnson

Our lab is conducting research aimed at several aspects of Swiss needle cast disease of Douglas-fir. This disease currently affects over 52,611 hectares of forested lands in western Oregon and has become an increasingly important concern as a threat to a major economic forest resource and ecologically dominant forest tree species in the Oregon Coast Range and western Cascades. Research is underway to examine the biological, ecological, and physiological interactions between the pathogen, *Phaeocryptopus gaeumannii*, and Douglas-fir to help understand all the contributing causes of the current disease outbreak. The causal agent is endemic in the area and historically has been considered a pathogen of only minor importance. One of the puzzling aspects of the disease is its current severity in many coastal plantations—the present level of disease is causing unusually high levels of defoliation and growth loss. Several possible contributing factors are being examined to account for the reasons for this and to help develop management options to minimize future disease impact.

Our research efforts are directed in six main areas:

- 1) Disease impacts in field sites; Determine conditions for infection. Compare epidemiology at various sites in the Tillamook area. Three plots are maintained in each of three areas around Tillamook. Each plot cluster includes a severely or moderately diseased plantation and lightly diseased and relatively healthy units. In each plantation we are monitoring weather, spore release and tree phenology, and infection period. We have examined needle retention, tree volume and growth, and wood anatomy at each of our sites. Additional inoculation experiments and field infection experiments are underway.
- 2) Cooperate with PNW geneticists to describe the relationship between Douglas-fir genotypes and severity of SNC. Compare SNC development in known susceptible and resistant trees. We have installed 5 of our SNC plots in progeny test plantations. Two Forest Service families are being monitored on three Forest Service sites (Cedar North, Salal Departure, and Limestone) and two State families are being monitored at Acey Creek and Coal Creek. A preliminary analysis of these families is included in this report. Work on SNC development in susceptible and resistant trees has begun with a long term outplanting study and inoculation experiments utilizing different provenances of DF.
- 3) Controlled field and greenhouse inoculation studies; Several studies are underway to determine the optimum conditions for infection, host tissue colonization and disease development. Studies underway include type of inoculum, source of inoculum, host phenology, host provenance, and effects of fertilization. We are developing methods that can be used for large scale, standardized tests for susceptibility and resistance in cooperation with USFS PNW geneticists.
- 4) Laboratory studies on pathogen physiology, infection biology and genetics; and population biology. We continue to gather, culture, and extract DNA from *Phaeocryptopus* isolates. We are continuing to maintain and process a collection of a worldwide sample of PG populations. We have initial ITS sequences. Pathogenicity tests comparing Tillamook and other isolates have been conducted and others are in progress. Single ascospore cultures have been prepared from more than 200 isolates of *Phaeocryptopus*. DNA extraction

and RAPD amplification procedures have been worked out, and new, more efficient protocols are now being used.

- 5) Methods for detection and quantification. We have completed evaluation of detection methods based on needle clearing, epifluorescence and light microscopy of needle surfaces, and direct isolation of the fungus. We have completed development of PG-specific DNA probes for infection detection and quantification. Further observations on initial infection and needle colonization by the pathogen are reported here. We have also been working to develop more effective means for quantification of the fungus within foliage by means of ergosterol analysis. We are developing methods to use digital microscopy and image analysis. These methods are being developed to augment our analyses and to provide research tools for cooperating researchers.
- 6) Landscape level analysis of disease severity and spread. Preliminary results are reported on risk analysis of Swiss needle cast in western Oregon. Further analyses with remote sensing technology are in progress.

Summary of Specific Studies in Progress

Field studies

Monitoring of tree growth, climatic factors, and disease effects in nine sites in coastal Oregon.

1. temperature, humidity and rainfall data for each site
2. tree height and diameter growth in relation to disease

3. needle retention, canopy density, transparency, discoloration rating
4. assessment of pseudothecium production on field collected branches
5. comparisons of site factors in disease severity
6. comparisons of seedling provenance/family group in disease impact

Observations on timing of field infection:

1. trap tree (exposure timing) experiments

Monitoring of timing ascospore release and concentration

1. ascospore release ("spore shoot") from field collected foliage
2. weekly quantification of ascospores (spore sampling) during spring-summer

Interactions between PG and other foliage pathogens

1. Rhizoctonia needle blight

Inoculation studies

Controlled farm/greenhouse inoculations

1. Compare effects of ascospore and culture-based inocula on infection/disease
2. Effects of tree phenology on infection
3. Effects nutrients on infection and disease severity
4. Effects of tree source
5. Variation in virulence among PG isolates
6. Non-host inoculations

Laboratory Studies

Infection Biology of *P. gaeumannii*

1. Histological studies, light and electron microscopy

Physiology of *P. gaeumannii*

1. Growth optima
2. Effects of specific growth inhibitors (e.g. melanin, chitin synthesis inhibitors)
3. Carbon and nitrogen nutrition, saprobic growth

Genetics

1. Genetic variation in geographically different isolates of *P. gaeumannii*
2. Population biology of *P. gaeumannii*
3. Phylogeny of *P. gaeumannii*

Detection/quantification of fungal infection

Assessment of colonization of needles

1. pseudothecium counts
2. needle dissection and culture
3. optical and scanning electron microscopy
4. digital imaging/image analysis

Biochemical methods

1. PCR-based (nucleic acid) probe
2. Ergosterol content

Digital photography/image analysis

Landscape level analysis

1. Risk analysis
2. Remote sensing approaches

Preliminary Results

Climatic factors

Nine study plots are installed in three clusters each including one plantation with moderate or severe disease, one with visible but not obviously damaging disease, and one relatively disease-free site (Tables 1, 2). Each plot has a meteorological station, with continuous recording of rainfall, temperature and leaf wetness.

Ongoing activities at each plot include:

Needles with fruiting bodies are collected at intervals and tested for spore release potential.

Needles are collected and preserved weekly for later analysis of fungus development within needle tissues. Disease level is estimated by color and retention of needles.

Height growth increment and DBH are measured once each year.

Potted seedling inoculum exposure experiments are underway at 3 sites.

We have installed uniform weather monitoring equipment at our field sites: temperature, leaf wetness and tipping bucket raingauges. At three sites, temperature/leaf wetness sensors are deployed at the tree base and upper canopy to give upper-lower canopy comparisons. We have weather data for nine sites for the past two years, and we are analyzing these data to determine whether there are any trends in relation to disease severity. In particular we are comparing cumulative hours of leaf wetness within specific temperature limits (Table 3) for the optimal growth range for *P. gaeumannii*. There are small but consistent differences in temperature among sites, with the low elevation/higher disease sites being warmer and slightly drier much of the year (Figure 1). Rainfall is probably not limiting at any sites on the wet west side of the Coast Ranges. Rainfall during spring and summer 1998 and 1999 did not show a very good correlation with disease severity

Table 1. Field plots.

	AGENCY	PREVIOUS STAND
Nehalem area		
North Fork	ODF	? alder rehab after spruce and hemlock
Coal Creek Progeny	ODF	small DF and hemlock after spruce and hemlock
Acey Creek Progeny	ODF	hemlock, spruce and DF
Tillamook area		
Juno Hill	ODF	?alder rehab after spruce and hemlock
Lower Stone Rd	ODF	DF, spruce and hemlock
Upper Stone Rd	ODF	DF
Hebo area		
Salal Departure Progeny	USFS	hemlock spruce and DF
Cedar North Progeny	USFS	DF, hemlock, and spruce
Limestone Progeny	USFS	DF

Table 2. Characteristics of field plots.

Site	Disease Severity	Elevation (ft)	Miles to ocean/bay	Age (1996)	Seed Source	Aspect
JUNO HILL	Severe	380	2.25	14	Boundary 1800FT	NE
STONE RD LOWER	Mild	430	14.75	14	Boundary 1800FT	SW
STONE RD UPPER	Healthy	1700	14.5	14	Boundary 1800FT	N
N FORK COAL CRK	Severe	160	4.75	10	Boundary 1800FT	SW
PROGENY	Moderate	220	5	10	1600FT & 1400FT	SE
ACEY CRK PROGENY	Healthy	670	8	10	1600FT & 1400FT	E
SALAL PROGENY	Moderate	370	4	9	1000FT	NW
CEDAR NORTH PROGENY	Mild	1500	7.5	9	1000FT	NW
LIMESTONE PROGENY	Healthy	890	12.25	9	1000FT	N

Table 3. Cumulative leaf wetness hours (leaf wetness > 1) at two temperature ranges, 16–22 C and 12–26 C, at nine field sites during the main infection period in 1998 and 1999.

Location	4/1/98 to 8/31/98			4/30/99 to 8/25/99		
	plot rating	1998		plot rating	1999	
		16-22 C	12-26 C		16-22 C	12-26 C
Acey w. station	2	69	728	2	39	480
Coal cr. w. station	3	81	599	3	44	494
N. fork w. station	4	175	909	6	82	594
Acey tree top	2	23	396	2	30	436
N. fork tree top	4	77	697	6	29	463
Upper st. w. station	2	97	700	3	6	336 (1)
Lower st. w. station	3	57	639	3	9	202 (2)
Juno w. station	6	47	840	6	42	723
Upper st. tree top	2	18	198	3	8	276
Juno tree top	6	57	648	6	76	737
Limestone	2	4	384	3	9	202
Cedar north	3	50	578	3	44	446
Salal	4	212	1113	4	4	393
Limestone tree top		nd	nd	3	19	289
Salal tree top		nd	nd	4	44	588

notes

There was little or no contribution during April 1998. Only a few dataloggers were deployed during April 1999, and they gave little or no contribution.

(1) missing from 4/30/99 to 5/13/99

(2) missing from 8/6/99 to 8/27/99. During this period mean at all other sites was 217 (at 12-26 C).

in the sites. Because May and June are the months when spore release is the highest, total precipitation during these months would affect spore dispersal. June precipitation does not appear to be well correlated with disease (Figure 2).

The sites with the highest disease ratings, North Fork, Juno Hill, and Salal all had high leaf wetness values compared to the other sites. These sites generally had the most hours of leaf wetness within the temperature limits 16–22C or 12–26 for both 1998 and 1999, although this was not always true. North fork had the most leaf wetness hours in both temperature ranges in both years

for the north group of sites, Juno hill was the highest in the middle group at both ranges in 1999 and between 12–26 in 1998, Salal had the most

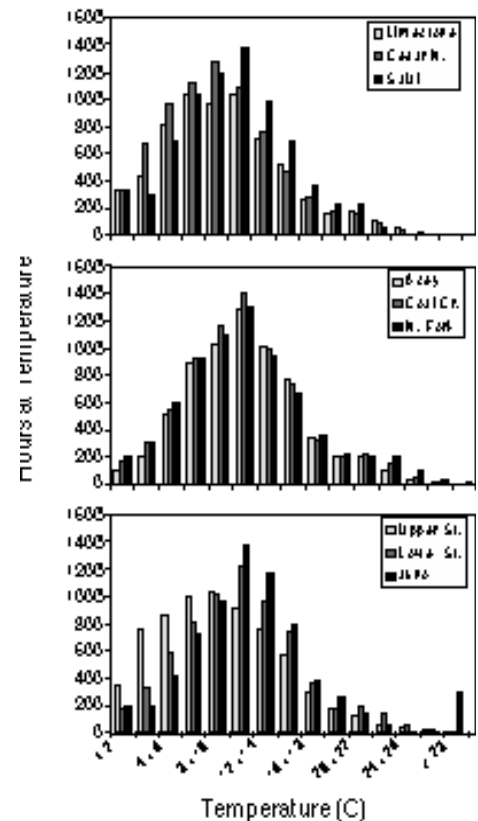


Figure 1. Temperature distributions for nine coastal sites Jan–Dec, 1998.

leaf wetness hours of the southern group for both temperature ranges in 1998 only. For the two years, the sites with the highest disease rating also had the most leaf wetness hours in both temperature ranges (Table 3, Figure 3).

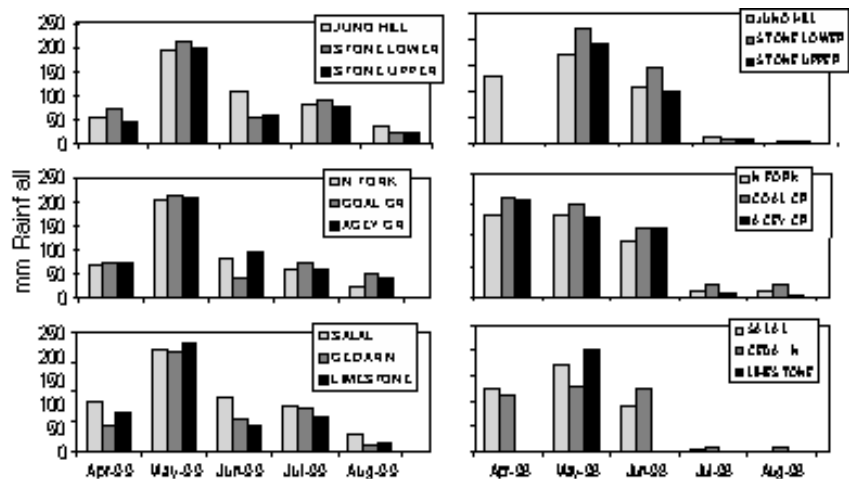


Figure 2. Spring and summer rainfall at nine coastal sites 1998 and 1999.

Seedling exposure experiments 1997-1998

Potted seedlings were exposed at the Salal site for two-week periods between March 6 and Sept 24, 1997. Groups of 20 trees were placed near infected trees at the Salal site and then returned to Corvallis for incubation to allow pseudothecium formation for one year. Five branchlets were clipped from each seedling in June 1999 to assess infection levels. The highest percent of needles that became infected were from seedlings exposed in the first two weeks of June, 1997 (Figure 4). There was apparently some background infection from the seedlings that had a minor level of infection in the nursery. Trees exposed at the Salal site between March 6 and 15 May had about 10% of their needles infected, which must have occurred at the OSU Botany Farm, since the 1998 needles that were scored for infection had not even been formed when the trees were exposed. Control seedlings that were

kept at the Botany Farm also had a low, approximately 10%, incidence of infection. Seedlings exposed in late May and early June had incidences of infection approaching 90%, much higher than the background levels. Infection that occurred after July 4 was very much lower, and because there was background infection at the OSU Farm, it is not possible to determine whether the late summer exposures at the Salal site led to the infections.

Density of pseudothecia was also higher in the seedlings that were exposed in May and June 1997. Seedlings exposed at the Salal site in May and June had pseudothecia densities of 70–80% (80% of stomata occupied), whereas trees apparently infected at the OSU farm had 20-30%. The greater number of pseudothecia formed on trees that also had a higher incidence of infection suggests that higher levels of inoculum lead to increased disease severity (density of pseudothecia), i.e. that multiple infections of a needle lead to a greater proportion of the needle

being colonized and greater numbers of pseudothecia. Trees exposed at Salal in April and early May also had higher pseudothecia densities than seedlings that remained at the OSU farm for the entire season or were exposed at Salal before budbreak (Figure 5). This probably reflects higher infection levels resulting from early sporulation at the site.

Incidence of infection in trees exposed in 1998 followed a similar pattern; highest incidence of infection was found in trees that were exposed in early May to early June. The proportion of needles infected was not as great as in 1997. The maximum incidence of needles bearing pseudothecia was about 50% in 1998 (Figure 6).

In 1997, there was a pronounced peak in infection in June that corresponded with rainfall during the period. There was low rainfall measured in late May and correspondingly low infection. In contrast, there was more precipitation early in the infection period in 1998 and the infection period began abruptly in mid May and extended into July. Even though the amount of measured rainfall in July was similar for both years, there was very little infection in July 1997 in contrast to 1998. Incidence of infection correlated well with rainfall during the period from early May through late June. Little infection occurred prior to mid May in both years, even though rainfall was adequate. Following pseudothecial maturation however, infection was closely correlated with rainfall until pseudothecia became depleted of spores in early to mid July. Even though rainfall was adequate, incidence of infection was low in early July in 1997 and late July in 1998.

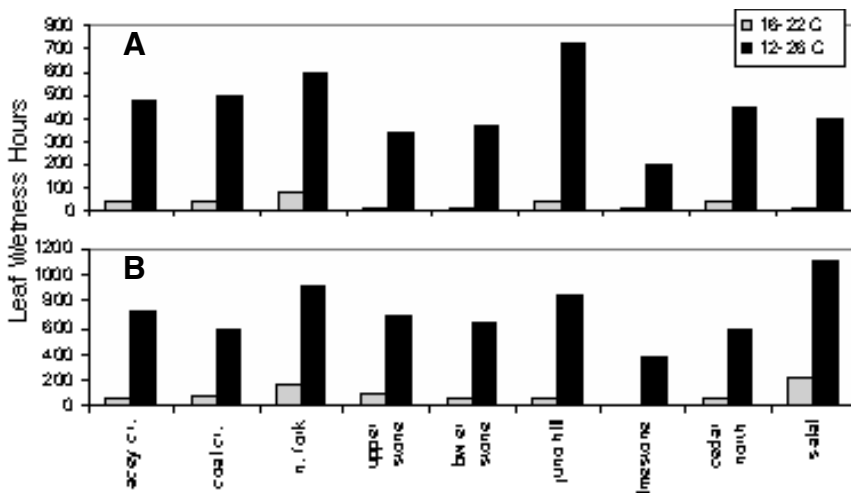


Figure 3. Comparisons of total hours of leaf wetness between 16–22 C and 12–26 C at nine coastal sites in 1998 (A) and 1999 (B).

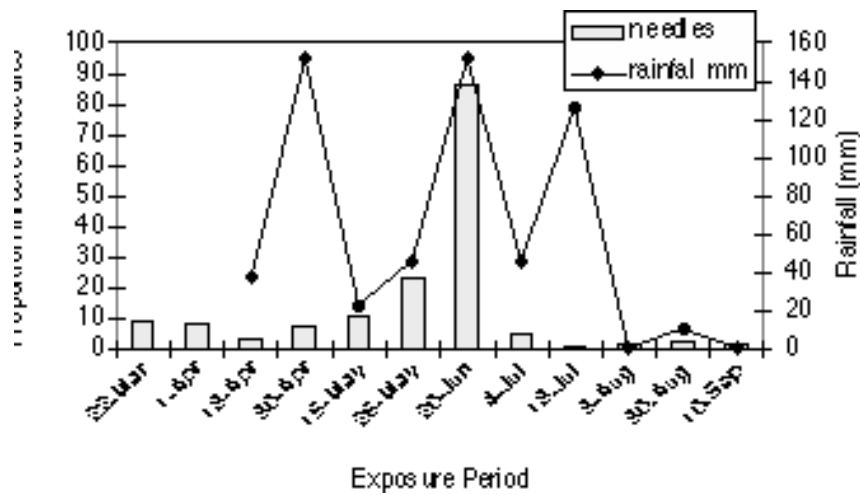


Figure 4. Incidence of infection (% needles infected) in seedlings exposed at the Salal site for two-week intervals in spring-summer 1997 in relation to rainfall.

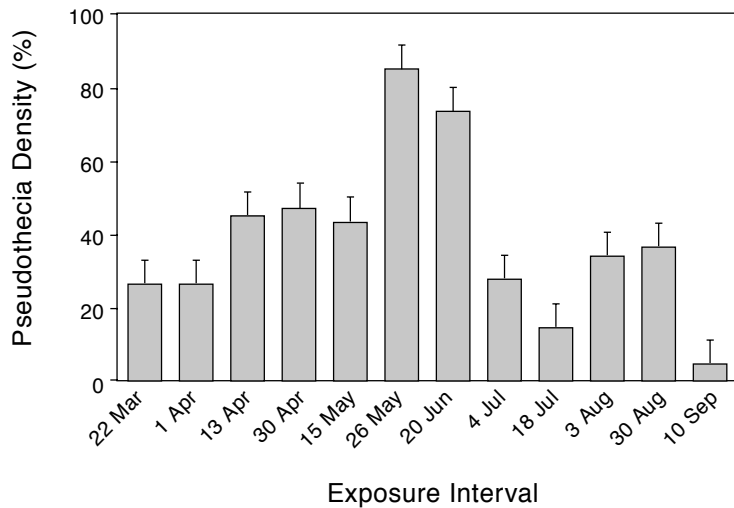


Figure 5. Density of pseudothecia on needles of potted seedlings exposed at the Salal site for two-week intervals in spring-summer 1997. Data are missing for the 2/24-3/2 and 6/9-6/24 periods.

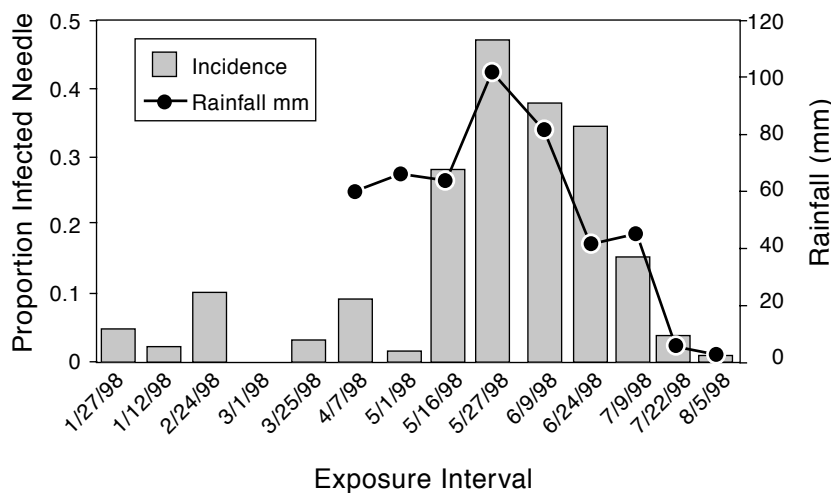


Figure 6. Incidence of infection in seedlings exposed for two-week periods at the Salal site in relation to rainfall. Missing infection data from the 6/9-6/24 interval.

Ascospore production and release is very seasonal. Maturation of pseudothecia appears to be almost synchronous, with a peak in early June, and depletion of ascospores combined with reduced rainfall to limit infections by mid July.

Impact of *Phaeocryptopus* infection on growth and needle retention of Douglas-fir.

Although the fungus is constantly associated with diseased trees, it is also present on trees with minimal symptoms of disease. It is therefore important to distinguish between the presence and the abundance of the pathogen, *Phaeocryptopus gaeu-mannii*, and disease severity. Presence of the pathogen is a necessary but not sufficient condition for Swiss needle cast disease. Severity of disease symptoms vary among sites and trees, and are apparently influenced by a variety of biological and environmental factors.

At each of our nine test sites, ten or twenty trees are marked and monitored twice each year. Growth, tree height, diameter, crown density, transparency and disease symptoms (color and needle retention) are recorded. On our progeny test sites, 10 trees of each of two families are monitored.

Needle retention of one-year-old needles was similar for all sites, and differences between 1999, 1998 and 1997 measurements were small from most sites. Only North Fork had markedly lower retention of one-year old needles in 1999 (**Figure 7**). Disease severity among sites is more appar-

ent in the retention of two-year-old needles. There were much lower values apparent at the Juno site for all three years. In general a greater proportion of the two-year-old needles were held in 1998 than in 1997 but less in 1999 than 1998 at all sites (Figure 7). Overall canopy density and transparency also had the most severe symptoms at the Juno site, with more minor variations among the other sites. A greater proportion of the trees at the Juno site are also severely chlorotic (Figure 8).

Density of pseudothecia, shown in figure 9 corresponds relatively well with needle retention. Sites with poorer needle retention (North Fork and Juno Hill) have the highest densities of pseudothecia. In general there is a greater density of pseudothecia in the two-year-old needles, except at the most severely diseased sites, where retention of two-year-old needles is poor. The most heavily infected two-year-old needles are abscised and the remaining attached two-year-old needles have lower pseudothecial densities.

A regression of pseudothecia density and needle retention is shown in Figure 10. Needle retention is well correlated with pseudothecia density within the plot groups, although across plot groups there are greater differences in pseudothecia density. Growth is severely affected by premature needle loss due to Swiss needle cast (Figure 11).

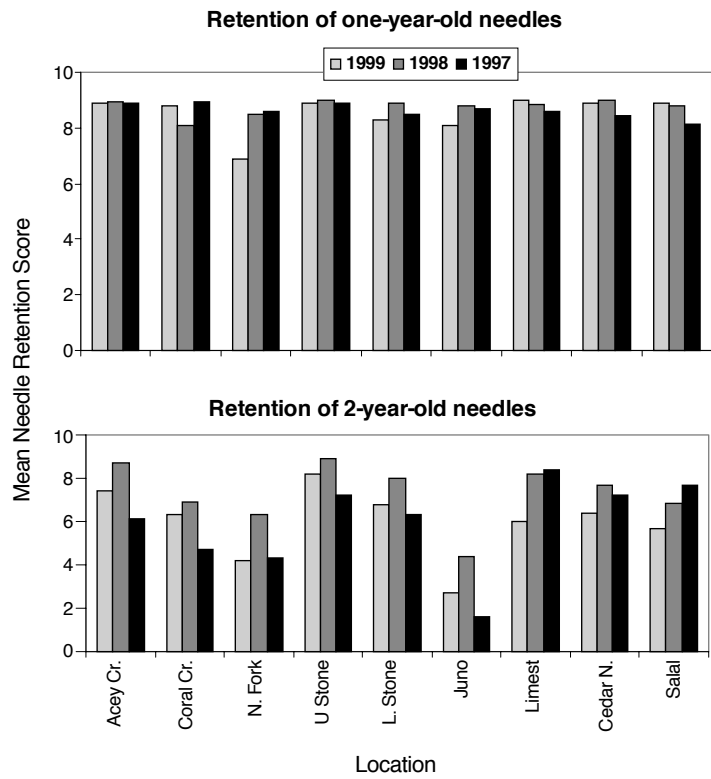


Figure 7. Retention of one- and two-year old needles at nine coastal sites for 1997, 1998, and 1999.

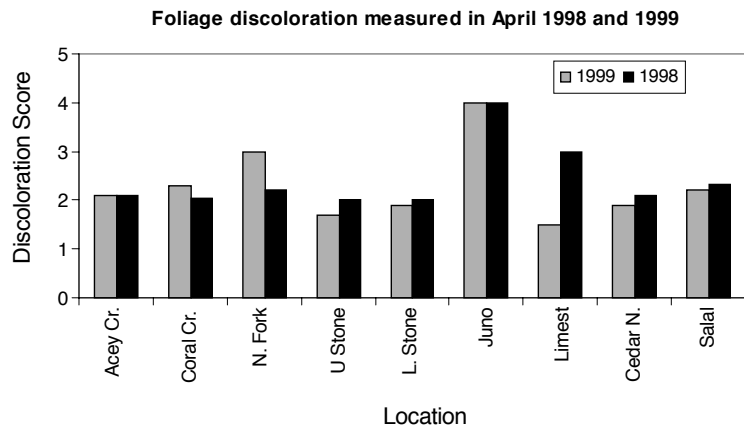
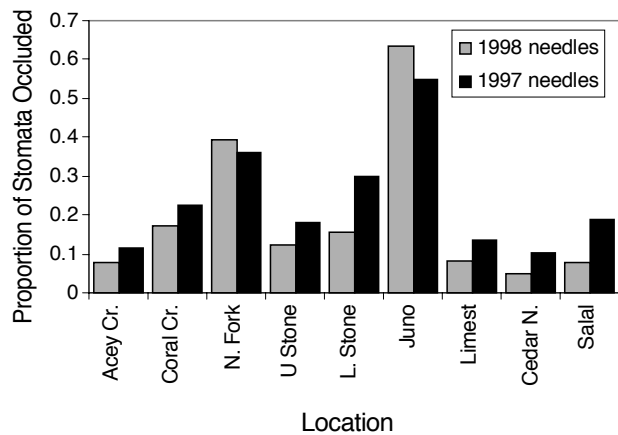


Figure 8. Foliage discoloration ratings for nine coastal sites, 1998 and 1999.

Figure 9. Density of pseudothecia on one- and two-year old needles measured in spring 1999 prior to budbreak.



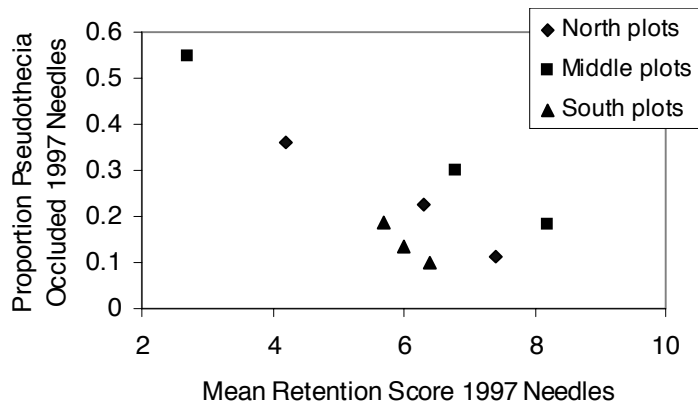


Figure 10. Relation between pseudothecia density and needle retention in 1999. $R^2 = 0.873$.

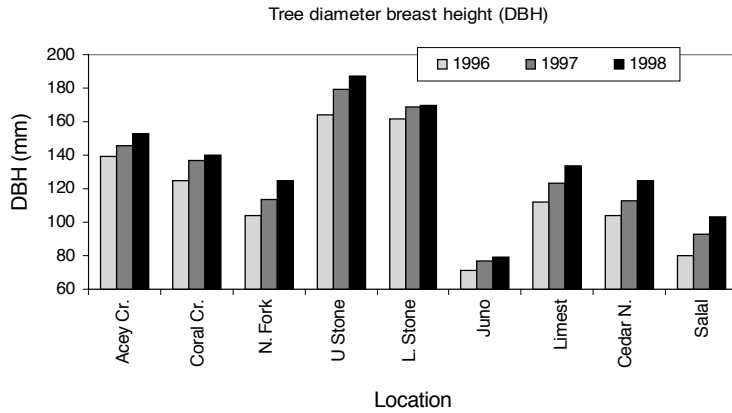


Figure 11. Tree diameter for nine coastal sites 1996–1998.

PART 2

Genetics of Phaeocryptopus

The hypothesis that current disease levels may be caused by a novel, more virulent *P. gaeumannii* strain has often been postulated but has never been tested. If the Tillamook epidemic is the result of a new or unique genetic strain, then it must be either: a) a native genotype that has changed at one or a few loci, or b) an import from elsewhere. If it is an import, then we might expect significant genotypic similarities between Tillamook populations at severe disease sites and populations in other high disease locations such as Europe or New Zealand. On the other hand, if it is a derived native genotype, then local populations should be more closely related to each other. To address these issues we have nearly completed an inoculation experiment designed to satisfy Koch's postulates and to test for differences in pathogenicity among isolates from different geographic origins. Also we are continuing a molecular population genetics study

to determine the possible origin of *P. gaeumannii* populations involved in the Tillamook epidemic.

Pathogenicity Tests

Experimental Design. Single-spore isolates from 4 sites (2 Tillamook severely diseased sites, 1 Tillamook mildly diseased site, and 1 mildly diseased site outside of the epidemic area) were grown in potato-dextrose broth (PDB) for 2 months. The mycelium was filtered, rinsed, weighed, and ground with a polytron homogenizer. A negative control was prepared from autoclaved mycelium. Each inoculum treatment was adjusted to .02 mg/ml dH₂O, and 25 ml were applied 2 weeks after budburst in May 1997 with an airbrush paint sprayer. Treated seedlings were incubated in a mist chamber for 4 days. 400 seedlings were randomly assigned to ten treatment combinations (**Table 4**) including two seed sources and 5 inoculum treatments. In May 1998 and May 1999, branches were collected from each seedling and evaluated for pseudothecial development. In Sept. 1998 and Sept. 1999 each seedling was measured for height, diameter, and needle retention.

Preliminary Results. Koch's postulates have now been completed. The inoculation method was successful, and one year after inoculation resulted in near absence of pseudothecia on the control seedlings (**Figure 12**). It is estimated that .9% of the control needles were infected one year after inoculation in spring 1998 (95% confidence interval from .5% to 1.3%). At this point it is unknown whether this is the result of infection acquired in the nursery or control branches touching non-control branches in the mist chamber. Because we inoculated with single-spore isolates and still obtained pseudothecia, it is probable that *P. gaeumannii* is capable of inbreeding. But because of the low amounts of infection on the control seedlings, we cannot rule out mating of inoculated strains with strains already residing in nursery infected seedlings. In a small companion study we inoculated each seedling with two different isolates. Some of these crosses resulted in higher pseudothecial formation than did the uncrossed inoculations (data not presented). This suggests that *P. gaeumannii* may also outcross. These results, although suggestive, are preliminary. The initial inoculation groups were small and the experiments need to be repeated.

On inoculated needles evaluated one year after infection (Spring 1998), there were generally higher levels of infection upon the Klamath Falls seed source than the Tillamook seed source (one-sided p-value = .0001). There is moderate evidence that infection level depends upon inoculum source alone (p-value = .028).

Table 4. Treatment combinations used in pathogenicity tests. The inoculum sources were obtained from stands expressing either mild or severe SNC as judged by needle retention and color.

Seed Source	Inoculum Source	SNC Disease Level
Tillamook	Negative Control	-
	Limestone	Mild
Klamath Falls	Cascade Mountains	Mild
	North Fork	Severe
	Juno Hill	Severe

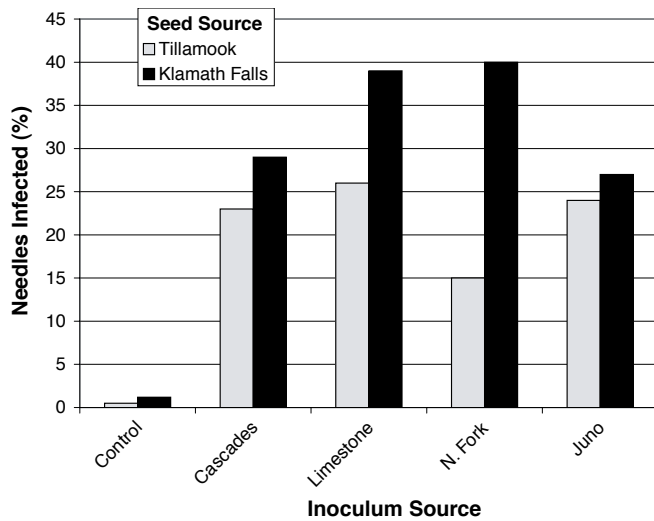


Figure 12. Average percentage of infected, artificially inoculated needles for the 40 seedlings in each treatment combination. In 1998, one year after inoculation, 100 of the 1997 needles were evaluated from each seedling.

However there is convincing evidence of an interaction between the seed and inoculum sources (p -value $< .0001$). It is interesting that, compared to the Juno Hill isolate, the North Fork isolate causes increased infection on Klamath seedlings and reduced infection on Tillamook seedlings. There is corroborating evidence. Both of these sites are severely diseased yet pseudothecial scores on field samples from these sites reveal far fewer pseudothecia on needles from North Fork (mean pseudothecial score = 2.5) than on those from Juno Hill (mean pseudothecial score = 4.3). In addition, hyphal abundance on needles collected from North Fork (480 $\mu\text{m}/\text{mm}^2$) is much less than would be expected when compared to Juno Hill (1062 $\mu\text{m}/\text{mm}^2$) and the relatively healthy Acey Creek site (843 $\mu\text{m}/\text{mm}^2$).

In Spring 1999, two years after inoculation, many seedlings had cast the inoculated 1997 needles. However 1998 needles, which were presumably naturally infected in

spring 1998 by ascospores from the needles inoculated artificially the previous year had an estimated 40% infection on the Klamath control seedlings and an estimated 8% infection on the Tillamook control seedlings (95% confidence intervals from 27% to 53% and 3% to 13% respectively) (Figure 13).

Needle Retention on inoculated needles 16 months after inoculation (Fall 1998) was higher on Klamath than on Tillamook seedlings (p -value = .0001) and on both seed sources there is ample evidence that inoculated seedlings retained fewer needles than unin-

oculated seedlings (p -value = .0001). There is also moderate evidence that needle retention depended upon inoculum source (p -value = .03) with the Juno Hill isolate causing about 10% less needle retention than isolates from the other three locations (95% confidence interval from 2% to 17%) (Figure 14).

On inoculated needles 2 years post inoculation (Fall 1999) there is no evidence that treatment groups alone differ in needle retention (p -value = .331). There is ample evidence, however, that seed sources still differ in needle retention (p -value $< .0001$) and slight evidence of an interaction effect between the

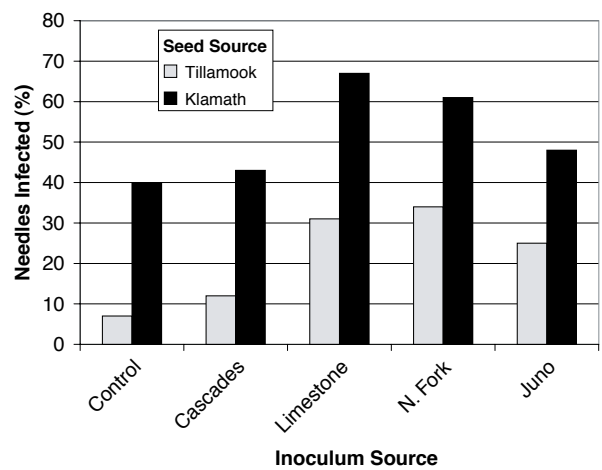


Figure 13. Average percentage of naturally infected, 1998 needles for the 40 seedlings in each treatment combination. In 1999, two years after inoculation of 1997 needles, 100 of the 1998 needles were evaluated from each seedling.

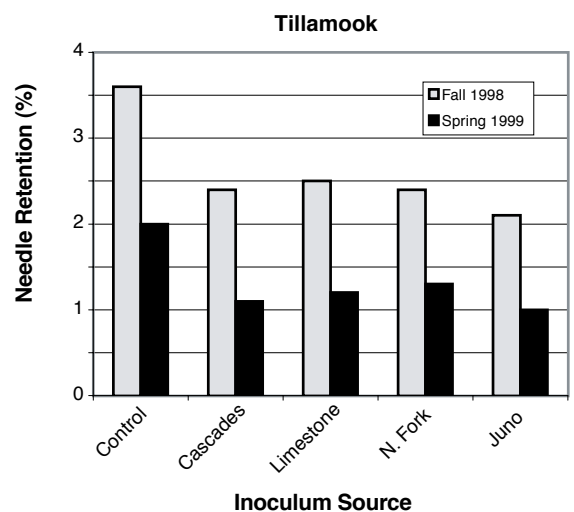


Figure 14. Average needle retention on the inoculated, 1997 internodes when evaluated in Sept. 1998 and May 1999. (1 = 0-20%, 2 = 20-40%, 3 = 40-60%, 4 = 60-80%, 5 = 80-100% needles retained).

treatment groups and seed sources (p-value = .053). While the Klamath Falls seedlings did not exhibit differences between the controls and the inoculum sources, the Tillamook seedlings exhibited an estimated 20% reduction in needle retention when comparing inoculated seedlings to control seedlings.

There is good evidence that both 1998 height and diameter growth (Figures 15 & 16) differed from the control for the Juno Hill inoculum on Klamath Falls seedlings (p-value = .0043). There is also suggestive, but inconclusive, evidence that treatment alone affected seedling height by Sept. 1999 (Figure 17), three growing seasons after inoculation (p-value = .078). Evidence for an interaction between the seed and inoculum sources is weak (p-value = .085). For Klamath Falls seedlings, only the Juno Hill strain reduced height growth compared to the control. For Tillamook seedlings, heights for the control seedlings were lowest, but not significantly.

Molecular Fungal Population Genetics

So far, we have a worldwide culture collection of about 825 single spore isolates, most of which are from the Pacific Northwest (Table 5). The samples collected from the 9 Tillamook test plots span 3 years in order to tell if fungal population structure has altered within this time as disease has increased. A preliminary study using RAPD (Random-amplified polymorphic DNA) fingerprinting as a means to estimate genetic diversity within *P. gaeumannii* has been com-

pleted. We used a small subset of our isolates for the pilot study: three populations in Washington, five in Oregon, three of which were in the Tillamook area, and two isolates from Pennsylvania.

In Figure 18, the length of the branches corresponds to relative similarity of the isolates fingerprints. Although the sample sizes and number of markers were too small for conclusions, it is evident that there is significant genetic variability in this fungus. There are slight suggestions of geographical clustering but no discernable correlation with pathogenicity. The unsuitability of these markers was revealed by the inability to reliably repeat these results. Also, Southern-blot hybridizations of the fingerprint gels suggested that most markers were linked, and therefore inappropriate. Although the RAPD

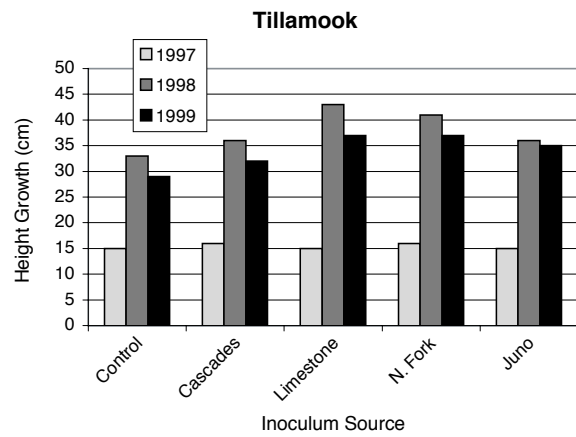


Figure 15. Average height growth of inoculated seedlings for the 1997, 1998, and 1999 growing seasons.

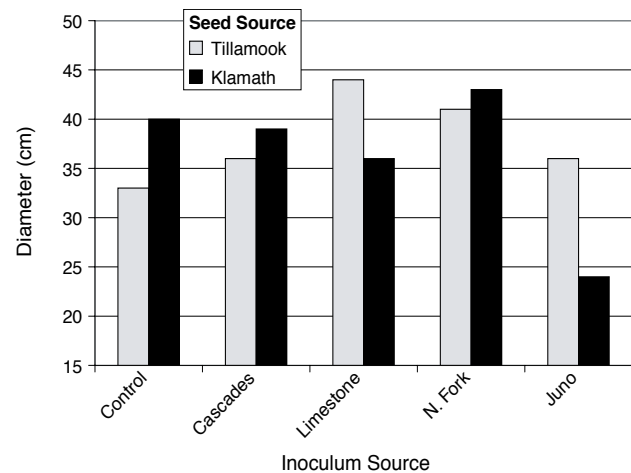


Figure 16. Average diameter of the inoculated seedlings after the 1998 growing season.

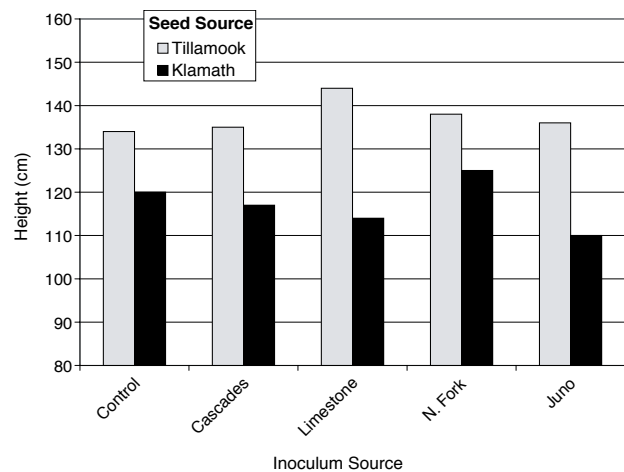


Figure 17. Average heights of the inoculated seedlings near the end of the 1999 growing season, 29 months after inoculation.

Table 5. Sample locations over three years for *P. gaeumannii* population genetic structure experiment.

1996	1997	1998
Cedar North	Cedar North	Cedar North
Salal Departure	Salal Departure	Salal Departure
Acey Creek	Acey Creek	Acey Creek
North Fork	North Fork	North Fork
Coal Creek	Coal Creek	Coal Creek
Limestone	Limestone	Limestone
Juno Hill	Juno Hill	Juno Hill
Upper Stone	Upper Stone	Upper Stone
Lower Stone	Lower Stone	Lower Stone
Sequim, WA	Mature stand near Coal Creek	Spokane WA
Forks, WA	Mature stand near Limestone	San Juan Island, WA
Pennsylvania	Mature stand near Upper Stone	
	Mature stand near Juno Hill	
	Near IFA Canby, OR	
	Near IFA Fipps, OR	
	Near IFA Toledo, WA	
	Corvallis, OR	
	Gold Beach, OR	
	Sweet Home, OR	
	Menagerie Wilderness, OR	
	Drift Creek Wilderness, OR	
	Hoquiam, WA	
	Forks, WA	
	Olympia, WA	
	Vermont	
	New York	
	New Mexico	
	England	
	Germany	
	France	
	Italy	
	Switzerland	
	New Zealand North Island	
	New Zealand South Island	

markers proved unsuitable for population genetic statistics, they did provide data suggesting high genetic variability that could be captured by more robust methods. We are therefore pursuing a sequence-based approach to detect nucleotide differences in the introns of coding genes. We have reliably detected polymorphic sites within the introns of 3 genes so far. This study will be completed winter 1999.

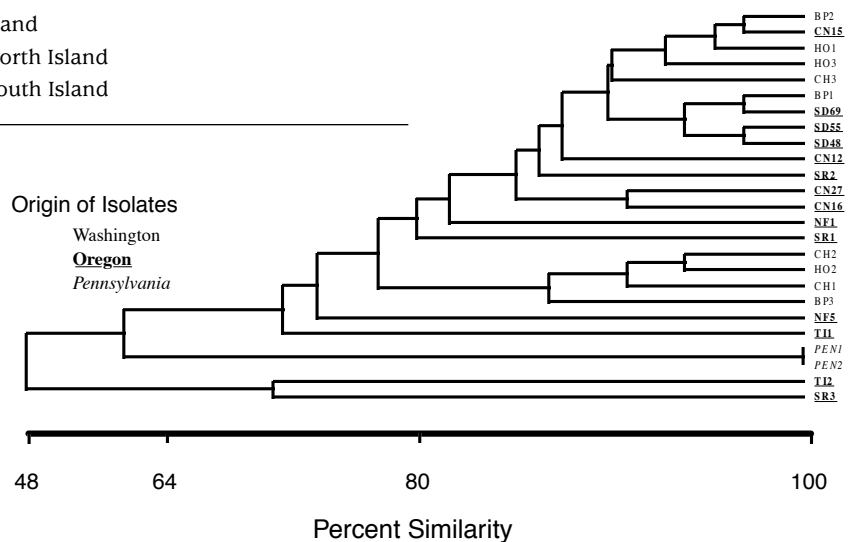


Figure 18. UPGMA phenogram for 17 markers of preliminary RAPD data. Isolates from Oregon are underlined, those from Pennsylvania are italicized, and those from Washington are in normal font.

Molecular Systematics

Current classifications place Phaeocryptopus as a member of the Venturiaceae, an ascomycete family consisting of 12 genera including Venturia. Venturia inequalis, causal agent of apple scab, has been considered the closest relative causing a well-studied disease. However, taxonomic treatments of the Venturiaceae rely heavily on subtle, variable, and evolutionarily suspect characters such as ascospore size and color. Molecular methods offer robust and independent data with which to test taxonomic classifications and which may more truly reflect genetic relatedness of fungal organisms. We have sequenced a portion of the nuclear gene coding for the ribosomal large subunit (LSU) of several members of the Venturiaceae as well as other Douglas-fir needle fungi. **Figure 19** depicts phylogenetic relationships of some members of the Venturiaceae and other fungi with bitunicate asci. Four points should be made about this tree: 1) the Venturiaceae, as pre-

sentedly defined, does not appear to be a natural group, 2) *P. gaumannii* does not appear to be closely related to any of the plant pathogens in the Venturiaceae such as *Venturia inaequalis*, *V. pyrina*, *Dibotryon morbosum*, or *Apiosporina collinsii*, 3) *P. gaumannii* does not appear to be a member of the Venturiaceae, and 4) the status of *P. nudus* is unclear. Although this analysis seems to support an anamorph-telomorph connection between *P. nudus* and *Rhizosphaera*, we have conflicting data presented below. It is possible that the DNA extracts may have been contaminated as it is very difficult to ensure that DNA from only one of two small, closely situated fungi has been extracted.

One of the current controversies in ascomycete systematics concerns monophyly of the bitunicate ascomycetes (loculoascomycetes). Although traditional classifications have usually treated these fungi as a natural group arising from a single, common ancestor, many molecular studies have contradicted this view. Unfortunately all of these studies have suffered from small sample sizes restricted to only a few of the bitunicate families. We have contributed to the large database of nuclear small subunit (SSU) ribosomal sequences by sequencing many of the bitunicate fungi encountered in studying the biology of *P. gaumannii*. **Figure 20** depicts phylogenetic relationships of the ascomycetes based on the SSU.

The inclusion of many previously unsequenced loculoascomycetes in this large comparative database has provided some support for a natural group of bitunicate fungi excluding the Chaetothyriales and Arthroniales. This unification of the Pleosporales and Dothideales although expected, has not been seen in most other molecular studies. Also note the distant placement of the two *P. nudus* sequences. While one sample supports a well delimited genus *Phaeocryptopus*, the other sample does not. Instead, by grouping with *Rhizosphaera* species and other members of the Dothideales, it suggests support for the unlikely, yet often suggested hypothesis that *Rhizosphaera* is the anamorph (asexual

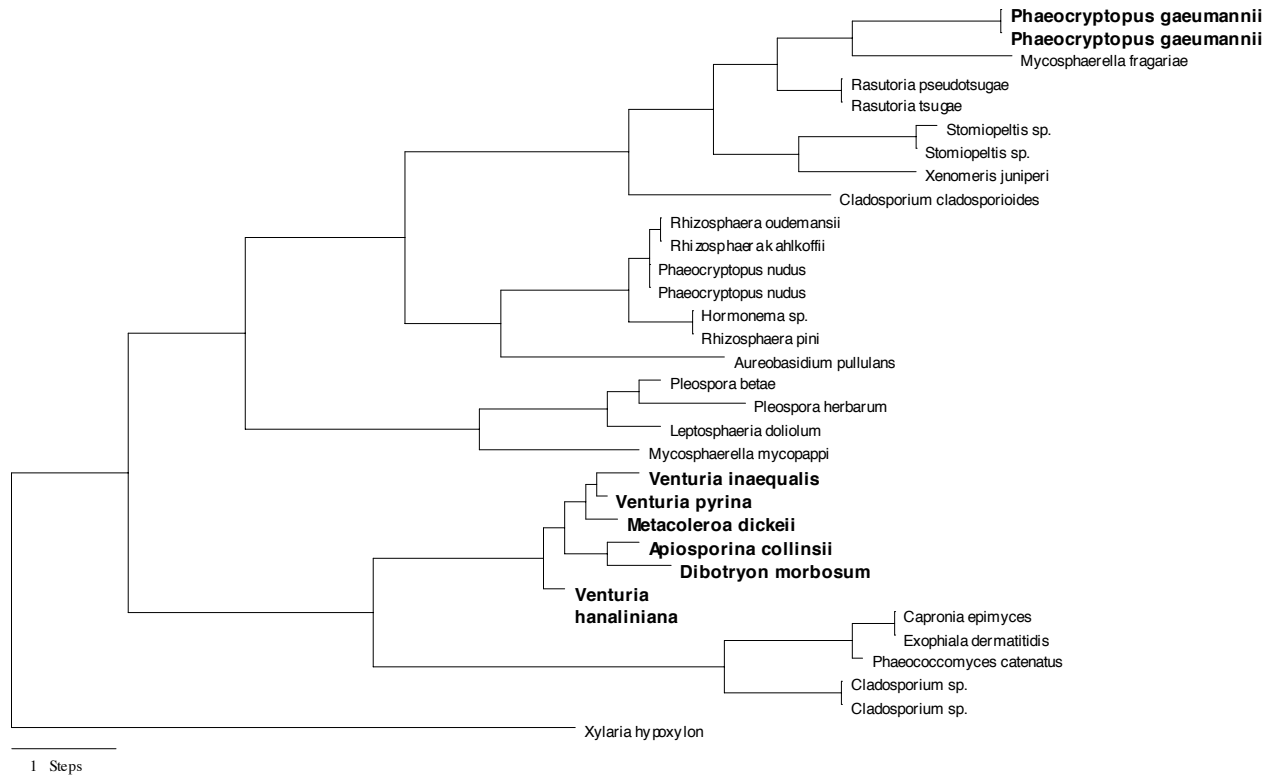


Figure 19. Single most parsimonious tree generated by maximum parsimony of LSU DNA sequences. Members of the Venturiaceae are in bold. *Xylaria hypoxylon* is the designated outgroup. The scale bar represents the number of DNA substitutions supporting the branch.

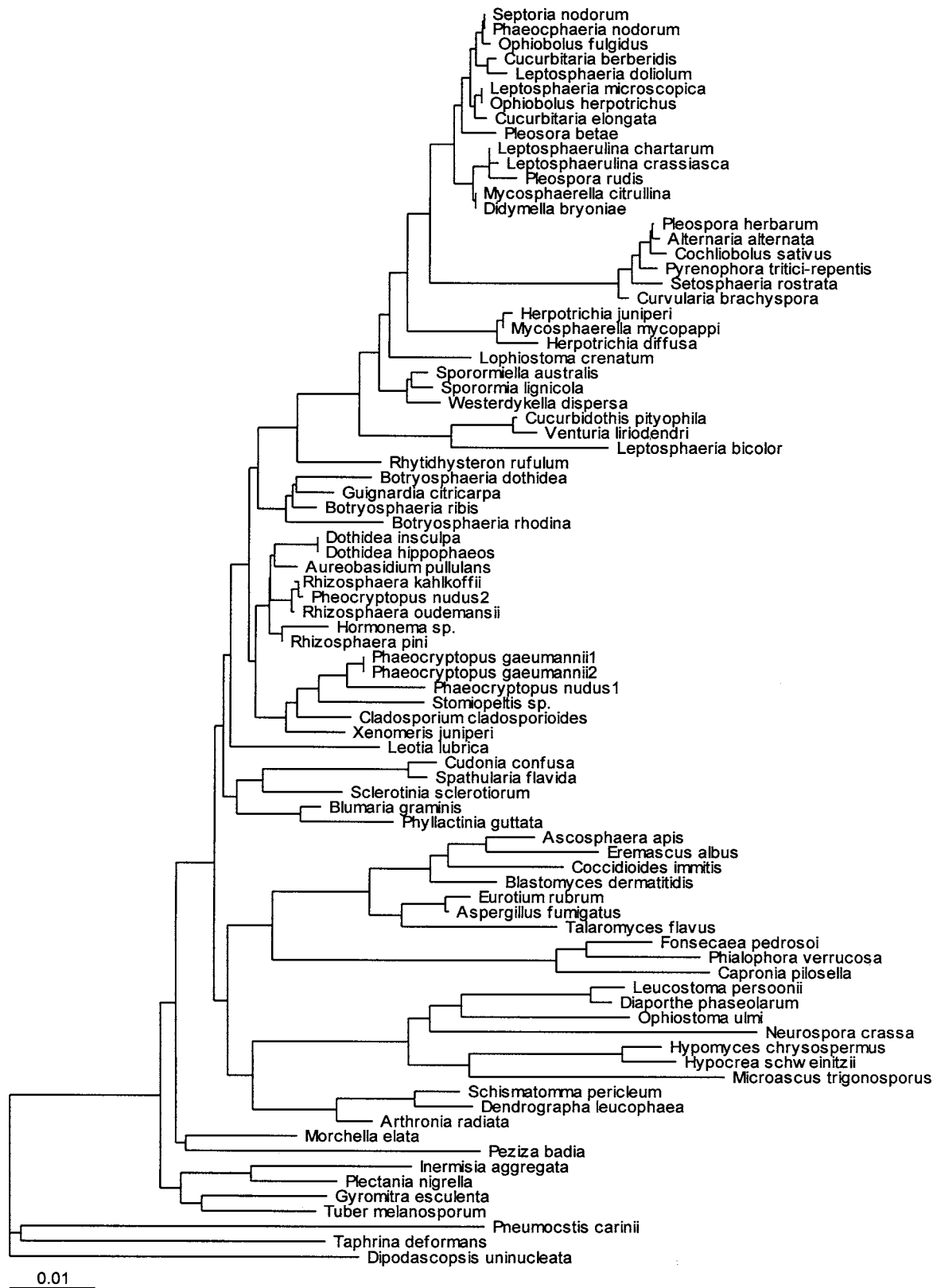


Figure 20. Neighbor-joining tree of SSU DNA sequences. The scale bar represents the percentage of sequence divergence.

state) of Phaeocryptopus. We suspect contamination in the DNA prep and are ordering a reference culture to clarify the situation.

Methods to detect and quantify the fungus in needles

DNA Probe

Improved methods to detect and quantify infection by *P. gaeumannii* will facilitate many studies already in progress or proposed by SNCC scientists for investigations on the effects of foliage infection and colonization by *P. gaeumannii*. It is now possible to quickly detect the presence of *P. gaeumannii* and to assess the total amount of *P. gaeumannii* DNA present within and on the surfaces of needles at any time of year regardless of the presence of pseudothecia. This should provide a very sensitive, standardized method for comparing total *P. gaeumannii* DNA within infected foliage that can be used in a number of planned or already in progress studies.

How it works

The probe is made highly specific to a short segment of *P. gaeumannii* DNA by first screening for short segments of DNA that are unique to *P. gaeumannii*. Next, a large number of copies that match exactly the sequence of bases of the unique *P. gaeumannii* DNA is produced. By linking these copies to a dye or radioactive label and applying it to a DNA extract from a sample, the DNA probe will adhere only to segments of DNA that have the complementary sequence and will

easily wash off non-complementary sequences. Selective binding should occur only in the DNA that came from the fungus *P. gaeumannii* and will be in proportion to the amount of *P. gaeumannii* present. Thus, the amount of dye visible adhering to a sample of DNA from a needle will be proportional to the amount of *P. gaeumannii* present.

Experimental Design. DNA was extracted from pure cultures of *P. gaeumannii* and several other Douglas-fir endophytes. Each sample was subjected to RAPD PCR that amplifies arbitrary sequences throughout the genome. The reaction products were examined side-by-side on a gel in order to identify a bands that are specific for *P. gaeumannii*. The candidate bands were excised from the gel and purified from the agarose matrix. The purified PCR products were labeled non-radioactively and hybridized separately to a nylon membrane that had sample DNA permanently bound to it (a dot-blot). To test the specificity of the probe three replicate dot-blots were prepared that contained DNA extracts of each of the fungal species used to identify the candidate probe as well as total genomic DNA of non-infected, newly flushed Douglas-fir needles. To test the sensitivity of the probe, another dot-blot was prepared in which dots had increasing amounts of *P. gaeumannii* DNA as well as dots with constant amounts of the total DNA extracted from infected Douglas-fir needles. Assay samples collected in spring 1999 of plot trees consisted of 10 randomly chosen one-year-old needles from each plot tree. Quantification of signal intensity was done

by densitometry to automatically quantify sample *P. gaeumannii* DNA by interpolation.

Preliminary Results. Ten different PCR fragments were tested at 4 different stringency regimes. Of the ten, a 900-base fragment was the most specific for *P. gaeumannii* while still retaining enough sensitivity to detect the fungus in lightly infected needles. When tested against a variety of purified DNA from fungi commonly isolated or found on Douglas-fir, the 900-base probe showed good specificity for *P. gaeumannii* (**Figure 21**) but on all three blots also hybridized weakly to the fungus *Rasutoria pseudotsugae*, a close relative of *P. gaeumannii*. Other near relatives of *P. gaeumannii* had essentially no reaction, and the probe did not bind to purified Douglas-fir DNA, which of course would be present in any foliage sample. On one blot the probe also generated a signal on the dot containing DNA extracted from *Allantophomopsis lycopodina*, the most genetically distant fungus included in the sample. It is unlikely that this binding was due to homology of the probe with a segment of DNA within the *A. lycopodina* genome. We think it was a false positive caused by damage to the membrane during preparation of the blot. The replicate blots confirmed this assumption as they did not reveal a signal for this fungus.

When hybridized to blots prepared from the total DNA extracted from samples of 10 Douglas-fir needles (**Figure 22**), the probe detected the presence of *P. gaeumannii* DNA within needles. The intensity of the staining also was proportional to

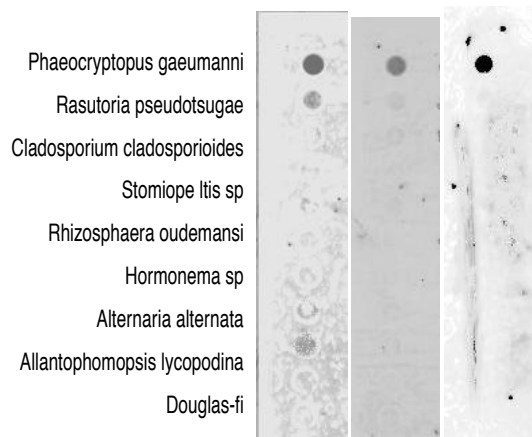


Figure 21. DNA Probe. Dot-blot demonstrating specificity of the DNA probe. Each circle contains 1 μ g of total genomic DNA. The darker the dot the more probe hybridized to the target DNA. In the first blot, the membrane was damaged when *A. lycopodina* was applied and the signal is an artifact.

different concentrations of purified *P. gaeumannii* DNA and also corresponded to the level of infection indicated by the pseudothecial score. The highest levels of infection in the 1996 and 1997 Juno foliage had apparently greater amounts of DNA than were included in the test standard (purified *P. gaeumannii* DNA).

It is evident that younger needles contained less *P. gaeumannii* DNA than older needles and each of the sites differed in amount. Juno Hill, unquestionably our most severely diseased site, had very strong signals

for both 1997 and 1996 needles and a detectable signal for 1998 needles, in which surface hyphae but no pseudothecia were visible. Upper Stone needles had more *P. gaeumannii* DNA for each age class than needles from Coal Creek. These data generally correspond with pseudothecial counts in foliage collected before budbreak in spring 1998.

Probe Assay Results. Although spanning at least 3 days, it takes only 15.5 man-hours to process 150 prepared samples and costs approximately \$.75/sample if 96 samples are processed at a time. There is ample evidence (F-test p-value < .0001) that sites differ in *Phaeocryptopus* DNA (**Figure 23**). There is overwhelming evidence that Juno Hill, our worst site by all measures, had much more *Phaeocryptopus* DNA than any other site (p-value < .0001). It is estimated that *Phaeocryptopus* DNA at Juno Hill is 489 ng higher than at the other sites (95% confidence interval from 386 to 592 ng). There is convincing

evidence that *Phaeocryptopus* DNA at N. Fork was higher than at Cedar N. and Limestone (p-values < .001) but the evidence is inconclusive as to whether N. Fork differs from Acey Cr., it's low disease companion site (p-value = .07). There is also weak evidence that U. Stone differs from Cedar N. (p-value = .022).

Table 6 shows results from correlations of probe DNA measurements with other measures of needle colonization by *P. gaeumannii*. Probe DNA correlates well with pseudothecial counts of occupied stomata (dna X severity = .712), less well with ergosterol (dna X erg = .499) and poorly with the percentage of infected needles (dna X incidence = .111) because most needles had at least a few pseudothecia.

Quantitative PCR

Real-time quantitative PCR has recently become available on campus. This method has the advantage of speed, technical simplicity, very low detection limits, and unparalleled specificity. The method utilizes fluorescent dyes in a conventional PCR reaction. As amplification of

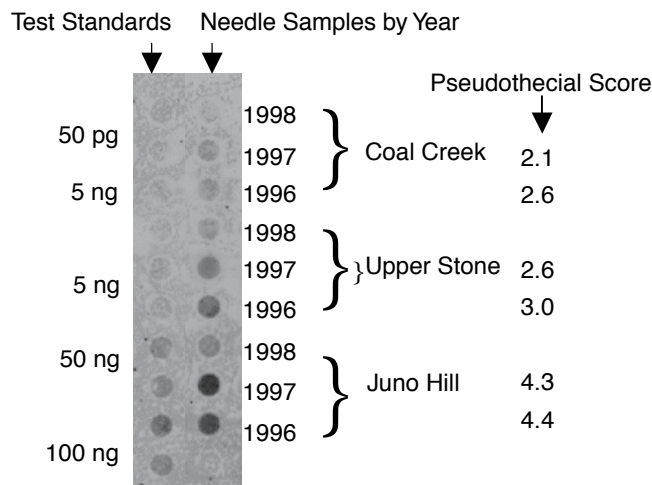


Figure 22. Dot-blot demonstrating quantitative use of the DNA probe. The first column contains increasing amounts of *P. gaeumannii* DNA for use as a comparison standard. The second column contains total genomic DNA extracted from field samples of Douglas-fir needles collected from sites expressing different levels of disease (Coal Creek = moderately diseased, Upper Stone = mildly diseased, Juno Hill = severely diseased). At each site, needles were collected separately from the 1998, 1997, and 1996 internodes. Pseudothecial scores are from Figure ? and is a visual estimate of the number of pseudothecia on needles.

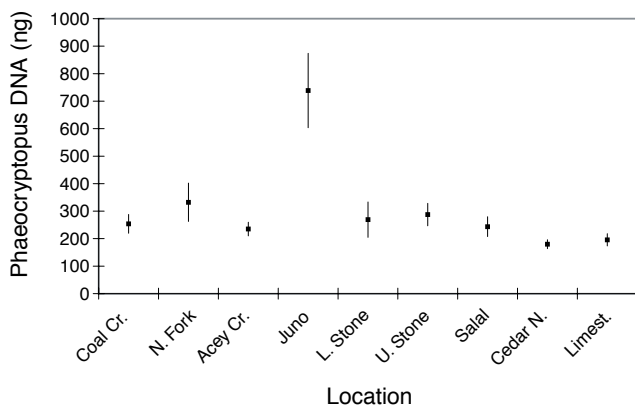


Figure 23. DNA Probe. Average *P. gaeumannii* DNA in 10 needles from each of 10 or 20 trees from each site as determined by dot-blot hybridization. Lines show 95% confidence intervals.

Table 6. Pearson Correlation Coefficients for comparisons of measures used for foliage colonization by *Phaeocryptopus gaeumannii* of 1-year-old needles.

	Dna	Erg	Severity	incidence
Dna	1			1
Erg	0.499*	1		1
Severity	0.712*	0.465*	1	1
Incidence	0.11	0.05	0.19	1

* Correlations significant at $p < .05$.

target molecules progresses, there is an increase in fluorescence. This is the only method to date suitable for detection and quantification of *P. gaeumannii* ascospores from aerial samplers as well as newly infected needles. We have completed initial tests on the EPA's quantitative PCR TaqMan instrument using *P. gaeumannii*-specific primers designed from variable regions of the beta-tubulin gene. There was no amplification of any of the other Douglas-fir needle fungi used for the probe development. Quantitative PCR detected differences in *P. gaeumannii* DNA in needles infected only one

month previous to the sample date (Figure 24). In addition, there was a difference of nearly two orders of magnitude between needles infected for one month and one year. Quantitative PCR also revealed the potential to provide quantitative information from aerial spore trap tapes. Small segments of the tapes were extracted in different volumes of buffer in order to determine the most efficient volume. Figure 25 reveals a clear relationship between extraction volume and DNA content and demonstrates successful amplification of *P. gaeumannii* DNA from spore trap tapes.

One of our main objectives has been to develop methods for quantification of fungal colonization of needles. This will help us in comparing disease resistance in trees and enable us to investigate the progress of needle colonization over time and in relation to various nutritional, environmental, and chemical factors. One method we have been using to quantify fungal colonization of needle tissue is the ergosterol assay.

Advantages of this method are that it is less technically diffi-

cult to use than the DNA probe, it is relatively inexpensive, it is rapid and it can be applied to a large number of samples. Measurement of ergosterol is less cumbersome than counting pseudothecia on individual needles, and is sensitive enough to quantify fungal biomass in needles not yet producing pseudothecia. The chief application of ergosterol analysis will be for comparative purposes. Ergosterol, a component of fungal cell membranes, can be used to assess fungal biomass in combination with pseudothecia counts or the DNA probe as a separate indication of total fungal biomass present. Measurement of ergosterol content of needles between and among trees and sites will provide an alternative quantitative measure of the levels of fungal colonization of the needles. This would be most useful in combination with pseudothecium counts, since extensive needle colonization occurs in advance of pseudothecium formation. In trees and sites with moderate to heavy colonization by *P. gaeumannii*, the relative contribution of other fungi within and on needle surfaces is probably minimal and

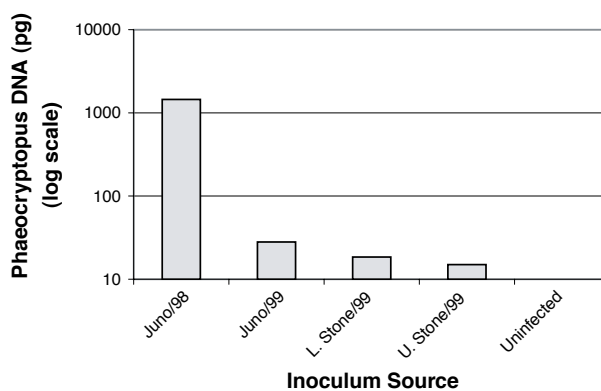


Figure 24. Quantitative PCR. Average *Phaeocryptopus* DNA in .5ul aliquots of total genomic DNA extracted from 10 needles/sample. (98 = infected for one year, 99 = infected for one month).

so ergosterol can be used as an approximate measure of *P. gaeumannii* biomass.

How it works

Ergosterol is a chemical component of fungal membranes, rarely found in plants. Thus, it has been used as an index of fungal biomass present in plant tissues (e.g., Martin et al. 1990). Samples are collected and weighed and ergosterol is extracted from foliage samples by a process involving several solvents. The concentration of ergosterol is then determined by comparing the sample with a series of known concentrations of pure ergosterol run through a high performance liquid chromatography apparatus (HPLC). The HPLC separates compounds of different composition as they move through a separation column in a chemical solvent. Separated compounds are detected according to the time it takes them to move through the column and wavelength of light they absorb. Compounds are quantified according to the amount of absorption at the peak wavelength compared to the pure standards.

Ergosterol Content from Field Sites with Varying Degrees of Swiss Needle Cast Symptoms

A comparison of measures of ergosterol content (i.e., fungal biomass) and symptom development is currently being conducted. **Fig. 26** shows the relationship between ergosterol content over the past year for our field sites. Each observation represents the mean and standard

error of ergosterol content extracted from 1998 needles from one branch on each of ten trees at each site.

The trends in ergosterol content do not always show the increasing ergosterol over time that we would expect. At some sites, ergosterol values decrease either gradually over time, or in some cases more abruptly in the spring. Decreasing ergosterol values may be due to abscission of needles during the winter. Also, the ergosterol amounts measured in the needles does not correlate well with disease symptoms. No obvious relationship between ergosterol values and symptom development.

One limitation of ergosterol is that it is non-specific, since it is a component of fungal membranes, any fungi on needles will

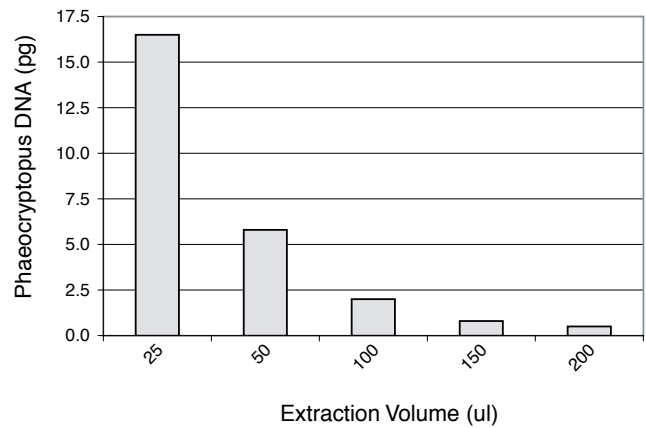


Figure 25. Quantitative PCR. Average *P. gaeumannii* DNA in .5ul aliquots of total genomic DNA extracted from one centimeter segments of spore trap tape suspended in 25-200 ul extraction buffer.

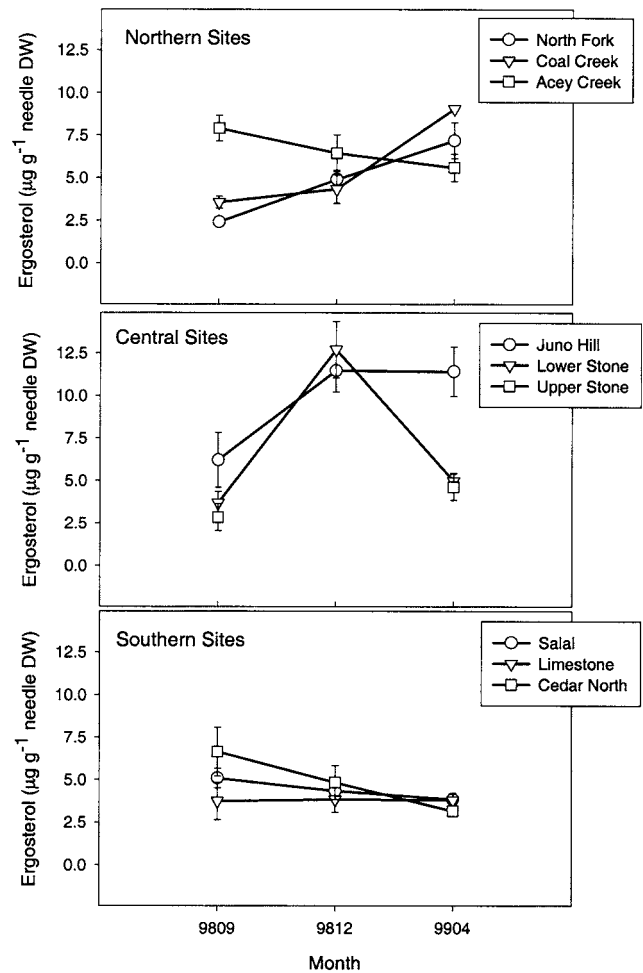


Figure 26. Development of Ergosterol Content, Hansen Field Sites, 1998 Needles only. Each symbol represents the mean of 10-20 trees; error bars are the standard error of the mean.

contribute to the total ergosterol, and lead to an erroneously high estimate of *Phaeocryptopus* levels. The DNA probe is much more specific for *Phaeocryptopus*, and was much better correlated with disease severity measures than ergosterol (see above). A second problem with the use of ergosterol can be variation in ergosterol content of cells over time. The amount of ergosterol can

change with time and in response to temperature and availability of some nutrients. The high variation in the ergosterol content measured for the nine sites in 1998 may reflect a combination of both these limitations. We are continuing to try to find a solution to these problems. Ergosterol may still prove to be a useful technique to estimate fungal biomass in needles.

SWISS NEEDLE CAST RISK ANALYSIS AND MODELING

Pablo Rosso and Everett Hansen

Introduction

The question of "why SNC here and now" has obviously a complex answer. Implicit in the question is the fact that something has changed in the Douglas-fir-Phaeocryptopus interaction that resulted in disease. This change could have been genetic and/or environmental. But in both cases the environment is a fundamental aspect of the disease development. The ecology of the disease, or epidemiology, has the role of conceptually placing the host and the pathogen within the framework of the environment. Having this framework not only helps in understanding the cause of the disease, it makes the disease more predictable, and hence, manageable.

SNC occurs in some areas and not in others. It is also evident that the sole presence of the pathogen does not determine the presence of the disease, because the pathogen is everywhere. In terms of understanding this, we could ask: "where is SNC now?" and "where next?". These questions can be re-phrased in terms of "what are the risks of SNC occurring in a certain area?"

The answer can be approached through the construction of a model that: a) understands the conditions for disease development and expression, and b) simulates these condi-

tions and assigns a level of risk at any point in space. This model has a very important geographic component. Geographic information systems (GIS) is a generic name for techniques and tools capable of dealing with entities (stands, plots, etc.) that have a spatial component, which means that their location is also an attribute as important as their structure, composition, size, etc.

The question about the risks of SNC is a question posed at a regional scale. The presence of symptomatic trees does not seem to depend on the location of a tree within a particular stand, or on the proximity of other stands with symptomatic trees, etc. The disease seems to affect whole diverse areas that are not always directly connected. The regional scale needs to be addressed with information about phenomena that operate at that scale.

Since the infection of a needle by a fungus is a process that occurs at a microscopic scale, and this process determines the presence of the disease at the regional scale, a risk assessment model needs to understand the connection between both scales. There are two ways of doing that. One is the "bottom-up" approach, which consists of a gradual scaling up (from needle to branch, to tree, to

stand, etc.) of the factors that allow the infection process to occur. The problem with this approach is that it needs a detailed understanding of the microscopic process, and how to translate this process from scale to scale. It also requires information at the microscopic scale to be able to reconstruct the conditions to determine the risk level of a stand or a certain area. This approach cannot be used at the present level of knowledge of SNC in the Pacific Northwest.

The "top-down" approach starts from factors operating at the regional or landscape scale and tries to establish a connection between these factors and the "end product" of the infection process, the stand severity level. Although this approach does not take primarily into account the mechanics of the infection process, it is more realistic in the sense that it does not need (at least, initially) a detailed knowledge, which is often not available. The "bottom-up" and the "top-down" approaches are not mutually exclusive, and it is possible to combine them as new knowledge of the processes involved is acquired.

The objective of the present study is to build a model to represent the conditions under which SNC develops and expresses itself. Given the

available information, a “top-down” approach was chosen, using environmental variables at the regional, landscape and stand scale. GIS was the basic tool used for preparing, combining and manipulating all the information.

Methods

Data characteristics and sources (Table 1):

Temperature and precipitation data are raster-based (grids) outputs from a climate prediction model called PRISM. Grids have an approximate cell resolution of 4x4 km (2.5 arc-minute). Temperature and precipitation grids of the months considered more relevant from the epidemiological point of view (Capitano 1999) were selected from the 5 most recent available years (1989-1993). After some analysis, each month was averaged over the 5 years. Of the months selected, June and November appeared to better describe the total variability in disease severity.

Fog/low cloud occurrence was estimated using daily images obtained with the GOES satellite (NOAA). This satellite produces an 8-km resolution grid image in which low clouds and high clouds are represented by different pixel values. Images for June and July 1998 were obtained and average pixel values of each month were calculated. (Note: 4-km resolution images for 1999 are presently available and are currently being processed).

Ambient vapor pressure deficit is a measure of the water content of the atmosphere. It was calculated

based on the average maximum and minimum temperatures (Monteith and Unsworth 1990).

Distance to the coast, elevation and landscape slope aspect were obtained from topographic maps. Landscape slope aspect describes the general orientation of the slope where the stand is located, regardless of what the slope aspect of the stand itself is.

Slope inclination, slope position and aspect were measured in situ. Slope position describes the location of the stand with respect to the bottom of the slope, and it had 4 possible values: low, medium, high or mountain ridge. Slope aspect was converted from azimuth angle values to 8 cardinal directions: N, NE, E, SE, S, SW, W, NW.

Categorical variables were initially used with all the categories (in the form of indicator variables). A merging of categories to produce

fewer groups was done based on the result of consecutive analyses.

The 1936 stand composition variable was extracted from a polygon coverage produced by the Forest Service based on a map by H.J. Andrews and Cowlins (US Forest Service 1936). Stands were separated according to whether or not they had Douglas-fir as the dominant species in 1936.

The stand SNC disease severity variable (the response variable) was based on the rating system (values 1-6) of the 1998 ground survey. Rating values 5 and 6 (only 1 stand) were merged into value 5, so the rating system resulted in 5 values total. The total number of plots considered in this analysis (sample size) was 170. These plots included the SNC Cooperative ground survey, and ground surveys from the Astoria, Forest Grove, Tillamook and Western Oregon ODF districts. A digital map of the ground survey SNC plots was

Table 1: Variables considered in the analysis. In bold type are variables included in the final model.

Variables	Min.-Max./Average
<u>Independent:</u>	
June precipitation (mm)	34-119 / 71.75
June avg. maximum temperature (C)	16.6-22.2 / 19.30
June avg. minimum temperature (C)	6.3-9.9 / 8.23
November precipitation (mm)	152-565 / 288.69
November avg. maximum temperature (C)	5.5-12.7 / 9.80
November avg. minimum temperature (C)	0.8-5.1 / 2.83
June fog/low cloud occurrence	- (arbitrary scale)
June ambient vapor pressure deficit (Pa)	471.21-792.36 / 607.85
Distance to the coast (mi)	0.6-45 / 15.42
Elevation (ft)	98-3367 / 1046.90
Slope inclination (%)	1-154 / 32.3
Slope position (categorical, initially 4 cat., finally 2 cat.)	High, Low
Stand slope aspect (categorical, initially 8 cat., finally 2 cat.)	W/SW/S/SE, NW/N/NE/E
Landscape slope aspect (categorical, 8 cat.)	N,NE,E,SE,S,SW,W,NW
1936 stand composition (categorical, 2 cat.)	Doug-fir, Non-D-fir
<u>Response:</u>	
Stand SNC severity rating (ordered categorical, 5 cat.)	1-5 / 2.56

displayed on a Landsat TM satellite image, and the correct location of each plot was tested using a ground-based map.

Analyses:

All variables were either contrasted individually or in pairs with the stand disease rating. The strength of the relationship between the independent variables and the response was graphically assessed. Groups of variables were then analyzed with multivariate approaches to better understand the data structure and the relationship between variables.

After the initial data selection was done, the resulting variables were used to construct a model for SNC severity in young plantations. The model was based on a multiple regression analysis. For the selection of the best model, two variable selection techniques called “Cp statistic” and “BIC” were used. These techniques assign the best value to those regression models that better explain the response variable with the least number of independent variables. In the search for the best model, quadratic terms and interaction effects were also investigated. The response variable was transformed to logarithm to fulfill the regression model assumptions.

Once a set of candidate variables was obtained, a series of regression analyses were used to include or exclude individual variables. The contribution of these individual variables to the general model was assessed with the corresponding F-statistic.

Results and Discussion

The best model found was:

Mean { log(SNC rating + 1) } =

1.46 + 0.0082 **November max. T** – 0.0073 **June max. T** + 0.0056 **June ppt.**

+ 0.0012 **slope inclin.** – 0.061 **slope pos.** (U,R) – 0.084 **slope asp.** (NW,N,NE,E)

where:

max. = maximum, T = Temperature, ppt. = precipitation, inclin. = inclination, pos. = position, U = upper, R = Ridge, asp. = aspect. Slope position equals “1” when it is located in the “upper” slope or “ridge” and “0” otherwise. Slope aspect equals “1” when the aspect is “NW”, “N”, “NE” or “E”, and “0” otherwise. (see more details on Table 2).

The resulting model is a good indicator of the kind of factors that may be related to Swiss needle cast disease expression. According to the model, there is a strong association between the disease and the climate and topography of the stands. Keeping in mind that higher values of the response correspond to higher disease severity, then, higher November maximum temperatures seem to be associated with higher disease levels, whereas higher June maximum temperatures appear to decrease the disease severity. Higher precipitation in June is related to higher disease levels. These results appear to correspond with basic biological principles. Higher temperatures in colder months may favor the development of organisms, such as *Phaeocryptopus gaeumannii*. In contrast, high temperatures in summer months could be detrimental to the fungus and the host, especially when it is combined with dry periods. From the point of view of fungal growth, this also explains why higher precipita-

tion in a dry month could be favoring the disease development.

These climate variables have a very coarse resolution (cells sizes of more than one km), and although they can determine a general trend, they have to be complemented with more detailed information, probably at the stand scale or smaller, in order to be related to processes that show high variability at lower scales such as fungal growth, canopy transpiration, infection, etc. Quite possibly topography would adequately represent this scale.

The fact that the West-South East facing stands are associated with higher disease severity may be related to the fact that surfaces facing South and (to some degree) West tend to receive more radiation because they are more directly exposed to the sun than the surfaces facing North and East (Jones 1992, Rosenberg et al. 1983). On the other hand, the landscape slope aspects, which represent not necessarily the direction towards which the stand is

facing, but the aspect of the whole slope in which the stand is located, did not result significantly associated with the disease. This may be indicating that climatic factors that may have a strong influence at that scale, such as wind, might not have as much importance as radiation does. In consequence, stands exposed to higher radiation may be either subject to detrimental effects of radiation or temperature over the tree host, or the fungus could be favored by higher temperatures.

Higher slope inclination (steeper slopes) was found to be associated with higher disease severity. Because the sun radiation impacts more directly on flat surfaces (zero inclination), irradiance is higher on more gentle slopes (Jones 1992, Rosenberg et al. 1983). The effect of radiation due to slope inclination may appear in contradiction with its effect due to slope aspect, however, the relationship between these two topographic variables could be quite complex. For example, while the effect of radiation on slope aspect may be similar all year long, the effect on inclination may vary from season to

season. In winter, when the sun orbit is lower, the relative percentage of direct radiation over diffuse radiation is much less than in summer. So it is possible that slope inclination plays a much more important role in summer, when, as it was seen before, higher temperatures (higher radiation on gentle slopes) means lower disease severity.

The fact that stands on lower and medium topographic position seem to experience higher disease severity might be related to the tendency of cloud and fog (either of coastal or local origins) accumulation on valley bottoms. An additional observation in favor of this explanation is the fact that it is not the absolute height what matters (which would have been the case of a significant association with elevation), but the relative topographic position, which is more related to local air movement patterns.

Although in this discussion some attempts were made to explain the possible reasons of why certain variables are associated with the disease, interpretations should be taken with caution. As mentioned before,

possible effects and mechanisms involved in the disease expression may be numerous and interactions can be complex. For example, the three topographic variables discussed here have been used in combination to predict soil moisture availability (Parker 1982), because of their obvious influence on soil water movement and distribution, particularly in mountainous terrain.

A mechanistic, complete explanation of why these variables may be associated with the disease is not an objective of this research. The purpose of this model is to sort out the main variables that influence the disease expression. Once these variables have been found, then, the generation of likely hypotheses follows. For example, going back to the previous discussion about the influence of topography, given the characteristics of SNC disease, the effects of topography on air (and canopy) humidity and temperature are likely to be more important than the effects of topography on soil moisture. Based on what is known about the physiology of the disease, symptoms appear to be more a result of host deficiencies derived from abnormal stomatal functioning rather than soil water availability.

Another main objective of this work is to obtain a model to estimate the probability of a certain area or stand to express SNC symptoms. The adjusted r-squared of the regression (Table 2) indicates that approximately 40 % of the variability observed cannot be explained with the model. 60 % of the variability explained by the model is a good percentage for biological systems, in which typically,

Table 2: Regression analysis

Variable	D. of F.	Estimate	Std. error	
Intercept	1	1.4614	0.3118	
November max. temp.	1	0.0082	0.0008	
June max. temp.	1	-0.0073	0.0015	
June precipitation	1	0.0056	0.0009	
slope inclination	1	0.0012	0.0006	$r^2 = 0.59$
slope position: upper, ridge	1	-0.0611	0.0278	
medium, low	0	0	-	
slope aspect: NW,N,NE,E	1	-0.0840	0.0277	
W,SW,S,SE	0	0	-	

the complexity and uncertainties are too high to be captured by a simple set of variables.

Three tests were done to assess the prediction ability of the model. First, the ground-based SNC rating of the 170 plots used in this study were compared with the predicted value from the model presented above (Figure 1). Points in Fig. 1 were jittered around each SNC rating class to facilitate their visualization. The diagonal shows the one-to-one line, and the short lines, the average predicted values within each SNC rating class. Even when the model did not show a one-to-one relationship between true and predicted ratings, it seems to represent the trend in which higher SNC rating values correspond to higher predicted values (Figure 1). When predicted values of each SNC rating class were averaged, the means of the classes 2 and 3 matched the one-to-one diagonal, class 1 was slightly above, and 4 and 5, markedly below (Figure 1). The dispersion of the points around each average line indicates the non-explained variability already mentioned above.

The second test consisted of using a set of plots that were not previously used in the construction of the model. These were 21 plots measured by ODF to be used in a thinning study (called the “PCT” plots). Plots were well distributed over the same geographical area of the study, and they represented the whole SNC severity rating range.

The predicted values showed similar dispersion and the same deviations from the one-to-one diagonal as shown in the general analysis. This suggests that the model is consistent

over the area of study.

For the third test, a set of 27 plots from the Elliot State Forest, not previously included, were used. This set of plots is special because it occurs outside the area of study, close to Coos Bay, about 50 miles south of the closest plots used in the model. Since there was no topographic information of these plots, and to simulate the range of possible SNC rating outcomes, the disease severity prediction model was applied twice

on each plot. Once with the “worst” topography scenario, that is, the topographic conditions for highest disease severity under the corresponding climate values (100% slope inclination, upper or ridge slope position, and SE, S, SW or W slope aspect). And once with the “best” scenario (0% slope inclination, lower or medium slope position, and NW, N, NE or E slope aspect). Although the ground survey SNC rating values were not available either, it was known that

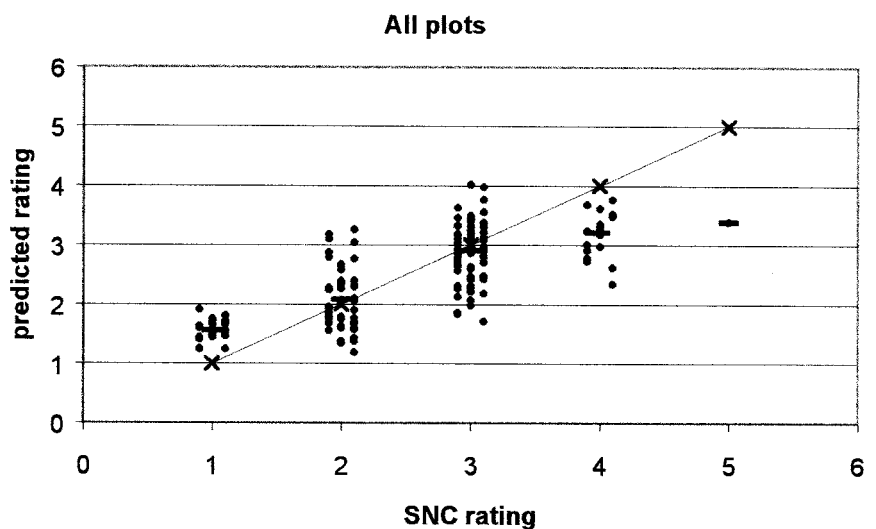


Figure 1: Comparison between the ground-based SNC disease rating and the predicted rating based on the model presented in this study.

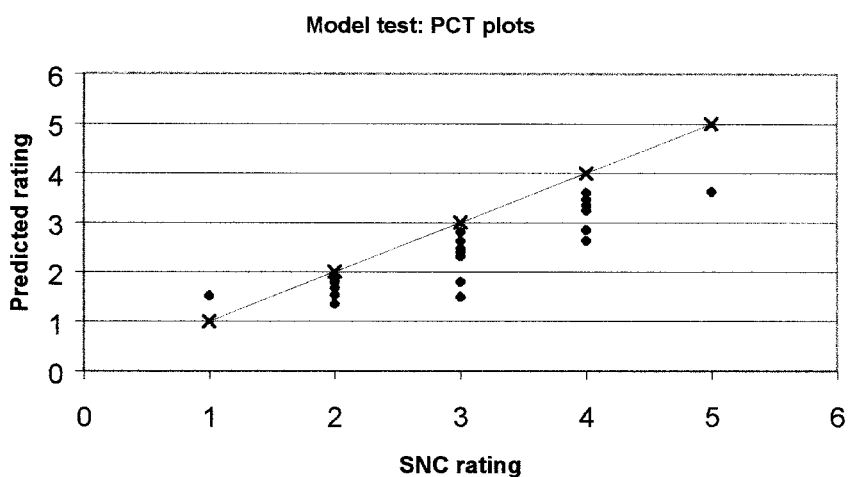


Figure 2: Comparison between the ground-based SNC disease rating and the predicted rating of 21 plots not used in the design of the model.

the SNC severity is low in the Elliot State Forest area.

Figure 3 depicts the resulting SNC rating for both extreme scenarios in the Elliot plots. The model predicted that most of the plot rating values would range from about 2.5 to 3.5, substantially higher than the severity levels known to occur in the field. The predicted high rating may be due to the influence of increasing November maximum temperature towards the South (Table 3).

From the statistical point of view, this clearly confirms the usual recommendation against applying regression models on data outside

the range of the original population. From the epidemiological point of view, one can assume that the model is missing one or more variables that could account for the low disease severity levels observed in the field in the southern portion of the Oregon coast (since the model as it is, predicts high values). The other possible assumption is that there exists a threshold in temperature and/or precipitation beyond which SNC is unlikely to occur.

The SNC disease model as it is, seems to be useful in sorting out the main factors that are involved in the disease expression. It also appears capable of predicting whether or not

extreme rating values, 1 or 4-5, are likely to occur at a certain location. However, its accuracy may not be high enough for the development of an adequate disease management strategy. How can this model be improved? Table 4 presents a theoretical summary of all the variables that could potentially be involved in the disease expression, and how these variables could be represented or estimated.

As can be noticed, some variables, such as soil characteristics have not yet been evaluated. Others, such as wind, have not been well documented or modeled and cannot be incorporated as such, but have to be indirectly estimated.

Result of this preliminary analysis, mostly based on “raw” variables, provided a basis for the next step in model refinement, which is the incorporation and analysis of more elaborated variables. For example, if the interpretation of the regression model is accurate, radiation, a variable that is estimated using sun characteristics and topography, is likely to improve the model accuracy. Another example of an elaborated variable that might be important in disease development and prediction is leaf wetness duration. However, it represents a real challenge when it has to be estimated and applied at the larger scale.

Time is a dimension that has not been addressed up to now and that also represents a potential source of model inaccuracy. There are at least three main factors that may make time relevant in the case of SNC disease development: changes in inoculum load (for example, spore

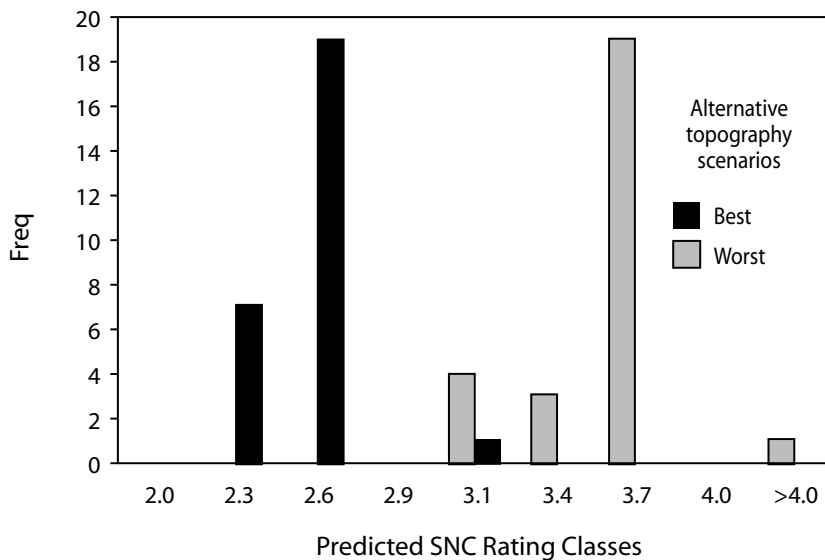


Figure 3: Number of Elliot plots at predicted SNC severity classes after using extreme topographic values to simulate the range of possible rating outcomes.

Table 3 : Comparison of average, standard deviation (parentheses) and min.-max. values of the climatic variables between Elliot plots and the plots used to build the regression model.

	November max. T	June max. T	June precip.
Elliot plots (Coos bay)	13.6 (0.6), 12.3-14.4	21.3(0.4), 20.4-22.1	61.7(5.9), 52-74
All plots (Columbia River to Newport)	9.8(1.9), 5.5-12.7	19.3(1.2), 16.6-22.2	71.8(19.4), 34-119

Table 4 : List of variables and related data potentially involved in disease expression.

What	Is affected by ...	Which can be estimated or tested using ...
Fungal growth		Air temperature radiation (slope aspect, slope inclination)
	Leaf (canopy) wetness and Ambient moisture	air/needle temperature radiation (slope aspect, slope inclination), wind (slope aspect, position, stand density) vapor pressure deficit (temperature) precipitation fog/clouds
?	Tree (stand) nutritional status	soil type seed source previous stand composition
?	Tree (stand) water status	Precipitation water loss (topography, soil texture and structure) radiation (slope aspect, slope inclination), wind (slope aspect, position, stand density) vapor pressure deficit (temperature) fog/clouds stand density
Symptoms	Fungal abundance	Direct measurement or see "Fungal growth"
	Tree health	See "Tree nutritional and water status"
	Climate	Precipitation wind (slope aspect, position, stand density) radiation (slope aspect, slope inclination), vapor pressure deficit (temperature)

density in air), changes in climate from year to year, genetic changes in both the host and/or the fungus. The model, so far has been built assuming that none of these factors exist.

In terms of inoculum load, it has been the assumption that since the fungus is always present everywhere, local changes in fungal abundance do not substantially impact regional distribution of inocula. Climate is known to change at different time scales (years, decades, centuries, etc.) and any model that depends on climate variables has to be adjusted accordingly. This means that a SNC model should be continuously tested against these changes and, ideally, these

changes have to be incorporated in the model itself. Genetic changes are also assumed not to occur during the development of the model, although

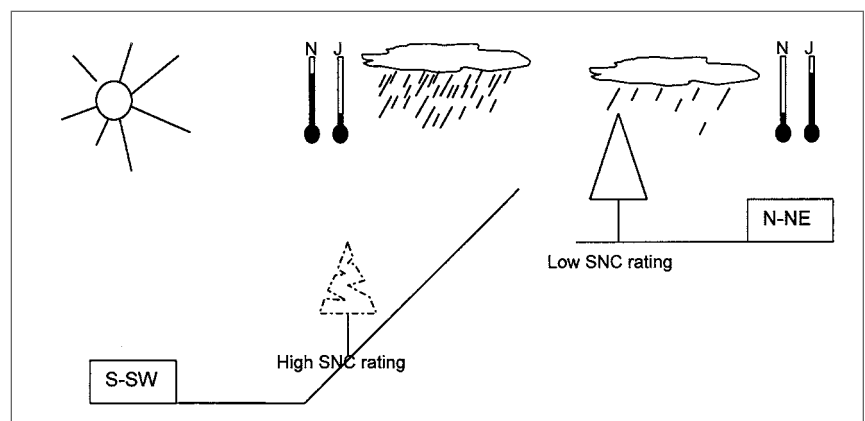


Figure 4: Schematic representation of the association between the variables and the disease expression

this a factor that has to be addressed one way or another.

Conclusions:

- November and June maximum temperatures, June precipitation, slope aspect, inclination and position are the variables that showed closest association with SNC disease expression. A schematic depiction of their effects is presented in Figure 4.
- The regression-based model accounts for 60 % of the variability present in the plots.
- An improvement of the model prediction accuracy is proposed by incorporating elaborate variables, that could more closely reflect the type of processes involved in disease development and expression.

References

- Capitano, B. 1999. The infection and colonization of Douglas-fir by *P. gaeumannii*. Oregon State University thesis, 81 pp.
- Jones, H. 1992. Plants and microclimate. 2nd ed., Cambridge University Press, 427 pp.

Monteith, J.L. and Unsworth, M.H. 1990. Principles of environmental physics. 2nd ed., London: Edward Arnold.

Parker, A.J. 1982. The topographic relative moisture index: an approach to soil-moisture assessment in mountain terrain. *Physical Geography*, 3, 2: 160-168

Rosenberg, N.J.; Blad, B.L. and Verma, S.B. 1983. *Microclimate. The biological environment*. 2nd ed., J. Wiley & Sons, 495 pp.

US Forest Service, 1936. Forest type map, State of Oregon. NW quarter. US Pacific NW Forest Experimental Station.

Objections and notes:

-Temperatures of Nov(5-12 C) and June and fungal development (opt germin: 11-22, Vent.. 18-22,Bryan)

-make a map of stands and rating. Are ratings spatially aggregated?

BACKGROUND AND ORGANIZATION

The Swiss Needle Cast Cooperative (SNCC) was established in January 1997. Damage caused by Swiss needle cast, a native foliage disease that affects Douglas-fir, has made it imperative that new research be conducted to learn practical methods of disease detection and management to maintain the health and productivity of Douglas-fir plantations. A well-run cooperative is an efficient means of increasing and accelerating the level of forest disease research in the region. Because members participate directly in problem identification and research solutions, communications of results is speeded and results are applied more rapidly and effectively.

SNCC is located in the College of Forestry at Oregon State University. The Membership is comprised of private, county, state, and federal organizations. Membership dues vary depending on forestland ownership. One annual report, project reports, and newsletters are distributed to members each year. All projects are carried out in cooperation with specific members on their land holdings.

PURPOSE

The focus of SNCC will be Swiss needle cast research for forest land owners in western Oregon and Washington. The purpose of SNCC is to provide the following services:

1. Conduct research on the biology, detection, and management of Swiss needle cast in coastal Douglas-fir as related to basic infection biology and genetics, tree physiological dysfunctions, aerial and ground survey technology, disease hazard and risk rating, growth and yield impacts, and strategies for control.
2. Conduct training and workshops on reassert and survey results
3. Provide newsletters and reports on research and surveys, and
4. Serve as a focal point for information on Swiss needle cast.

